

|              |   |
|--------------|---|
| Title        | Degradation control of polysaccharide by Malaprade oxidation for tissue engineering |
| Author(s)    | CHIMPIBUL, WICHCHULADA  |
| Citation     |   |
| Issue Date   | 2016-06   |
| Type         | Thesis or Dissertation  |
| Text version | ETD   |
| URL          | <a href="http://hdl.handle.net/10119/13725">http://hdl.handle.net/10119/13725</a>   |
| Rights       |   |
| Description  | Supervisor: 松村 和明, マテリアルサイエンス研究科, 博士  |

# **Degradation control of polysaccharide by Malaprade oxidation for tissue engineering**

by

Wichchulada Chimpibul

Supervisor: Associate Professor Kazuaki Matsumura

School of Materials Science

Japan Advanced Institute of Science and Technology

June 2016

**Referee-in-chief:** Associate Professor Dr. Kazuaki Matsumura  
*Japan Advanced Institute of Science and Technology*

**Referees:** Professor Dr. Kohki Ebitani  
*Japan Advanced Institute of Science and Technology*

Professor Dr. Tatsuo Kaneko  
*Japan Advanced Institute of Science and Technology*

Professor Dr. Masayuki Yamaguchi  
*Japan Advanced Institute of Science and Technology*

Professor Dr. Supason Wanichwecharungreung  
*Chulalongkorn University*

## ***Abstract***

Polysaccharide is one of the biopolymers which has been attracted by tissue engineering application due to biodegradability, low toxicity, low manufacture costs [1]. Polysaccharide comprises a numerous of hydroxylic group which are suitable for derivatization and subsequent chemical and physical crosslinking. Malaprade oxidation is glycol cleavage reaction of vicinal diol by periodate ion. The carbon–carbon bond in a vicinal diol (glycol) is cleaved and replaced with two carbon–oxygen double bonds. Depending on the substitution pattern in the diol, either ketones or aldehydes may be formed [2]. In this thesis, I focused on oxidizing dextran and cellulose. Dextran is a bacterial polysaccharide, consisting of  $\alpha$ 1-,6 linked D-glucopyranose residue. For several years, dextran was oxidized with sodium periodate to investigation the degradation but no report about the mechanism of degradation or how oxidized dextran and other polysaccharide were degrade by Malaprade and Schiff base reaction. In chapter2, I reveal the degradation mechanism of oxidized dextran using 2D NMR technique and gel permeation chromatography. The results showed that the oxidation of polysaccharide was controlled by varying the concentration of periodate and primary amino acid. The degradation was started after adding amino acid which related which Schiff base reaction. Moreover, the degradation of oxidized polysaccharide is related with Maillard reaction due to the appearance of methyl group which is one component of deoxyosone in Maillard pathway. A second aspect of partially oxidized polysaccharides is the chemical properties of the oxidized residues, and in particular the hydrolytic ability, which may provide a basis for biomaterials with increased biodegradability. In chapter 3,

I used the cellulose as non-soluble polysaccharide for fabricating the tissue engineering scaffold using NaCl leaching technique. The results indicated that the degradation of oxidized polysaccharide scaffold was controlled by varying the concentration of periodate. Furthermore, the degradation was initially started by adding the primary amino acid which correlated with oxidized dextran degradation in chapter 2. To further investigate the suitability of these scaffolds for tissue engineering applications, biocompatibility was checked using CCK-8 kit assay. In addition, scanning electron microscopy and *in vivo* experiment were demonstrated to show the ability of cells to attach to scaffold surfaces and a biocompatibility of matrices with cells, respectively. The result indicated that the oxidized cellulose scaffold showed good biocompatibility, cell viability and degradation which are important properties of scaffold for tissue engineering. In this thesis, I can explore the mechanism of oxidized polysaccharide by Malaprade oxidation via oxidized dextran which directly related with Schiff base and Maillard reaction. In addition, I use this mechanism for controlling the oxidized polysaccharide scaffold via cellulose scaffold for tissue engineering.

**Keywords:** polysaccharide, Malaprade oxidation, Schiff base reaction, Maillard reaction, tissue engineering.

## **References**

1. Khan, F. and S.R. Ahmad, *Polysaccharides and their derivatives for versatile tissue engineering application*. Macromol Biosci, 2013. **13**(4): p. 395-421.
2. Singh, M., A.R. Ray, and P. Vasudevan, *Biodegradation studies on periodate oxidized cellulose*. Biomaterials, 1982. **3**(1): p. 16-20.

## Content

|  |        |
|--|--------|
| <b>Chapter1</b> .....  | 1      |
| 1.1 Research background.....                                   | 1      |
| 1.2 Polysaccharide.....  | 2      |
| 1.2.1 Dextran.....   | 3      |
| 1.2.2 Cellulose.....   | 4      |
| 1.3 Polysaccharide degradation.....                            | 5      |
| 1.3.1 Dextran degradation.....                                 | 5      |
| 1.3.1.1 Enzymatic degradation dextran.....                     | 5      |
| 1.3.1.2 Physical degradation dextran.....                      | 6      |
| 1.3.1.3 Dextran degradation by Malaprade oxidation.....        | 7      |
| 1.3.2 Cellulose degradation.....                               | 8      |
| 1.3.2.1 Cellulose enzymatic degradation.....                   | 8      |
| 1.3.2.3 Cellulose degradation by oxidation with periodate..... | 9      |
| 1.4 Polysaccharide chemical modification reaction.....         | 10     |
| 1.4.1 Malaprade reaction.....                                  | 10     |
| 1.4.2 Schiff base reaction.....                                | 11     |
| 1.4.3 Maillard reaction.....                                   | 13     |
| 1.5 Polysaccharide for tissue engineering.....                 | 14     |
| 1.5.1 Dextran for tissue engineering.....                      | 16     |
| 1.5.2 Cellulose for tissue engineering.....                    | 18     |
| 1.6 Research objective.....                                    | 19     |
| References.....  | 20     |
| <br><b>Chapter 2</b> .....                                     | <br>28 |
| 2.1 Introduction.....  | 28     |
| 2.1.1 Dialdehyde polysaccharide.....                           | 28     |
| 2.1.2 Hemiacetal formation.....                                | 29     |

|  |           |
|--|-----------|
| 2.1.3 Maillard reaction.....   | 31        |
| 2.1.4 Mechanism of formation in Maillard reaction.....   | 34        |
| 2.1.5 Strecker degradation.....  | 35        |
| 2.1.6 Melanoidin.....  | 36        |
| 2.2. Material and method.....  | 36        |
| 2.2.1 Dextran oxidation.....   | 36        |
| 2.2.2 Aldehyde content determination.....  | 37        |
| 2.2.3 Molecular weight determination by GPC.....   | 37        |
| 2.2.4 NMR spectroscopy.....  | 38        |
| 2.3 Results and discussion.....  | 38        |
| 2.3.1 Oxidation of dextran with periodate.....   | 38        |
| 2.3.2 Molecular weight determination.....  | 39        |
| 2.3.3 NMR analysis.....  | 45        |
| 2.4 Conclusion.....  | 56        |
| References.....  | 57        |
| <b>Chapter 3.....</b>  | <b>59</b> |
| 3.1. Introduction.....   | 59        |
| 3.1.1 The oxidation of cellulose.....  | 59        |
| 3.1.1.1 Oxidation cellulose with nitrogen dioxide.....   | 60        |
| 3.1.1.2 Oxidation cellulose with phosphoric acid, sodium borate,<br>sodium chlorate and sodium chlorite..... | 60        |
| 3.1.1.3 Oxidation cellulose with phosphoric acid, sodium nitrite or<br>sodium nitrate.....                   | 61        |
| 3.1.1.4 Oxidation cellulose by periodate.....  | 62        |
| 3.1.2 Scaffold biofabrication technique.....   | 63        |
| 3.1.2.1 Particulate leaching and solvent casting.....  | 63        |
| 3.1.2.2 Gas foaming.....   | 64        |
| 3.1.2.3 Phase separation.....  | 64        |
| 3.1.2.4 Melt molding.....  | 65        |
| 3.1.2.5 Freeze drying.....   | 66        |

|  |           |
|--|-----------|
| 3.1.2.6 Electrospinning.....   | 67        |
| 3.1.3 Ionic liquids and their interaction with cellulose.....          | 67        |
| 3.2 Material and method.....   | 69        |
| 3.2.1 Cellulose membrane degradation.....                              | 69        |
| 3.2.1 Cellulose scaffold fabrication.....                              | 69        |
| 3.2.2 Oxidized cellulose scaffold.....                                 | 70        |
| 3.2.3 Degradation of oxidized cellulose scaffold <i>in vitro</i> ..... | 70        |
| 3.3 Results and discussion.....  | 71        |
| 3.3.1 Aldehyde introduction in oxidized cellulose membrane.....        | 71        |
| 3.3.2 Cellulose scaffold characterization.....                         | 75        |
| 3.3.3 Aldehyde introduction in oxidized cellulose scaffold.....        | 79        |
| 3.3.4 Degradation of oxidized cellulose scaffold <i>in vitro</i> ..... | 81        |
| 3.4 Conclusion.....  | 85        |
| References.....  | 86        |
| <b>Chapter 4.....</b>  | <b>88</b> |
| 4.1 Introduction.....  | 88        |
| 4.1.1 Protein adsorption.....  | 88        |
| 4.1.1.2 Relevance.....   | 88        |
| 4.1.2.2 Protein and surface interaction.....                           | 89        |
| a. Protein properties.....   | 89        |
| b. Surface properties.....   | 92        |
| 4.1.2 Cell and polymer interaction.....                                | 92        |
| 4.1.3 Effect of polymer chemistry on cell behavior.....                | 94        |
| 4.1.3.1 Synthetic polymer.....   | 94        |
| 4.1.3.2 Biodegradable polymer.....                                     | 96        |
| 4.2 Material and method.....   | 97        |
| 4.2.1 Protein adsorption.....  | 97        |
| 4.2.2 Cell growth investigation.....                                   | 97        |
| 4.2.3 Cell fixation on oxidized cellulose scaffold.....                | 98        |

|  |            |
|--|------------|
| 4.2.4 Animal implantation.....                           | 98         |
| 4.2.5 Histological study.....                            | 99         |
| 4.3 Results and discussion.....                          | 100        |
| 4.3.1 Protein adsorption.....                            | 100        |
| 4.3.2 Pore size effect to cell growth.....               | 101        |
| 4.3.3 The degree of oxidation effect to cell growth..... | 103        |
| 4.3.4 Animal test.....                                   | 105        |
| 4.4 Conclusion.....                                      | 110        |
| References.....  | 111        |
| <b>Chapter 5.....</b>                                    | <b>116</b> |
| Conclusion.....  | 116        |
| Achievement.....   | 119        |
| Acknowledgement.....                                     | 121        |

# Chapter 1

---

## General introduction

### 1.1 Research background

For several years, polysaccharide has been frequently used for biomedical and pharmaceutical application, mainly hyaluronic acid, alginate and chitosan as wound dressing, drug carrier and scaffold for tissue engineering. The different degradation mechanisms were reported including the enzymatic degradation related with their biodegradability. However, the degradation of polysaccharide by enzymatic degradation is consistent related with complicated processing combining with many technique and high value, such as isolation and purification enzyme processing. Therefore, the role of chemical modification of polysaccharide for degradation increased its importance. By another reason, the controlling of polysaccharide degradation via chemical modification is facile and simple than enzymatic degradation. The chemical reactions for conjugate and modification of polysaccharide are required the active functional groups such as carbodiimide, hydrazide, aldehyde, radical and ester. Malaprade reaction has been considered because this reaction is favorably used for polysaccharide modification through glycol cleavage reaction without catalytic system. In previous research, many researchers used Malaprade reaction for polysaccharide oxidation resulting to dialdehyde polysaccharide which can react with amine

group to form Schiff base. The degradation rate was controlled by varying the degree of oxidation. However, the mechanism of dialdehyde polysaccharide degradation has not been clarified. Hence, the mechanism for polysaccharide degradation by Malaprade reaction are studied and reported in detail in this thesis.

## 1.2 Polysaccharide

Polysaccharides are biopolymer which composed of long chains of monosaccharide units bound together by glycosidic linkages and are hydrolysis give the constituent oligosaccharides or monosaccharides. The structure of polysaccharide can be both linear and branch. Natural saccharides are generally of simple carbohydrates called monosaccharides with general formula  $(\text{CH}_2\text{O})_n$  where  $n$  is three or more. Examples of monosaccharides are glucose, fructose, and glyceraldehyde. Polysaccharides which contain only one kind of monosaccharide are called homopolysaccharides (homoglycans); when they are established by two or more different monomeric units they are named heteropolysaccharides (heteroglycans). The number of monosaccharide units in a polysaccharide is termed degree of polymerization or d.p. The size of a polysaccharide varies between approximately 16,000 and 16,000,000 daltons (Da).

Polysaccharides are produced by a variety of species, including plant, algae, microbes and animals. It is an important class of biological polymers. Their function in living organisms is usually either structure- or storage-related. Starch is frequently used as a storage polysaccharide in plants, being found in the form of both amylose and amylopectin. In animals, the structurally similar glucose polymer is the more densely branched glycogen. Its properties allow it to be metabolized more rapidly, which suits the active lives of moving animals. The structural polysaccharides are chitin and cellulose (see 1.2.2). Chitin is polysaccharide which contains nitrogen side branches for increasing its strength. It is usually found in arthropod exoskeletons and

in the fungi cell walls. It also has multiple applications such as surgical threads. Cellulose is used as plants cell walls and other organisms which it is most abundant organic molecule on earth. It has many application such as an important role in the paper and textile industries. For polysaccharide producing from microorganism, xanthan and dextran (see 1.2.1) are examples. Xanthan is made from bacteria *Xanthomonas campestris*. It have important role in food and pharmaceutical industries. Xanthan is normally used for increasing the suspension viscosity and increasing food stability at acid high concentration of acid.

### 1.2.1 Dextran

Dextran is a polysaccharide which synthesized by fermentation of *Leuconostoc mesenteroids* bacteria, when grown on sucrose containing media [1]. The straight chain consists of  $\alpha$ -1,6 glycosidic linkages between glucose molecules, while branches begin from  $\alpha$ -1,3 linkages. Dextran fractions are supplied in molecular weight from 1,000 Daltons to 2,000,000 Daltons. It is certainly soluble in water and electrolyte solution to form clear, stable solution, easy to functionalize through its reactive hydroxyl chemistries.

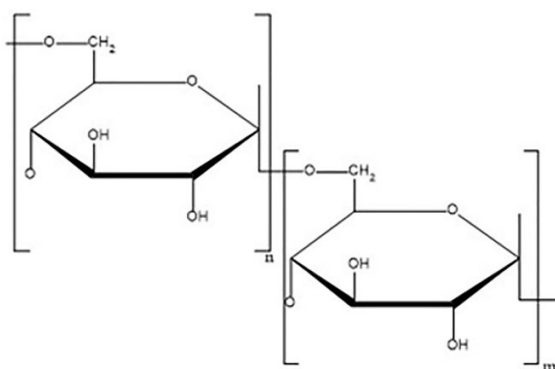


**Figure 1.1** Dextran structure.

Dextran had concerned consideration from the biotechnology field. It was accepted as a plasma volume expander because its linear structure, high water solubility, and specially owing to

its  $\alpha$ -1,6 linkage, more related to biological applications, slowly degraded by human enzymes as compared to other polysaccharides [2]. The biodegradation of dextran usually occurs through natural enzymatic partitive of saccharide bonds by dextran-1,6-glucosidase found in liver, spleen, kidneys, lungs, brain and muscle tissue as well as by dextranases expressed by bacteria in the colon [3, 4]. Therefore, dextran has also been imposed that it lacks nonspecific cell binding and resists protein adsorption, which is attracted as a biomaterial [5, 6]. Moreover, it has been used as macromolecule carrier for drug and protein delivery, to increase the longevity of therapeutic agents in systemic circulation [7-9].

### 1.2.2 Cellulose

Cellulose is a natural polymer which is important component in plant cell wall with the formula  $(C_6H_{10}O_5)_n$ , a polysaccharide consisting of a linear chain of several hundred to many thousands of  $\beta$  (1 $\rightarrow$ 4) linked D-glucose units (**Figure 1.2**). It is most abundant polymer on world and can be made from plant and microorganism.

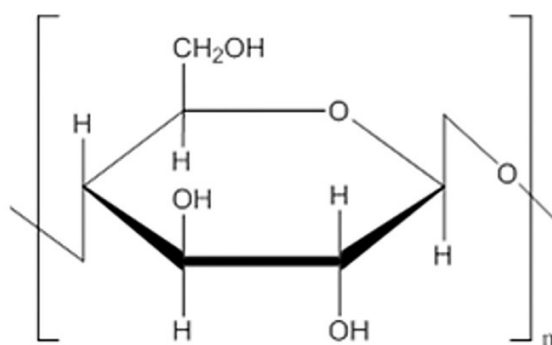


**Figure 1.2** Cellulose structure.

Cellulose is no taste, odorless, hydrophilic, insoluble in water and biodegradable [10]. Compared to starch, cellulose has much more crystalline. Whereas starch undergoes a crystalline

to amorphous transition when heated up to 60–70 °C in water, cellulose obliges a temperature of 320 °C and pressure of 25 MPa to turn into amorphous in water. Strong crystalline structures of cellulose are corresponding to the location of hydrogen bonds between and within strands.

### **1.3 Polysaccharide degradation**

#### **1.3.1 Dextran degradation**

Dextran is frequently attracted in biomedical field. Due to high molecular weight of dextran, it may be increased the sedimentation tendency of red blood corpuscles [11]. Therefore, dextran such a material using for blood expander, it is important to control the molecular size. The procedure which use for depolymerize dextran are acid hydrolysis, enzyme degradation and ultrasonic vibration [12].

##### **1.3.1.1 Enzymatic degradation dextran**

Dextran is depolymerized by enzyme dextranase which catalyze the endohydrolysis of 1,6- $\alpha$ -glucosidic linkages in dextran (Figure 3). Dextranase is an enzyme which catalyzed the dextran degradation in to low molecular weight fraction [13]. It usually made from bacteria such as *Paccilomyces lilacinus* [13], *Penicillium funiculosum*[14]. Chalet et al. purified the dextranase from *Penicillium funiculosum*, dextran was degraded yield 27,000 isomaltose reducing units in 2 hours by 1 mg dextranase [14]. Moreover, the controlled released of protein from dextran microsphere was carried out by enzymatic degradation. The dextran microsphere were degraded by co-encapsulation of endo-dextranase [15]. Furthermore, enzymatically-degrading dextran hydrogels were investigated as matrices for the delayed release of proteins. In the absence of dextranase, protein was released very slowly for a period of 250 days, whereas, the gels containing dextranase showed the release profile which was highly dependent on the concentration of

dextranase present in the hydrogel [16]. However, the dextranase from microorganism have been carried out on crude or ammonium sulphate precipitation enzyme preparation. Therefore, the complicate process and vast outlay are cooperated.

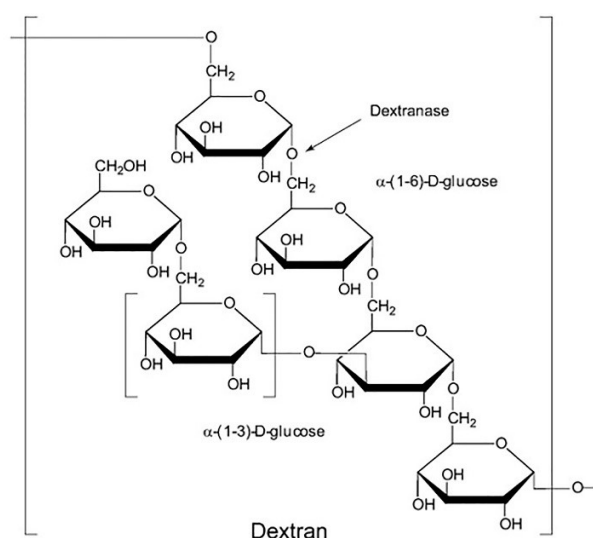


**Figure 1.3** Enzymatic dextran degradation by dextranase.

### 1.3.1.2 Physical degradation dextran

Dextran is depolymerized by physical method such as jet-cooking under high steam pressure, extrusion under harsh environmental conditions and ultrasonication. The three physical methods, the ultrasonic treatment causes the greatest degradation, yielding dextrans with much lower molecular weight and less viscous solutions than the other two methods [17]. Ultrasonication is one of the most promising approaches for the degradation of polymer, leading to an irreversible lowering of the chain length caused by cleavage and not necessarily any chemical changes. Molecular weight and polydispersity index of dextran decreased with increasing time of ultrasonic treatment [18].

### 1.3.1.3 Dextran degradation by Malaprade oxidation

For several years, dextran was oxidized with periodate ion by Malaprade reaction (see 1.4). Dextran was oxidized with periodate ion which is a catalysis-free aqueous reaction. The yield is purified product with simple dialysis step, followed by freeze-drying. First disclose, the Malaprade reaction was used for characterization and explanation the polysaccharide structure, through the complete oxidation and degradation product analysis [19-21]. The dextran oxidation by periodate is a strong reaction that leads to chain degradation and modifies dextran physico-chemical properties. Mirgorodskaya et al. introduced aldehyde group into dextran, showing that in the reaction dialdehyde-dextran with different degrees of oxidation of the monomer units can be formed [22]. The new derivative of dextran was prepared by oxidation of dextran and the oxidation of dextran enhances the flexibility of the backbone and decreased the molecular weight [23]. Oxidized dextran is slightly soluble in water and more viscous than regular dextran [24, 25]. The degree of oxidation is also reflected on the glass transition temperature according to dynamic mechanical thermal analysis. The glass transition temperatures shift is in direct accordance with the molecular weight decrease, but do not give much insight on the structural consequences of the oxidation [24].

To control the degree oxidation in dextran is most importance for final properties and application. Degree oxidation of effect on final monomer properties which results to the efficient design of nanoparticle [26], hydrogel [27, 28], drug immobilization [29, 30] and surface coating [5]. Lee et al. fabricated the hydrogel film by crosslinking gelatin with dialdehyde dextran for controlling the polypeptide release system. The crosslinked gelation with dialdehyde dextran showed the appropriate releasing profile for sustained delivery of epidermal growth factor (EGF) [28]. Furthermore, nanoparticle was synthesized by oxidized dextran conjugated with cholic acid

hydrazide. The particle showed the self -aggregation and depended on oxidation and substitution degree [31]. Oxidized dextran can be a crosslinker for preparation gelatin microsphere. It showed the slow release of antitumor drug and indicated that oxidized dextran could be crosslinker to form gelatin microsphere for controlled release of drugs [32].

### **1.3.2 Cellulose degradation**

#### **1.3.2.1 Cellulose enzymatic degradation**

Cellulose is degraded by enzyme which is produced from microorganism such as bacteria, fungi and protozoa. Microorganism is efficient for the degradation of cellulose by together working with different enzyme specificity. Cellulase hydrolyzes the  $\beta$  1,4 glycosidic linkage of cellulose which divides into two classes, endoglucanase and cellobiohydrolase. Both enzymes can degrade amorphous cellulose but only cellobiohydrolase can degrade crystalline structure. However, cellulase and cellobiohydrolase degrade cellulose and release cellobiose molecule. Therefore,  $\beta$ -glucosidase is required for breaking down the cellobiose to release glucose molecule (Figure 4).

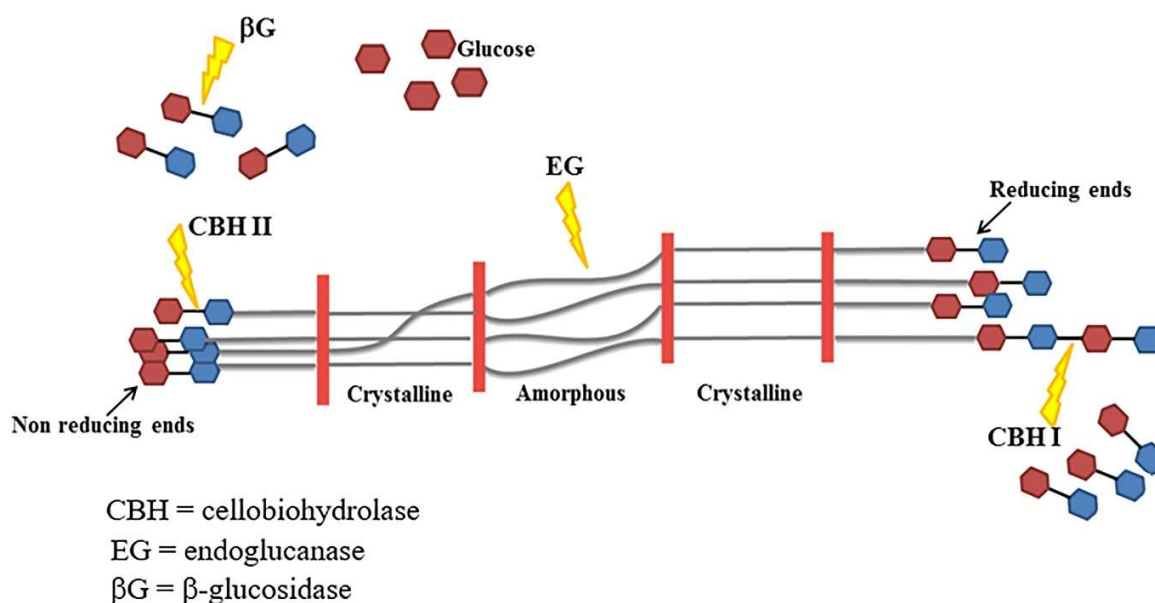


**Figure 1.4** Enzymatic cellulose degradation.

Almost mechanisms for cellulose degradation by enzymatic microorganism usually occur under anaerobic condition. Some microorganisms require quite high temperature for cellulose degradation. Therefore, cellulose enzymatic degradation is attained through the complicated process for operation and purification.

### 1.3.2.3 Cellulose degradation by oxidation with periodate

Oxidation of cellulose using sodium periodate is widely interested. The C<sub>2</sub> and C<sub>4</sub> vicinal hydroxyl group is selectively cleaved to yield a product with 2, 3 dialdehyde unit along with cellulose chain. Maekawa and Koshijima found that the kinetics of the reaction depended on the physical form of the cellulose, such as film, fiber, powder, etc. [33]. Because of rich reactivity of aldehyde group, dialdehyde can promote as intermediate for derivatization of cellulose. Due to the degree of oxidation can be certainly controlled by the amount of periodate added, functional

utilization of partially oxidized cellulose have been used for drug release [34], column packing [35-37], absorbent of heavy metal ion [33, 38] and tissue engineering [39-41].

However, dialdehyde cellulose is not soluble in water or organic solvent, even after complete oxidation. The insolubility of dialdehyde cellulose has been mentioned to hemiacetal formation of aldehyde group with cellulose's remaining hydroxyl group. Kim et al. found that the completely oxidized dialdehyde cellulose was soluble in water by simple heating [42].

In addition, crystallinity of dialdehyde cellulose was changed when compared with native cellulose. The wide angle X-ray diffraction peak was located at  $2\theta = 22.7^\circ$  for oxidized cellulose, which the crystalline of cellulose, was showed to decrease proportionately to the degree of oxidation of cellulose. The crystallinity differentiation results to their hydrogen bonding ability with adjacent molecule. Their ability to hydrogen bond with water is reflected in their water absorption capacity [43].

## **1.4 Polysaccharide chemical modification reaction**

### **1.4.1 Malaprade reaction**

Malaprade reaction is an oxidation of adjacent diols with periodic acid or its salt in aqueous solution. In this reaction, solvents such as ethanol, methanol and acetic acid, can be added to the reaction solution to increase the solubility of organic substrates. Malaprade reaction is similar to glycol oxidation which is assumed to involve an acidic cyclic ester intermediate that decomposes to yield ketone or aldehyde. The hydroxyl group is oxidized to an aldehyde or a ketone group, the carbonyl group is oxidized to a carboxyl group, and the amino group is converted into an

aldehyde group and ammonia (or a substituted amine in the case of a secondary amine). This reaction has been successfully used for the degradation of carbohydrates and in structural analysis [44].

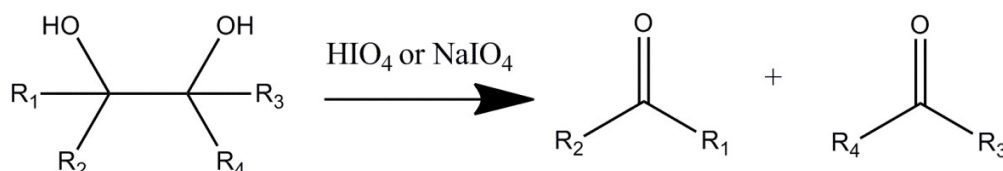


**Figure 1.5** General Malaprade oxidation.

#### 1.4.2 Schiff base reaction

A Schiff base is a nitrogen analog of an aldehyde or ketone in which the C=O group is replaced by C=N-R group. It is usually formed by condensation of an aldehyde or ketone with a primary amine according to the following scheme (Figure 5). Where R, it may be an alkyl or an aryl group. The formation of a Schiff base from an aldehydes or ketones is a reversible reaction and generally takes place under acid or base catalysis, or upon heating.

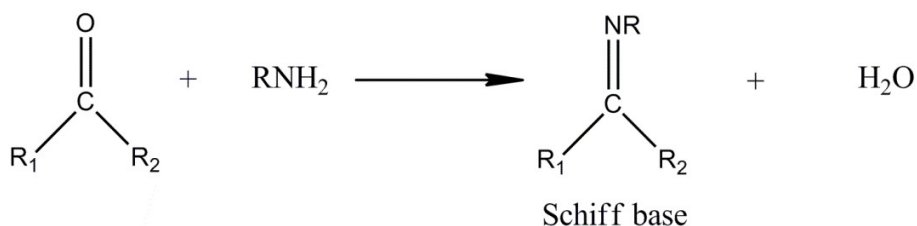


**Figure 1.6** Schiff base reaction.

Schiff bases perform to be an important intermediate in a number of enzymatic reactions involving interaction of an enzyme with an amino or a carbonyl group of the substrate. One of the

most important types of catalytic mechanism is the biochemical process which involves the condensation of a primary amine in an enzyme usually that of a lysine residue, with a carbonyl group of the substrate to form an imine or Schiff base.

In addition, Schiff base reaction is usually used for preparation of self-crosslinking hydrogel for biomedical application because the formation of Schiff base via an aldehyde or ketone encouraged rapid crosslinking of gel precursor [45]. This has specifically been investigated for the preparation of crosslinked proteins such as gelatin [46, 47] and albumin [48] and amine containing polysaccharides [49]. Furthermore, amine and vinyl group was investigated *in situ* crosslinking hydrogel because its fast reaction time and flexibility in forming with multiple type of bond [50]. The formation via Schiff base is an alternative procedure to avert using the toxic chemical crosslinker. Glutaraldehyde as favorite crosslinker is toxic even if it was applied at low concentration. Our previous study, the hydrogel was formed between the oxidized dextran and  $\epsilon$ -poly-L-lysine via Schiff base reaction (Figure 7). The gelation time of the hydrogel was easily controlled by the extent of oxidation in dextran and of the acylation in  $\epsilon$ -PL by anhydrides. The cytotoxicity of oxidized dextran and  $\epsilon$ -PL were 1000 times lower than that of glutaraldehyde and poly (allylamine) [51].

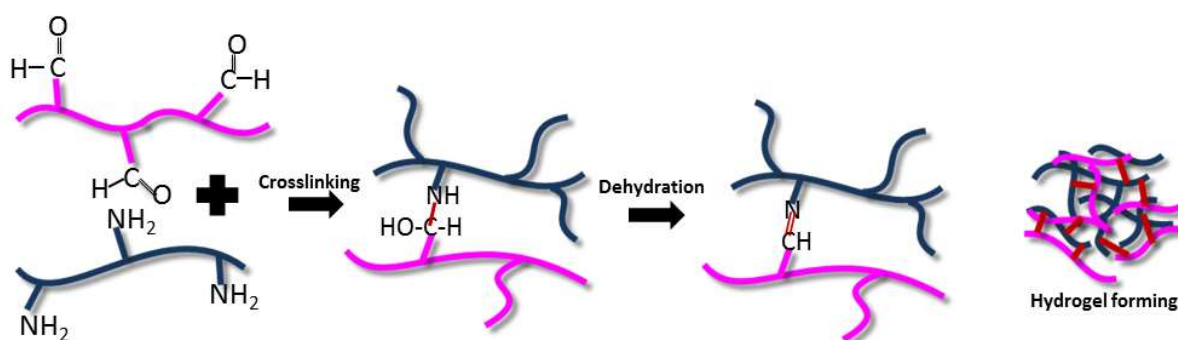


**Figure 1.7** Oxidized dextran and  $\epsilon$  poly L-lysine hydrogel forming scheme.

The hydrogel color was changed from clear to brown indicating that the reaction between the oxidized dextran aldehyde and the poly-L-lysine amino may be induced by a Maillard reaction (see 1.4.3) via Schiff base formation [52].

### 1.4.3 Maillard reaction

The Maillard reaction is a reaction between reducing sugars and amino acids that provide browned food its desirable flavor. The reducing sugar condenses with free amino acid group to give a condensation product N-substituted glycosilamine, which changes to the Amadori rearrangement product (ARP). Subsequently, the Amadori product degradation depends on the pH. At pH > 7, the Amadori product degradation is rearranged to Fission product including acetol, diacetyl and pyruvate which are reactive compounds. Carbonyl groups are attacked with free amino groups resulting to the incorporation of nitrogen into the reaction products. Dicarbonyl compounds are reacted with amino acids with the aldehyde formation of  $\alpha$ -aminoketones via Strecker degradation. At pH 7 or below, the Schiff base of hydroxymethylfurfural (HMF) will be formed (Figure 8).

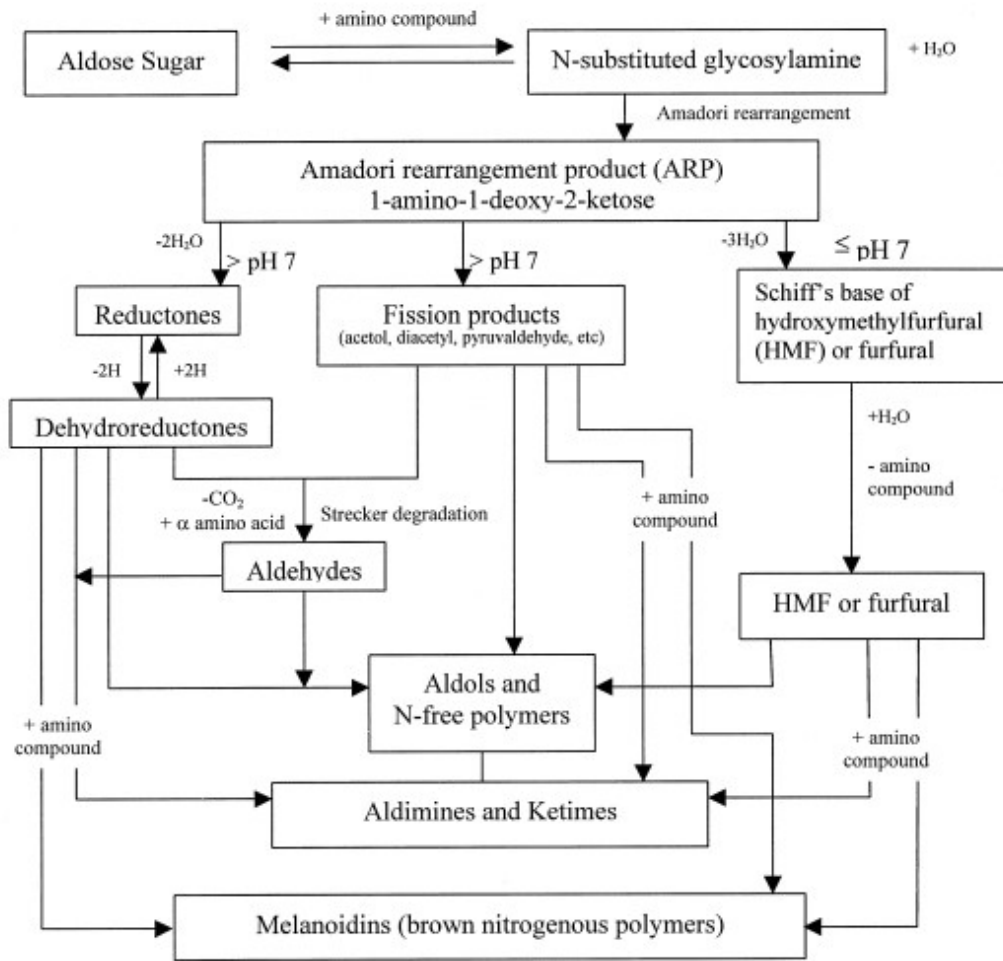
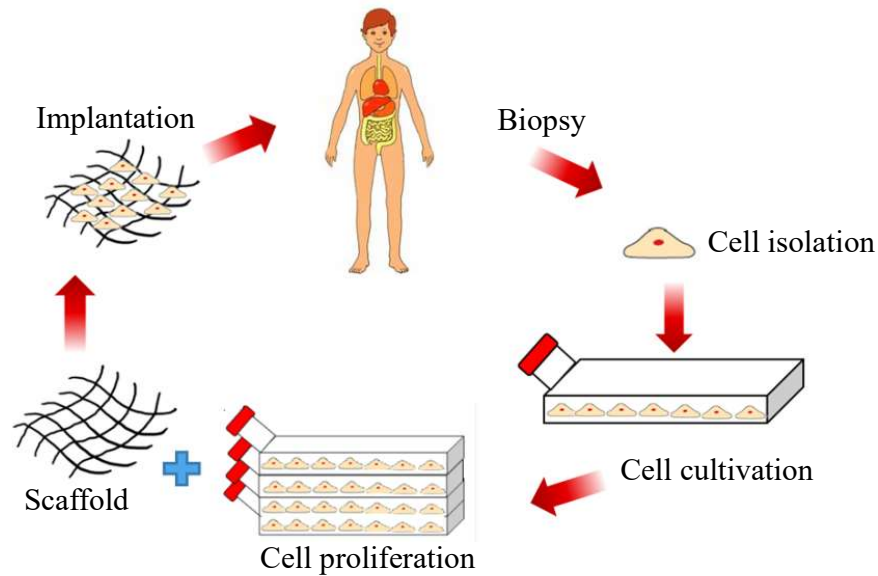


Figure 1.8 Millard reaction scheme by Hogde [53].

### 1.5 Polysaccharide for tissue engineering

The tissue engineering is the interdisciplinary field which is gainful to plan of artificial scaffold. It is related to biomaterial development. The aim of tissue engineering is to gather functional constructs for keeping, maintenance or improvement the injured tissue or organ. The basic tissue engineering principle is illustrated in **Figure 1.9**. Cells are isolated from living organism or patient's body and cultured in cultured dish in laboratory. The sufficient cells are

seeded in the polymeric material as scaffold and allowed to culture in incubator or bioreactor. When the construct is developed enough, it is implanted in the area of defect to patient's body.



**Figure 1.9** Tissue engineering principle.

In present day, the tissue engineering application is really used in hospitals such as artificial cartilage [54], bone [55, 56], tendon, ligament [57], skin [58], esophagus [59], liver [60], nerve [61]etc. Nevertheless, the scaffold for tissue engineering is found to be the less than ideal application, not only lack of the mechanical stiffness which is important for implantation but also lack of the interconnected pore that permits cells growth and penetration. The important purposes of tissue engineering scaffold are permit cell attachment and migration, delivery and retain cell and biochemical factor, enable diffusion of vital cell nutrient and product expression. Consequently, the production and creation a proper scaffold material is first priority. In crucial stage, the selection of suitable raw material is primary consideration.

Natural polymers have usually been studied in tissue engineering area because their properties are similar to natural extracellular matrix (ECM). It presents a unique complex structure

and may offer a diversity of capability application in tissue engineering field because their diverse properties, such as gelation ability, water adsorption capacity, pseudoplastic behavior and biodegradability. Moreover, they have many functional group accessible for chemical modification; reduction, oxidation, esterification and crosslinking reaction. The congenital characteristic of natural polymer is ability to be degraded by enzyme which indicates the leaning of this material to be metabolized by physiochemical mechanism. Another essential perspective for using natural polymer as scaffold, is that they induce unpleasing immune response because the presence of endotoxin and impurities.

Polysaccharide is popular natural polymer which frequently used as tissue engineering scaffold. Due to the difference in monosaccharide arrangement, molecular weight, chain form and linked type control their properties including the gelation potential, solubility, interfacial and surface properties[62].

### **1.5.1 Dextran for tissue engineering**

Dextran hydrogel are specifically interested as scaffold for soft tissue engineering because it has been expressed to resist cell adhesion [63-65] and protein adsorption [65] permit to create a scaffold without the specific site for cell recognition (it present in poly(ethylene glycol(PEG)). In previous study, the dextran have been regularly study as hydrogel for drug delivery [66] but not as scaffold for tissue engineering, since the pore size of dextran hydrogel was smaller than scaffold which suit for cell regeneration and penetration. Another important reason, hydrogel lack the mechanical property for supporting and cell growth promoting. Therefore, interconnectivity, pore size and porosity have been developed. Dextran hydrogel can be designed by either chemical or physical crosslinking through the hydroxyl group.

Levesque et al. prepared the macroporous interconnected pore dextran scaffold using radical liquid-liquid immiscibility of methacrylate dextran with polyethylene glycol (PEG) by controlling the methacrylate substitution degree to create microporous [67].

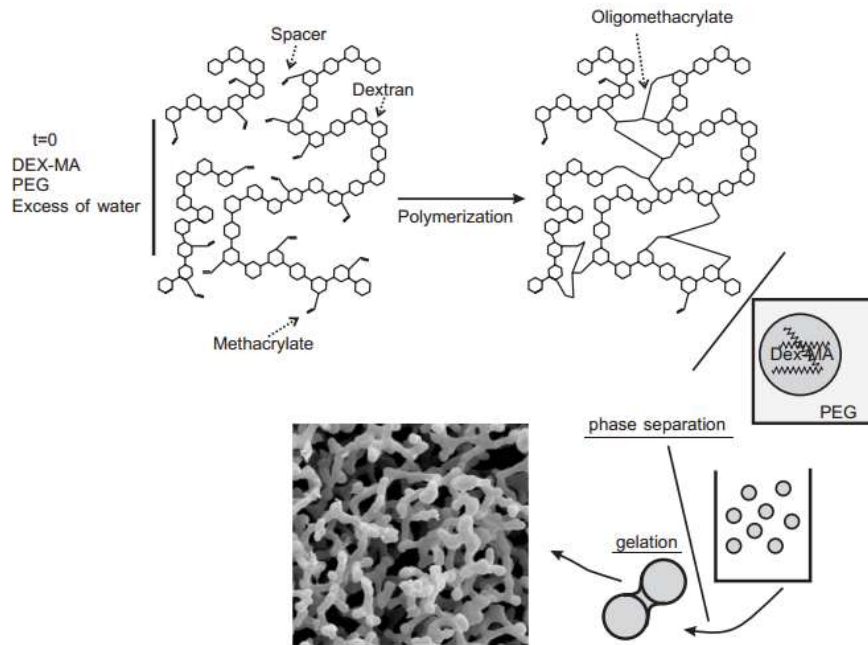


**Figure 1.10** Illustration of the formation of macroporous beaded dextran hydrogels of methacrylate dextran and polyethylene glycol (PEG)[67].

The hybrid hydrogel including of dextran tyramine grafted to hyaluronic acid as injectable hydrogel for cartilage tissue engineering via enzymatic crosslinking. The storage modulus of hydrogel was controlled by varying the concentration of polymer and tyramine degree substitution [68].  $\text{CO}_2$  water emulsion polymerization has been prepared for highly interconnected pore and thin wall porous dextran hydrogel. Potassium peroxydisulphate as the initiator cooperated with super critical  $\text{CO}_2$  water emulsion generated the interconnected porous in dextran hydrogel. The pore and adjacent pore can be controlled by increasing the  $\text{CO}_2$  volume fraction[69].

### 1.5.2 Cellulose for tissue engineering

Cellulose has the special character as the strong mechanical material. Due to  $\beta$  linked glucopyranose formation in cellulose, results to stabilize chain structure and minimize its adaptability. These unique property of chemical stability and mechanical property lead to insoluble polymer with little degradation in vivo [70]. The cellulose biodegradation is limited because of the deficiency of hydrolase enzyme which can attack the  $\beta$ 1,4 linkage in cellulose chain [71]. Together with complicated cellulose processing, it is greatest restrict factor for using cellulose in tissue engineering area. Nevertheless, the modification for partially degradation of sponge cellulose fabrication was reported [72]. Miyamoto et al. reported that cellulose and its derivatives can be changed to biocompatible materials by chemical or/and physical transformation [73]. The cellulose acetate (CA) scaffolds showed the promoting cardiac cell growth and increasing cell connectivity. The degradation of scaffold was controlled by de-acetylation of cellulose acetate, hydrolysis and cellulase enzyme [70]. Moreover, bacterial cellulose (BC) and modified BC showed as the new scaffold material for cartilage because its unique properties and biodegradability. Native BC and modified BC which modified with chemical sulfation and phosphorylation showed the high amount of chondrocyte cell growth [74]. BC is also available for tissue engineering blood vessel [75]. The fabrication of BC scaffold had been successfully produced with various method, most is porogen using. Bäckdahl et al. fabricated the BC tube using starch and paraffin wax as the porogen. Interconnectivity and pore size were controlled by varying the paraffin particle size [76]. Furthermore, Rambo et al. made BC membrane which controlled pore size of membrane by varying the pin template between 60-300  $\mu$ m [77].

## 1.6 Research objective

Although the oxidized dextran is various advantages in biomedical field as modified polymer and crosslinker in hydrogel, the mechanism and the controlling of degradation are not clear. If the mechanism of polysaccharide degradation can be explored, it will be expanded and applied it for biomedical application. Therefore, in this research, we attempt to reveal the polysaccharide degradation mechanism and the degradation controlling via oxidized dextran. Moreover, we also considered to cellulose because it is the most abundant polysaccharide in the world. However, the application of cellulose is limited because it is not soluble in water and other solvent and partially degraded. Hence, the procedure for increasing the cellulose degradation is required. Furthermore, cellulose can be fabricated as scaffold for tissue engineering with simple, easy and green method. This report, I will report the degradation of cellulose scaffold and the important role of cellulose scaffold for cell growth and cell attachment *in vitro* and *in vivo*.

## References

1. Qader, S.A.U., A. Aman, and A. Azhar, *Continuous Production of Dextran from Immobilized Cells of Leuconostoc mesenteroides KIBGE HAI Using Acrylamide as a Support*. Indian Journal of Microbiology, 2011. **51**(3): p. 279-282.
2. Hamdy, M.K., et al., *Factors Affecting the Degradation Processes for Dextran*. Ohio Journal of Science 1956. **56**(1): p. 41-51.
3. Rosenfeld, E.L. and I.S. Lukomskaya, *The splitting of dextran and isomaltose by animal tissues*. Clinica Chimica Acta, 1957. **2**(2): p. 105-114.
4. Sery, T.W. and E.J. Hehre, *Degradation of dextrans by enzymes of intestinal bacteria*. Journal of Bacteriology, 1956. **71**(3): p. 373-380.
5. Massia, S.P., J. Stark, and D.S. Letbetter, *Surface-immobilized dextran limits cell adhesion and spreading*. Biomaterials, 2000. **21**(22): p. 2253-2261.
6. Österberg, E., et al., *A collection of papers presented at the Symposium on Surface Modification-Principles and Applications (with special relevance to biotechnical problems) Comparison of polysaccharide and poly(ethylene glycol) coatings for reduction of protein adsorption on polystyrene surfaces*. Colloids and Surfaces A: Physicochemical and Engineering Aspects, 1993. **77**(2): p. 159-169.
7. Pacelli, S., P. Paolicelli, and M.A. Casadei, *New biodegradable dextran-based hydrogels for protein delivery: Synthesis and characterization*. Carbohydrate Polymers, 2015. **126**: p. 208-214.
8. Van Tomme, S.R. and W.E. Hennink, *Biodegradable dextran hydrogels for protein delivery applications*. Expert Review of Medical Devices, 2007. **4**(2): p. 147-164.
9. Varshosaz, J., *Dextran conjugates in drug delivery*. Expert Opinion on Drug Delivery, 2012. **9**(5): p. 509-523.

10. Bishop, C., *Vacuum Deposition onto Webs, Films, and Foils*. 2007: Elsevier Science. 495.
11. Ogston, A.G. and E.F. Woods, *Molecular Configuration of Dextran in Aqueous Solution*. *Nature*, 1953. **171**(4344): p. 221-222.
12. Hamdy, M.K., et al., *Factors affecting the degradation processes for dextran*. *Ohio Journal of Science*, 1956. **56**(1): p. 41-51.
13. Lee, J.M. and P.F. Fox, *Purification and characterization of Paecilomyces lilacinus dextranase*. *Enzyme and Microbial Technology*, 1985. **7**(11): p. 573-577.
14. Chalet, L., et al., *Isolation of a Pure Dextranase from Penicillium funiculosum*. *Applied Microbiology*, 1970. **20**(3): p. 421-426.
15. Franssen, O., R.J.H. Stenekes, and W.E. Hennink, *Controlled release of a model protein from enzymatically degrading dextran microspheres*. *Journal of Controlled Release*, 1999. **59**(2): p. 219-228.
16. Franssen, O., O.P. Vos, and W.E. Hennink, *Delayed release of a model protein from enzymatically-degrading dextran hydrogels*. *Journal of Controlled Release*, 1997. **44**(2-3): p. 237-245.
17. Cote, G.L. and J.L. Willet, *Thermomechanical depolymerization of dextran*. *Carbohydrate Polymers*, 1999. **39**(2): p. 119-126.
18. Zou, Q., et al., *Ultrasonic degradation of aqueous dextran: Effect of initial molecular weight and concentration*. *Carbohydrate Polymers*, 2012. **90**(1): p. 447-451.
19. Jeanes, A. and C.A. Wilham, *Periodate Oxidation of Dextran*. *Journal of the American Chemical Society*, 1950. **72**(6): p. 2655-2657.

20. Rankin, J.C. and A. Jeanes, *Evaluation of the Periodate Oxidation Method for Structural Analysis of Dextran*. Journal of the American Chemical Society, 1954. **76**(17): p. 4435-4441.
21. Sloan, J.W., et al., *Determination of Dextran Structure by Periodate Oxidation Techniques*. Journal of the American Chemical Society, 1954. **76**(17): p. 4429-4434.
22. Mirgorodskaya, O.A. and L.V. Poletaeva, *Periodate oxidation of dextrans*. Pharmaceutical Chemistry Journal, 1985. **19**(5): p. 347-351.
23. Rinaudo, M., *Periodate Oxidation of Methylcellulose: Characterization and Properties of Oxidized Derivatives*. Polymers, 2010. **2**: p. 505-521.
24. Maia, J., et al., *Insight on the periodate oxidation of dextran and its structural vicissitudes*. Polymer, 2011. **52**(2): p. 258-265.
25. Maia, J., et al., *Ocular injectable formulation assessment for oxidized dextran-based hydrogels*. Acta Biomaterialia, 2009. **5**(6): p. 1948-1955.
26. Lin, W., et al., *Preparation of sterically stabilized human serum albumin nanospheres using a novel Dextranox-MPEG crosslinking agent*. Pharm Res, 1994. **11**(11): p. 1588-92.
27. Bogdanov, B., E. Schacht, and A. Van Den Bulcke, *Thermal and rheological properties of gelatin-dextran hydrogels*. Journal of thermal analysis, 1997. **49**(2): p. 847-856.
28. Draye, J.-P., et al., *In vitro release characteristics of bioactive molecules from dextran dialdehyde cross-linked gelatin hydrogel films*. Biomaterials, 1998. **19**(1-3): p. 99-107.
29. Battersby, J., et al., *Sustained release of recombinant human growth hormone from dextran via hydrolysis of an imine bond*. Journal of Controlled Release, 1996. **42**(2): p. 143-156.
30. Behe, M., et al., *Biodistribution, blood half-life, and receptor binding of a somatostatin-dextran conjugate*. Medical Oncology, 2001. **18**(1): p. 59-64.

31. Yuan, X.-B., et al., *Self-aggregated nanoparticles composed of periodate-oxidized dextran and cholic acid: preparation, stabilization and in-vitro drug release*. Journal of Chemical Technology & Biotechnology, 2006. **81**(5): p. 746-754.
32. Cortesi, R., et al., *Dextran cross-linked gelatin microspheres as a drug delivery system*. European Journal of Pharmaceutics and Biopharmaceutics, 1999. **47**(2): p. 153-160.
33. Koshijima, T., et al., *Chelating polymers derived from cellulose and chitin*. Cellulose Chemistry and Technology, 1973. **7**: p. 197–208.
34. Liu, X.D., et al., *Chitosan coated cotton fiber: preparation and physical properties*. Carbohydrate Polymers, 2001. **44**(3): p. 233-238.
35. Boeden, H.F., et al., *Bead cellulose derivatives as supports for immobilization and chromatographic purification of proteins*. J Chromatogr, 1991. **552**(1-2): p. 389-414.
36. Kim, U.-J. and S. Kuga, *Ion-exchange chromatography by dicarboxyl cellulose gel*. Journal of Chromatography A, 2001. **919**(1): p. 29-37.
37. Kim, U.-J. and S. Kuga, *Ion-exchange separation of proteins by polyallylamine-grafted cellulose gel*. Journal of Chromatography A, 2002. **955**(2): p. 191-196.
38. Bhattacharyya, D., et al., *Novel poly-glutamic acid functionalized microfiltration membranes for sorption of heavy metals at high capacity*. Journal of Membrane Science, 1998. **141**(1): p. 121-135.
39. Li, J., et al., *Preparation and characterization of 2,3-dialdehyde bacterial cellulose for potential biodegradable tissue engineering scaffolds*. Materials Science and Engineering: C, 2009. **29**(5): p. 1635-1642.

40. Singh, M., et al., *Potential Biosoluble Carriers: Biocompatibility and Biodegradability of Oxidized Cellulose*. Biomaterials, Medical Devices, and Artificial Organs, 1979. **7**(4): p. 495-512.
41. Verma, V., et al., *2, 3-Dihydrazone cellulose: Prospective material for tissue engineering scaffolds*. Materials Science and Engineering: C, 2008. **28**(8): p. 1441-1447.
42. Kim, U.-J., M. Wada, and S. Kuga, *Solubilization of dialdehyde cellulose by hot water*. Carbohydrate Polymers, 2004. **56**(1): p. 7-10.
43. Varma, A.J. and V.B. Chavan, *A study of crystallinity changes in oxidised celluloses*. Polymer Degradation and Stability, 1995. **49**(2): p. 245-250.
44. Moe, O.A., S.E. Miller, and M.H. Iwen, *Investigation of the Reserve Carbohydrates of Leguminous Seeds. I. Periodate Oxidation I*. Journal of the American Chemical Society, 1947. **69**(11): p. 2621-2625.
45. Bulpitt, P. and D. Aeschlimann, *New strategy for chemical modification of hyaluronic acid: Preparation of functionalized derivatives and their use in the formation of novel biocompatible hydrogels*. Journal of Biomedical Materials Research, 1999. **47**(2): p. 152-169.
46. Tabata, Y. and Y. Ikada, *Synthesis of gelatin microspheres containing interferon*. Pharm Res, 1989. **6**(5): p. 422-7.
47. Yamamoto, M., et al., *Bone regeneration by transforming growth factor  $\beta$ 1 released from a biodegradable hydrogel*. Journal of Controlled Release, 2000. **64**(1-3): p. 133-142.
48. Willmott, N., et al., *Adriamycin-loaded albumin microspheres: preparation, in vivo distribution and release in the rat*. Biopharm Drug Dispos, 1985. **6**(1): p. 91-104.

49. Jameela, S.R. and A. Jayakrishnan, *Glutaraldehyde cross-linked chitosan microspheres as a long acting biodegradable drug delivery vehicle: studies on the in vitro release of mitoxantrone and in vivo degradation of microspheres in rat muscle*. *Biomaterials*, 1995. **16**(10): p. 769-75.
50. Hiemstra, C., et al., *Rapidly in Situ-Forming Degradable Hydrogels from Dextran Thiols through Michael Addition*. *Biomacromolecules*, 2007. **8**(5): p. 1548-1556.
51. Hyon, S.-H., et al., *Low cytotoxic tissue adhesive based on oxidized dextran and epsilon-poly-l-lysine*. *Journal of Biomedical Materials Research Part A*, 2014. **102**(8): p. 2511-2520.
52. Matsumura, K., et al., *Self-degradation of tissue adhesive based on oxidized dextran and poly-l-lysine*. *Carbohydrate Polymers*, 2014. **113**: p. 32-38.
53. Hodge, J.E., *Dehydrated Foods, Chemistry of Browning Reactions in Model Systems*. *Journal of Agricultural and Food Chemistry*, 1953. **1**(15): p. 928-943.
54. Kessler, M.W. and D.A. Grande, *Tissue engineering and cartilage*. *Organogenesis*, 2008. **4**(1): p. 28-32.
55. Hutmacher, D.W., *Scaffolds in tissue engineering bone and cartilage*. *Biomaterials*, 2000. **21**(24): p. 2529-2543.
56. Stevens, M.M., *Biomaterials for bone tissue engineering*. *Materials Today*, 2008. **11**(5): p. 18-25.
57. Caoa, Y., et al. *Tissue Engineering of Tendon*. in *MRS Proceedings*. 1995.
58. Cooper, M.L., et al., *In vivo optimization of a living dermal substitute employing cultured human fibroblasts on a biodegradable polyglycolic acid or polyglactin mesh*. *Biomaterials*, 1991. **12**(2): p. 243-8.

59. Watanabe, M., et al., *Artificial esophagus with peristaltic movement*. *Asaio j*, 2005. **51**(2): p. 158-61.
60. Cima, L.G., et al., *Tissue engineering by cell transplantation using degradable polymer substrates*. *J Biomech Eng*, 1991. **113**(2): p. 143-51.
61. Evans, G.R.D., et al., *In vivo evaluation of poly(l-lactic acid) porous conduits for peripheral nerve regeneration*. *Biomaterials*, 1999. **20**(12): p. 1109-1115.
62. Izydorczyk, M. and S.W. Cui, *Polysaccharide gums: structures, functional properties, and applications*. 2005: CRC Press Taylor & Francis Group. 263-307.
63. Massia, S.P. and J. Stark, *Immobilized RGD peptides on surface-grafted dextran promote biospecific cell attachment*. *J Biomed Mater Res*, 2001. **56**(3): p. 390-9.
64. McArthur, S.L., et al., *Effect of polysaccharide structure on protein adsorption*. *Colloids and Surfaces B: Biointerfaces*, 2000. **17**(1): p. 37-48.
65. McLean, K.M., et al., *Method of immobilization of carboxymethyl-dextran affects resistance to tissue and cell colonization*. *Colloids Surf B Biointerfaces*, 2000. **18**(3-4): p. 221-234.
66. Hovgaard, L. and H. Brøndsted, *Dextran hydrogels for colon-specific drug delivery*. *Journal of Controlled Release*, 1995. **36**(1-2): p. 159-166.
67. Levesque, S.G., R.M. Lim, and M.S. Shoichet, *Macroporous interconnected dextran scaffolds of controlled porosity for tissue-engineering applications*. *Biomaterials*, 2005. **26**(35): p. 7436-46.
68. Jin, R., et al., *Enzymatically-crosslinked injectable hydrogels based on biomimetic dextran-hyaluronic acid conjugates for cartilage tissue engineering*. *Biomaterials*, 2010. **31**(11): p. 3103-3113.

69. Partap, S., et al., *Supercritical Carbon Dioxide in Water” Emulsion-Templated Synthesis of Porous Calcium Alginate Hydrogels*. *Advanced Material*, 2006. **18**: p. 501–504.
70. Entcheva, E., et al., *Functional cardiac cell constructs on cellulose-based scaffolding*. *Biomaterials*, 2004. **25**(26): p. 5753-62.
71. Beguin, P. and J.P. Aubert, *The biological degradation of cellulose*. *FEMS Microbiol Rev*, 1994. **13**(1): p. 25-58.
72. Martson, M., et al., *Is cellulose sponge degradable or stable as implantation material? An in vivo subcutaneous study in the rat*. *Biomaterials*, 1999. **20**(21): p. 1989-95.
73. Miyamoto, T., et al., *Tissue biocompatibility of cellulose and its derivatives*. *Journal of Biomedical Materials Research*, 1989. **23**(1): p. 125-133.
74. Svensson, A., et al., *Bacterial cellulose as a potential scaffold for tissue engineering of cartilage*. *Biomaterials*, 2005. **26**(4): p. 419-31.
75. Bäckdahl, H., et al., *Mechanical properties of bacterial cellulose and interactions with smooth muscle cells*. *Biomaterials*, 2006. **27**(9): p. 2141-2149.
76. Bäckdahl, H., B. Risberg, and P. Gatenholm, *Observations on bacterial cellulose tube formation and ways to introduce microporosity*. 2008, Chalmers University of Technology: Göteborg, Sweden.
77. Rambo, C.R., et al., *Template assisted synthesis of porous nanofibrous cellulose membranes for tissue engineering*. *Materials Science and Engineering: C*, 2008. **28**(4): p. 549-554.

# Chapter 2

---

## *Dextran degradation by Malaprade reaction*

### **2.1 Introduction**

#### **2.1.1 Dialdehyde polysaccharide**

Dialdehyde polysaccharide is popular oxidative method for introduce aldehyde which usually used for treatment polysaccharide in industries, such as gum cellulose and starch because it is success for using as crosslinking derivative. Moreover, dialdehyde polysaccharide in industrial application are important role for paper industry as wet strength improver [1]. Dialdehyde polysaccharide via Malaprade oxidation is cleaved between C<sub>2</sub>-C<sub>3</sub> bonds in glucopyranose ring of polysaccharide chain. The hydroxyls on side chain or ring are oxidized to form aldehyde group. Consequently, cleaved pyranose ring is named dialdehyde derivative which are intra and inter hemiacetal and hydrated hemiacetal (see 2.1.2).

However, dialdehyde polysaccharide is overlooked as the component in foodstuff because it convince polypeptide chains to crosslink with globulins [2]. However, dialdehyde is still attracted in food industry because it can be the biodegradable plastic as packaging and raping. As 1.3.1.3, it mention about the benefit of oxidized dextran in biomedical application. Even though, oxidized polysaccharide is approached in varieties application. The mechanism of dialdehyde

polysaccharide is unclear. Therefore, in this chapter we will explain the related reaction and related product for dialdehyde polysaccharide.

### 2.1.2 Hemiacetal formation

The hemiacetal formation can divide into two partway, first is natural pathway. The aldehyde is attached with alcohol and underwent to hemiacetal (**Figure 2.1a**). Another pathway, it is fast reaction due to the presence of acid (**Figure 2.1b**). This reaction is continued by attacking the hemiacetal by another alcohol underwent to acetal. Acetal and hemiacetal are significant functional groups because it naturally present in sugars.

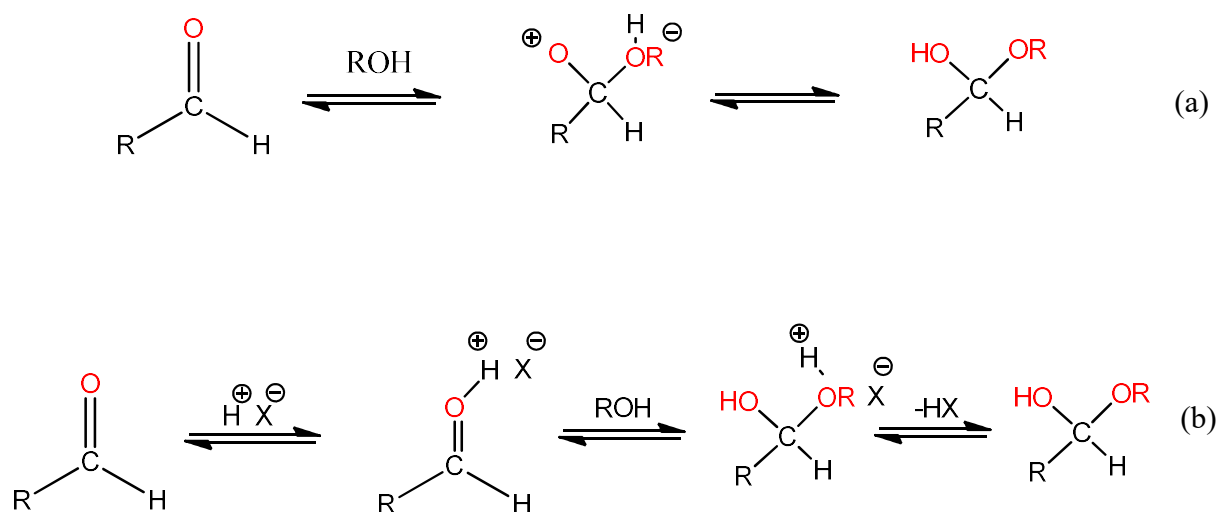


**Figure 2.1** Hemiacetal formation

The above reaction is easily reversible. Hemiacetal can easily convert to aldehyde and alcohol is released (**Figure 2.2**).

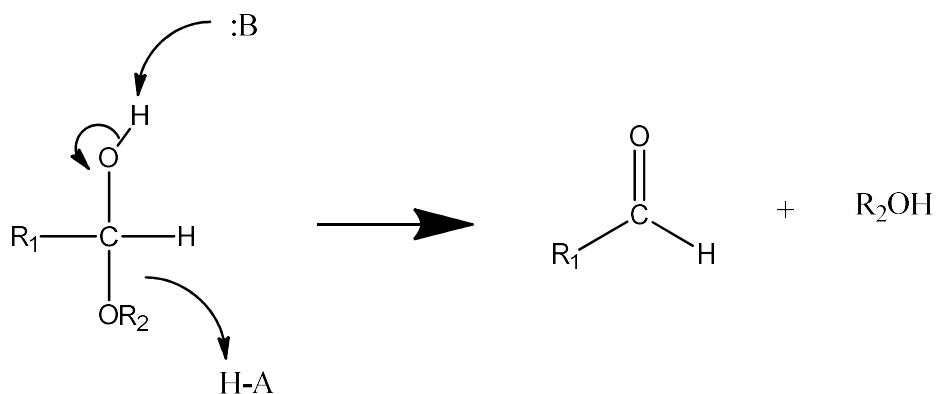


**Figure 2.2** The reversible reaction of hemiacetal.

When hemiacetal in aqueous solution, aldehyde group can be hydrate aldehyde. This reaction is easy by adding water to carbonyl group (**Figure 2.3**).

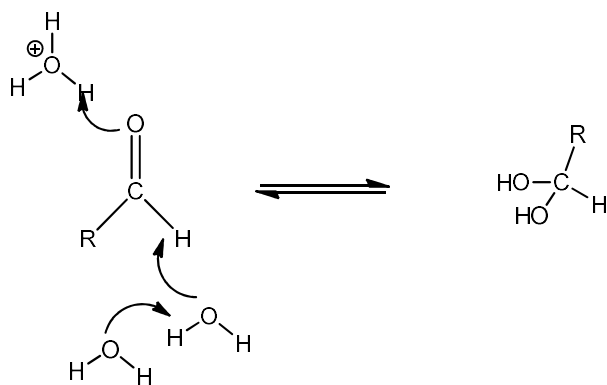


**Figure 2.3** Hydrate aldehyde formation.

The reaction of hemiacetal is main carbohydrate chemistry. Due to polysaccharide chain is compose of monosaccharide, such as glucose. As sugar molecule, it have multiple of hydroxyl

group and reducing end. In aqueous solution, straight chain of glucose rapidly converts to cyclic form resulting in hemiacetal formation. The sugar cyclization reaction is spontaneously occurred and reversed without enzyme (**Figure 2.4**).

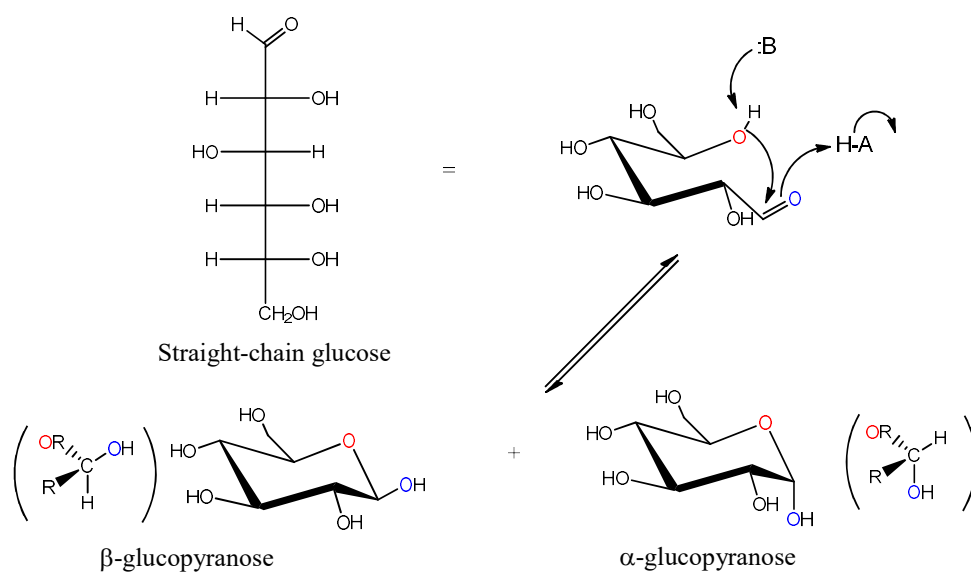


**Figure 2. 4** Hemiacetal formation from straight chain glucose.

### 2.1.3 Maillard reaction

Maillard reaction is reaction between reducing sugars and amino acid (**Figure 2.5**) and resulting in desirable flavor and browned food.

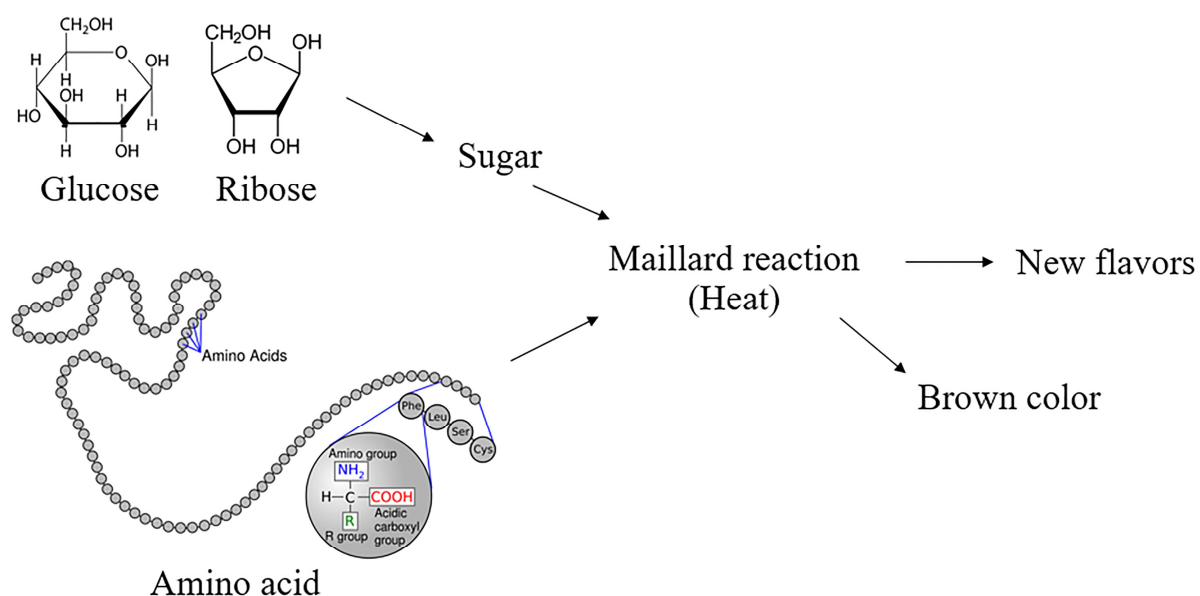


Figure 2.5 Simple Maillard reaction.

It is composed of seven stage (Figure 2.6). Stage one, aldose is attached by amino compound for glycosylamine formation (A). Subsequently, Amadori compound is formed and rearranged (B). The intermediate stage is dehydrated and undergo to Schiff base (C) and reductone and Fission product (D) formation. Accordingly, the pathway is separated into two way; aldehyde formation via Strecker degradation (E) and aldose formation (F). The final stage comprise of the conversion of carbonyl compound (F).

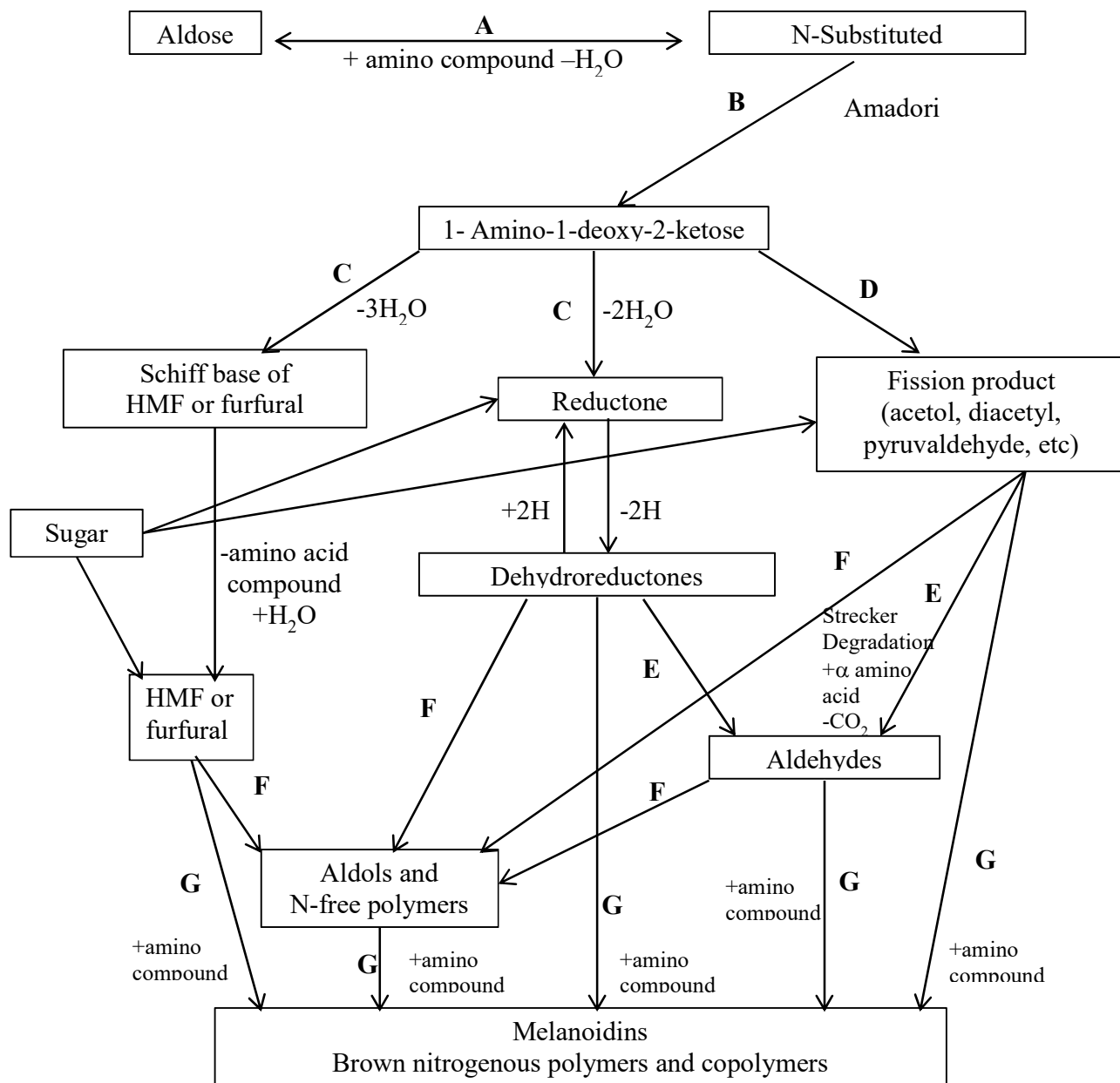
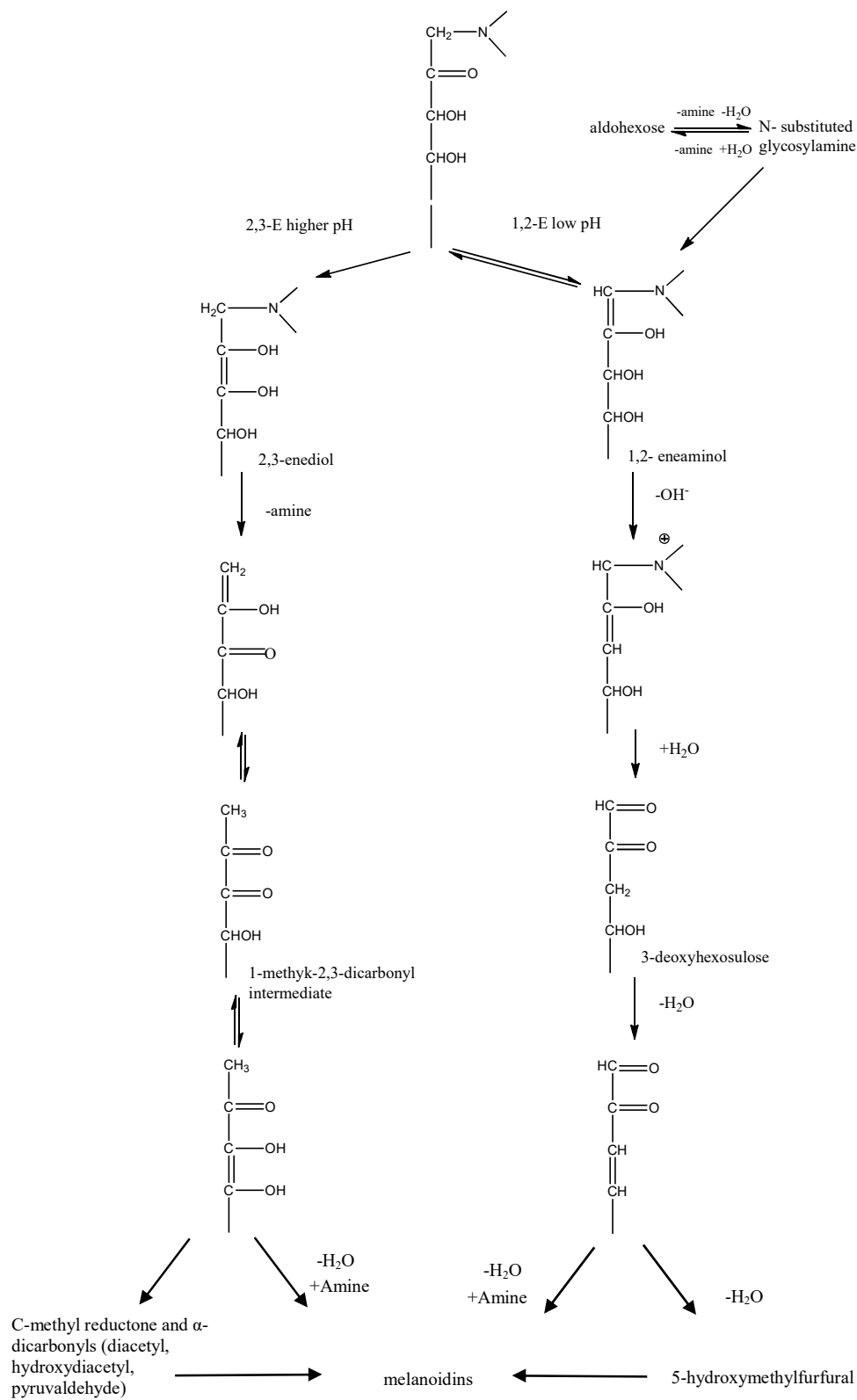


Figure 2.6 Non enzymatic browning reaction [3].

2.1.4 Mechanism of formation in Maillard reaction



**Figure 2.7** Maillard reaction : two major pathway from Amadori compound to melanioidins [3].

Amadori product is intermediated form in Maillard reaction. At difference pH, Amadori product are degraded to 1-, 3- and 4- deoxydicarbonyl compound (deoxyosone). At pH >7, it is purposed to be the pathway to flavor formation. Moreover, redox mechanism have been recognized, there are  $\alpha$ -dicarbonyl,  $\alpha$ -hydroxy carbonyls and formic acid. Formic and acetic acid are important degradation product of fructose, glucose [4] and lactose [5] in Maillard reaction. In this pathway, 2,3 enaminol as Amadori product can convert to 1-dexyhexosulose and 4-dexyhexosulose (deoxyosone) by amine elimination. At pH < 7, it is main line for Strecker degradation. 1,2-Enaminol via Amadori product can convert to 3-dexyhexosulose by amine elimination. The final product is formic acid which is main degradation (**Figure 2.7**).

### **2.1.5 Strecker degradation**

During the Maillard reaction, Strecker degradation is important reaction, in which amino acids are undergone degradation processes (decarboxylation and oxidative deamination) in the appearance of a dicarbonyls compound formed by Maillard reaction. The Strecker degradation undergo the aldehydes formation and aminoketone. The H<sub>2</sub>S, NH<sub>3</sub> are important intermediate products which are formed by Strecker degradation. The intermediate products can react with other compounds to produce high and low molecular weight end flavor compounds.

### **2.1.6 Melanoidin**

Melanoidin is a high molecular weight colored compounds which usually present in brown food, due to the interaction between amine group and carbohydrates. The structure of melanoidin is not certainly known, it have been usually defined as high molecular weight nitrogen-containing brown polymers.

## **2.2. Materials and method**

Dextran with molecular weight of 70 kDa was obtained from Meito Sangyo Co., Ltd. (Nagoya Japan). Sodium periodate, di-sodium hydrogen phosphate, sodium di-hydrogen phosphate, glycine, starch soluble were obtained from Nacalai Tesque, Inc., (Kyoto, Japan).

### **2.2.1 Dextran oxidation**

Aldehyde dextran was prepared by the oxidation of dextran with sodium periodate according to the method reported by Mo et al [6]. Briefly, 5 g of dextran was dissolved in 20 mL of distilled water, and different amount of sodium periodate (0-2.5 g) were dissolved in 10 mL of water. Both solutions were combined together. Then, the reaction proceeded at 50 °C for 1 h under gentle stirring. The reaction mixture was dialyzed using cellulose membrane (cut off molecular weight of 14,000, Viskase Companies, Inc., IL, USA) against distilled water for 16 h. Aldehyde dextran was recovered by air-drying for 48 h at 40 °C.

### **2.2.2 Aldehyde content determination**

The aldehydes introduced in dextran were evaluated by simple iodometry. Briefly, 10 mL of approximately 1 w/v% aqueous aldehyde dextran solution was added to 20 mL of I<sub>2</sub> solution (0.05 mol/L), followed by addition of 20 mL of NaOH (1 mol/L). The oxidation reaction proceeded for 15 minutes. After the addition of 15 mL of H<sub>2</sub>SO<sub>4</sub> (6.25 v/v%), the I<sub>2</sub> consumption by the reaction with aldehyde was titrated with 0.1 mol/L of Na<sub>2</sub>S<sub>2</sub>O<sub>3</sub> using a drop of aqueous 20 w/w% of starch solution as an indicator, where one mole of aldehyde group reacts with one mole of I<sub>2</sub> in alkaline condition, leading to the formation of carboxyl acid, and one mole of I<sub>2</sub> reacts with 2 moles of S<sub>2</sub>O<sub>3</sub><sup>2-</sup> ion. Triplicate readings were taken for each titration (n=3).

### **2.2.3 Molecular weight determination by GPC**

The oxidized dextran with 0–25% (w/w) NaIO<sub>4</sub> solution was dissolved in distilled water to give a final concentration of 20% (w/w). Then, the same volume of 10, 20, and 30% (w/w) glycine solution was added to the mixture. The molecular weight of oxidized dextran after addition of the glycine solution was determined by GPC (column, BioSep-s2000, Phenomenex, Inc., CA, USA) and was measured on a Shimadzu high-performance liquid chromatography data system using a refractive index detector. Phosphate buffer solution (pH 7.4, 0.1 M) was used as the mobile phase (flow rate = 1 mL/min) and pullulan was used as the standard. 10-μL aliquots of the sample solutions were taken out every 20 min for determination of molecular weight for 120 min.

#### **2.2.4 NMR spectroscopy**

All NMR data were recorded on Varian INOVA 600 MHz spectrometer at 25 °C for assignment of A-dex or at 37 °C for kinetic analysis of the degradation of A-dex reacted with glycine. <sup>1</sup>H-<sup>13</sup>C HSQC, 2D HSQC-TOCSY, <sup>1</sup>H-<sup>13</sup>C HMBC, TOCSY, and DQF-COSY were used for assignment of A-dex. For kinetic analysis experiments, the 20 % (w/w) a-dex in D<sub>2</sub>O solution and 10% (w/w) glycine in D<sub>2</sub>O solution were mixed with 1:1 on ice bath to delay the degradation i.e., final concentration was 10% a-dex and 5% glycine in D<sub>2</sub>O. The mixed solution was quickly set in NMR magnet, and then the temperature was raised. The first <sup>1</sup>H NMR spectrum was recorded after 12 min from raising temperature at 37 °C. The NMR spectra with presaturation were recorded every 5 min.

### **2.3 Results and discussion**

#### **2.3.1 Oxidation of dextran with periodate**

The aldehyde contents in periodate-oxidized dextran by was determined by iodimetry and the results are shown in **Figure. 2.8**. The degree of oxidation was evaluated as percentage oxidation per glucose unit, defined as number of C–C bonds cleaved in 1,2-diol in each glucose unit. From Fig.1, we successfully controlled the oxidation of dextran up to 40.3% by changing the concentration of NaIO<sub>4</sub>. In this report, oxidized dextran was denoted as x%OxDex with x% oxidation like 21.2%OxDex, 40.3%OxDex.

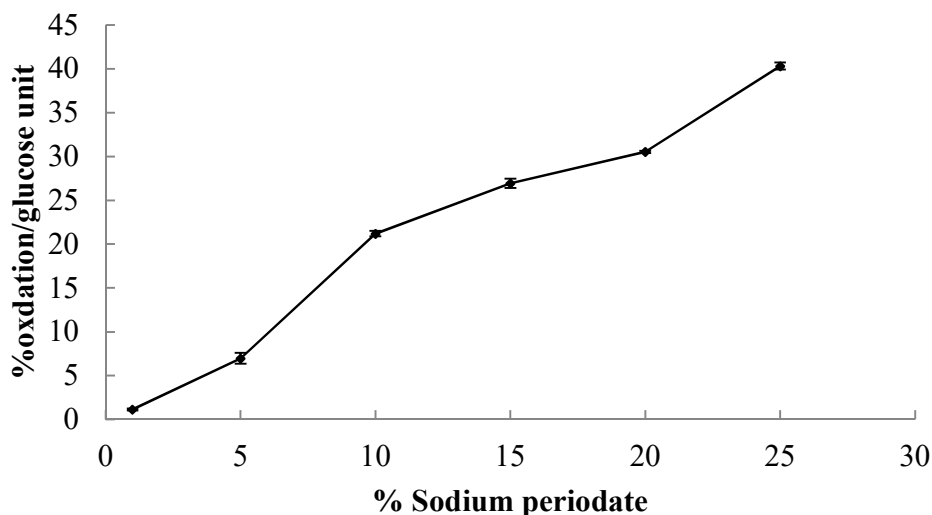


**Figure 2.7** Effect of periodate concentration on dextran oxidation

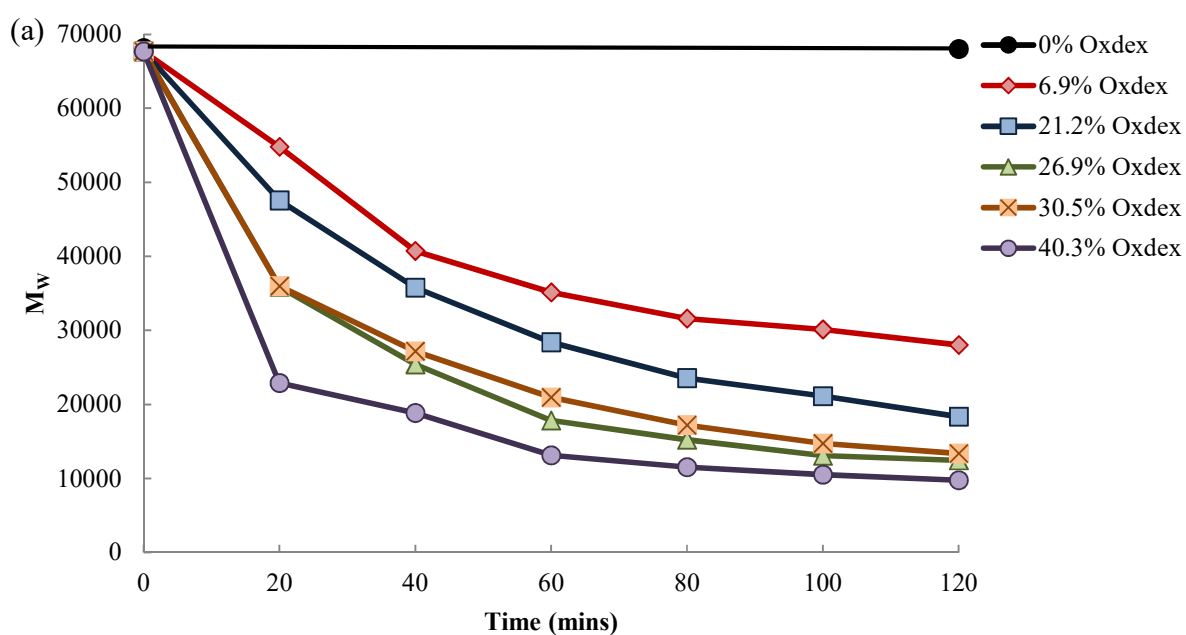
### 2.3.2 Molecular weight determination

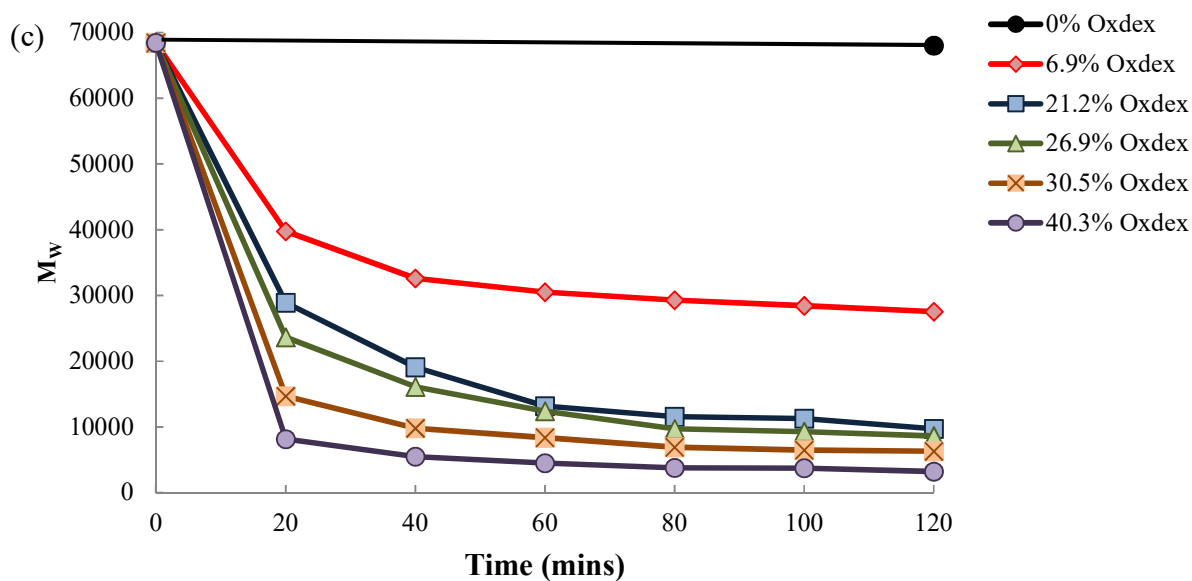
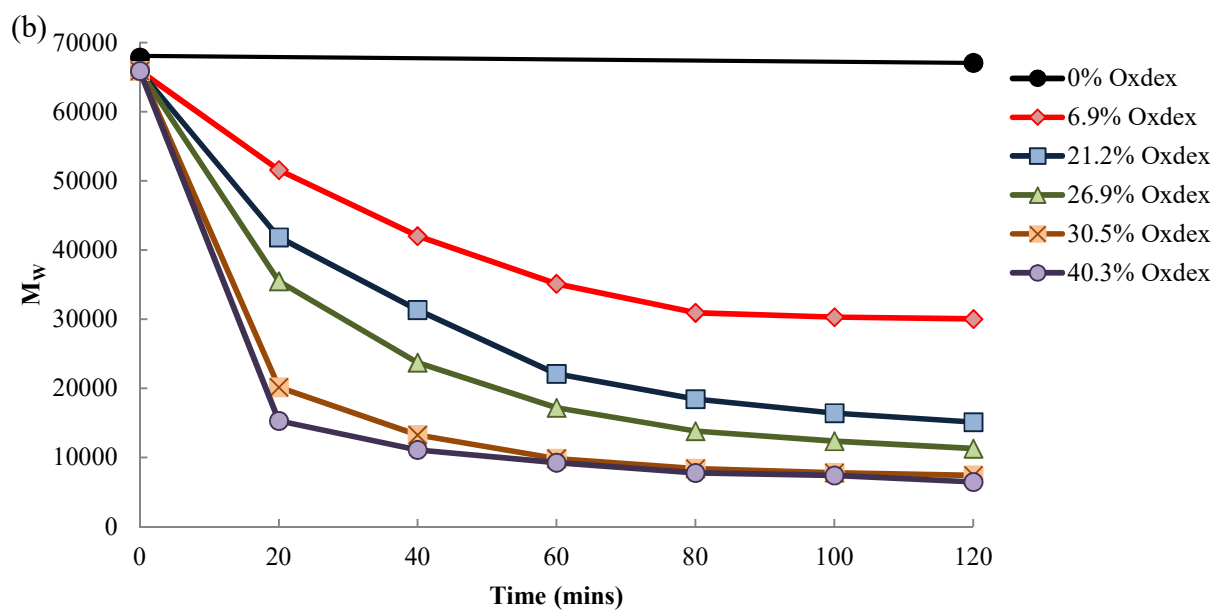
In a previous study, hydrogel formed by mixing oxidized dextran and  $\epsilon$ -PL showed degradation in phosphate-buffered saline (PBS).[7] In this report, we used glycine as the monoamine source to react with aldehyde in oxidized dextran. The molecular weights ( $M_w$ ) of various oxidized dextran samples with various aldehyde amounts after reaction with glycine solutions with various concentrations were recorded with GPC for 2 h. **Figure 2.9** (a)–(c) shows the weight-average  $M_w$  change under various concentration of glycine. The  $M_w$  of unoxidized dextran used in this study provided by the supplier was 70,000. Each figure shows almost similar  $M_w$  values before addition of glycine, which indicated that Malaprade oxidation itself did not degrade the dextran chain. It is reasonable that unoxidized dextran (0%OxDex) did not degrade in glycine solution. However, molecular weight of oxidized dextran gradually decreased in glycine

solution. Molecular weight reduction strongly depended on oxidation ratio (**Figure 2.9**) and glycine concentration (**Figure 2.10**). **Figure 2.9a** shows the effect of the oxidation degree of oxidized dextran on molecular weight reduction in 5% glycine. In the first 20 min, fast decreasing of molecular weight was observed. **Figure 2.9 a, b, and c** show that the concentration of glycine solution influenced the initial decrease of  $M_w$  in each oxidized dextran sample, e.g., at 20 min, 21.2%OxDex showed 20%  $M_w$  decrease in 5% glycine, while more than 40% decrease in  $M_w$  was observed in 15% glycine. Interestingly,  $M_w$  reduction saturated after ~60, 40, and 20 min in 5, 10, and 15% glycine, respectively, and dextran with lower oxidation degree showed saturation at higher  $M_w$ . These results suggested that degradation of oxidized dextran might be triggered by the reaction between the amino group in glycine and the aldehyde groups in dextran and the number of degradable points were decided by degree of oxidation.

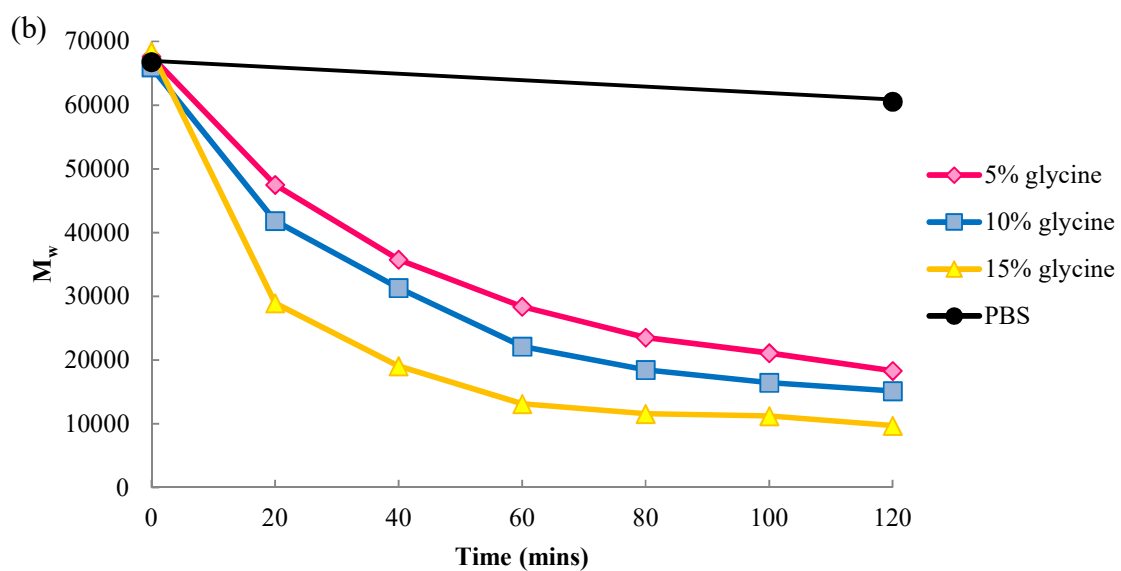
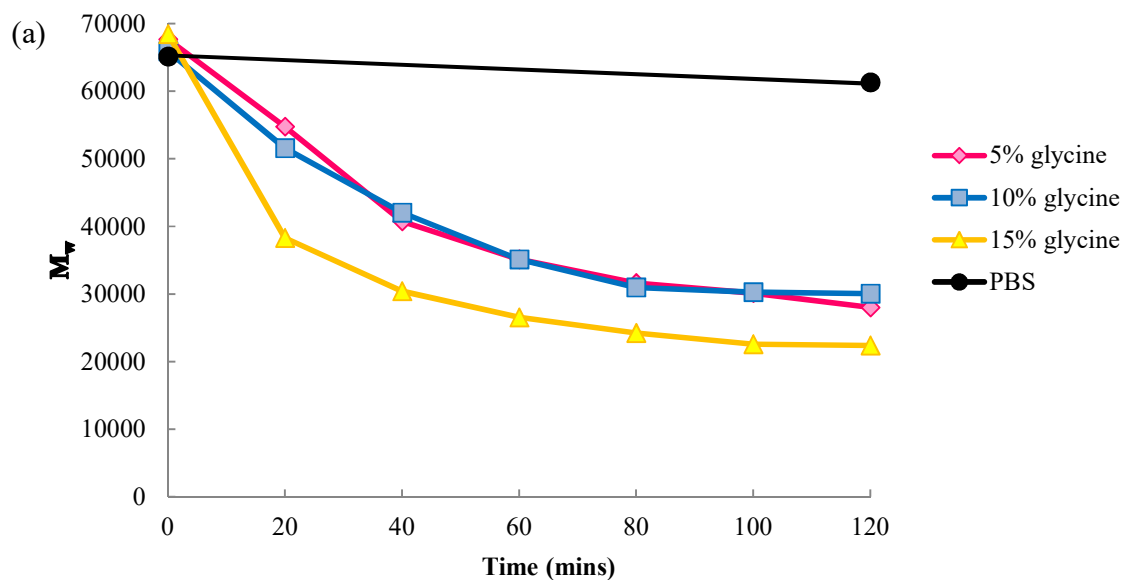
In addition, the effect of glycine concentration to each oxidized dextran sample was observed (**Figure 2.10**). **Figure 2.10** shows the molecular weight reductions of 6.9%OxDex when reacted with 5%, 10%, and 15% (w/w) glycine. The  $M_w$  reduction rate of 6.9%OxDex in 5% glycine before 20 min was quite moderate, and after 60 min it was constant. Meanwhile, the molecular weight reduction rate was high consistent with the concentration of glycine. Similar patterns were observed for 21.2%, 26.9%, 30.5% and 40.3%OxDex (**Figures 2.10b, 2.10c, 2.10d, and 3e**, respectively), while the molecular weights of none of the oxidized dextran samples were decreased in PBS. Dextran with highest oxidation ratio (40.3%OxDex) showed fastest reduction and reached the lowest  $M_w$ . The results obviously indicate that  $M_w$  is reduced through the reaction between aldehyde and amino groups. This reaction has already been confirmed in a previous report on hydrogel formation through multiple Schiff base formations [8].

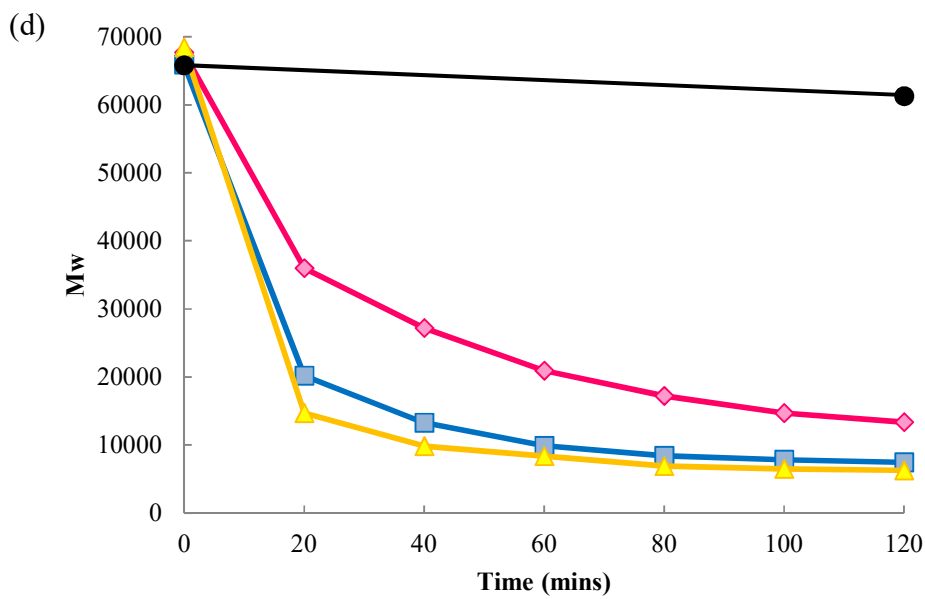
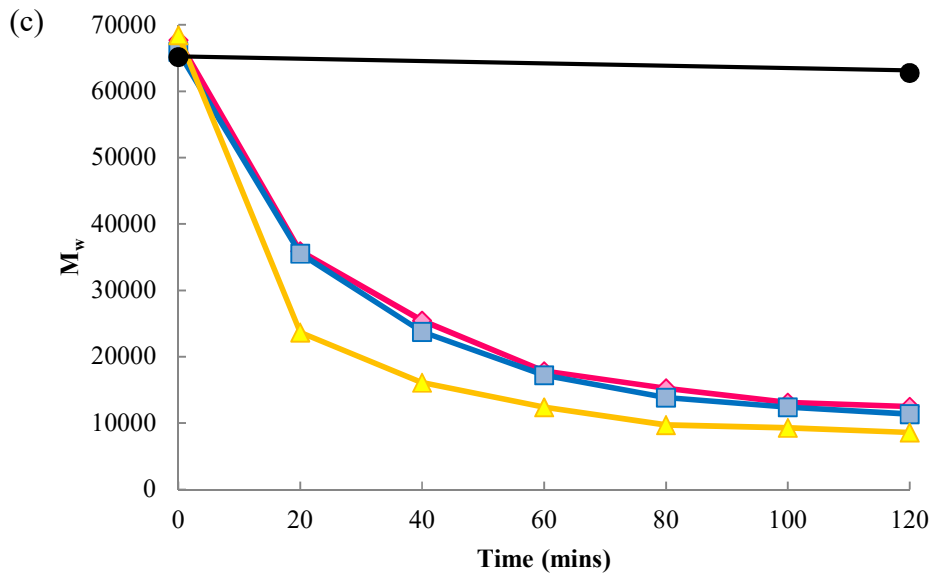
To investigate the nature of the reaction that occurred after Schiff base formation, time-dependent NMR signals were collected from the mixture of 21.2%OxDex with 10% glycine.





**Figure 2.8** The molecular weight determination of 0-40% oxidized dextran in 5%, 10% , 15% glycine respectively (2a, 2b, 2c) by GPC.





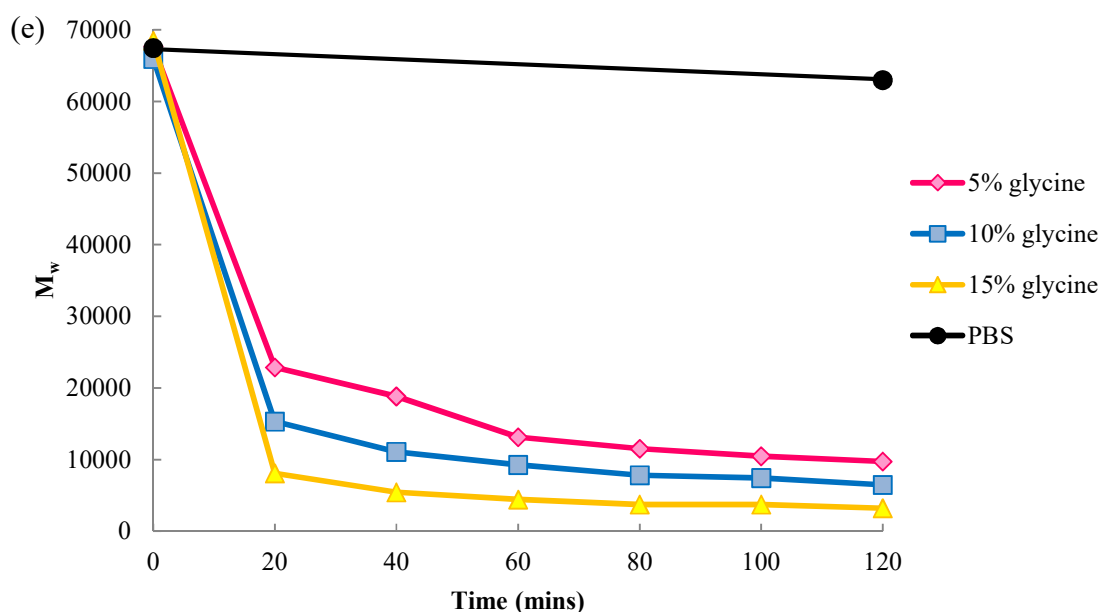


**Figure 2.9** The molecular weight determination of 6.9%, 21.2%, 26.9%, 30.5%, 40.3% oxidized dextran (a, b, c, d, e) submerged with difference glycine concentration by GPC.

### 2.3.3 NMR analysis

Although two aldehyde groups were produced by periodate oxidation of the diols of saccharides, signals from aldehyde were not observed in the  $^1\text{H}$  NMR spectrum of 21.2%OxDex, in contrast to the aldehyde content determined by iodimetry. This contradiction is explained by previous reports [9-12]. The produced aldehyde groups were reacted with hydroxyl groups to form hemiacetal structures. More than four hemiacetal substructures were observed in our oxidized dextran, including non-oxidized glucose (**Figure 2.11**). Sodium periodate putatively oxidized and cleaved only  $\text{C}_2\text{-C}_3$  and  $\text{C}_3\text{-C}_4$  bonds in the glucose moiety of dextran. When both bonds were cleaved,  $\text{C}_3$  was removed, and  $\text{C}_2$  and  $\text{C}_4$  were converted into aldehydic carbons. Thus two

aldehyde groups and a water molecule were converted to a hemiacetal structure (substructure 2, **Figure 2.11**). For C<sub>2</sub>–C<sub>3</sub> bond cleavage, oxidized glucose was converted into a hemiacetal structure (substructure 3, Scheme1). , Hemiacetal structure (substructure 4, **Figure 2.11**) was also obtained for C<sub>3</sub>–C<sub>4</sub> bond cleavage. Although other structures were found in the NMR spectra with abundance ratio comparable to substructures 2, 3, and 4, the respective structures were unknown. Assignments of these substructures were conducted with <sup>1</sup>H-<sup>13</sup>C HSQC, 2D HSQC-TOCSY, <sup>1</sup>H-<sup>13</sup>C HMBC, TOCSY, and DQF-COSY in <sup>13</sup>C- and <sup>1</sup>H-NMR. <sup>1</sup>H-<sup>13</sup>C HSQC NMR spectrum of freshly prepared 21.2%OxDex is shown in **Figure 2.12** and chemical shifts of the substructures are given in **Table 2.2**. Previous reports suggested that a seven-member structure was produced from C<sub>3</sub>–C<sub>4</sub> bond cleavage by sodium periodate oxidation [11]. The unassigned signals may be generated from these structures.

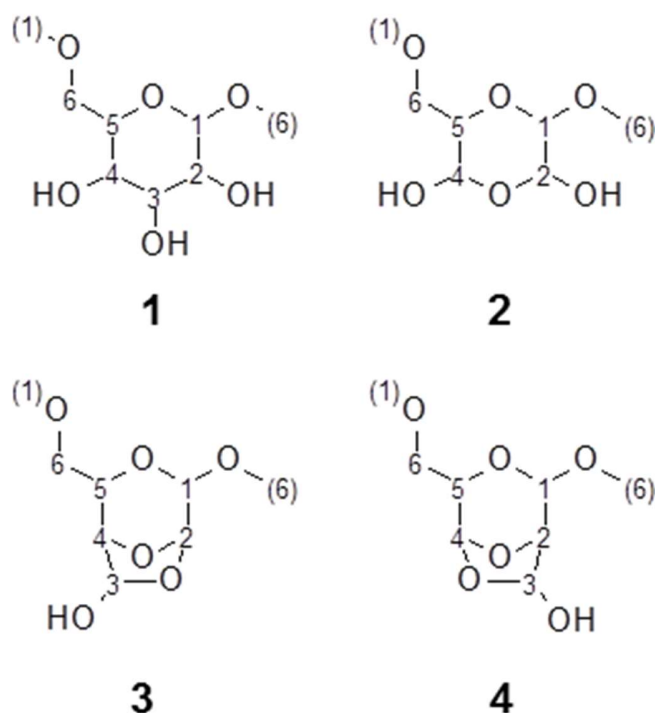


**Figure 2.10** Schematic of identified substructure in ald-dex chain. Glucose (1). C<sub>2</sub>-C<sub>3</sub> and C<sub>3</sub>-C<sub>4</sub> cleavages, C<sub>3</sub> desorption, hemiacetal structure (2). C<sub>2</sub>-C<sub>3</sub> cleavage, hemiacetal structure (3). And C<sub>3</sub>-C<sub>4</sub> cleavage, hemiacetal structure (4).

To investigate the dependence of oxidized dextran degradation on the nature of the substructure, kinetic analysis was performed for each substructure. The substructure 2 gave three NMR signals (H1, 2, 4) to analyze the time course and to fit with the single-exponential function (**Figure 2.13**). This time constant depended on the glycine concentration (**Figure 2.14**). Even when the glycine concentration was increased to 0.5 or 1.5%, glycine molarity was more than that of substructure 2 in 10% oxidized dextran. Thus, degradation kinetics of substructure 2 with glycine was considered a pseudo-first-order reaction. For this reason, we performed the single-exponential curve fitting to the kinetics of substructure 2. The average time constant of the degradation of

substructure 2 was  $1.5 \pm 0.43$  h, remarkably lower than substructures 3 and 4 (**Figure 2.13d, 2.13e**) (**Table 2.1**) and the unknown structures (data not shown). Furthermore, methylene groups were generated with a similar time constant, 1.8 h (**Figure 2.15**), by the deoxidation process in Maillard reaction.[13]

The glucose and glycine Maillard reaction pathways suggest that Amadori product is produced from the interaction between glucose and glycine, and were converted into 1- and 3-deoxyosone. The methylene group is certainly present during 3-deoxyosone formation through Amadori rearrangement, and leads to Strecker degradation and melanioidins formation that produces the brown color during polysaccharide degradation[14] (**Figure 2.16**).

**Table 2.1** Initial population of substructure in a-dex and time constants of a-dex reaction.

| Substructure |      | Initial population <sup>a</sup> / % | Time constant <sup>b</sup> / h |
|--------------|------|-------------------------------------|--------------------------------|
| 2            |      | 1.4±0.43                            | 1.5±0.11                       |
| 3            |      | 1.6±0.19                            | 89±48                          |
| 4            |      | 2.9±0.34                            | 34±1.7                         |
| Methylene    |      | n.d.                                | 1.8                            |
| Reducing end | α-H1 | n.d.                                | 1.4 / 42                       |
|              | β-H2 | n.d.                                | 1.2 / 37                       |

<sup>a</sup> Average percentile of <sup>1</sup>H NMR intensity of substructures as 100 % intensity of H1 proton in non-oxidized glucose

<sup>b</sup> Average time constants resulted in single- or double-exponential fitting.

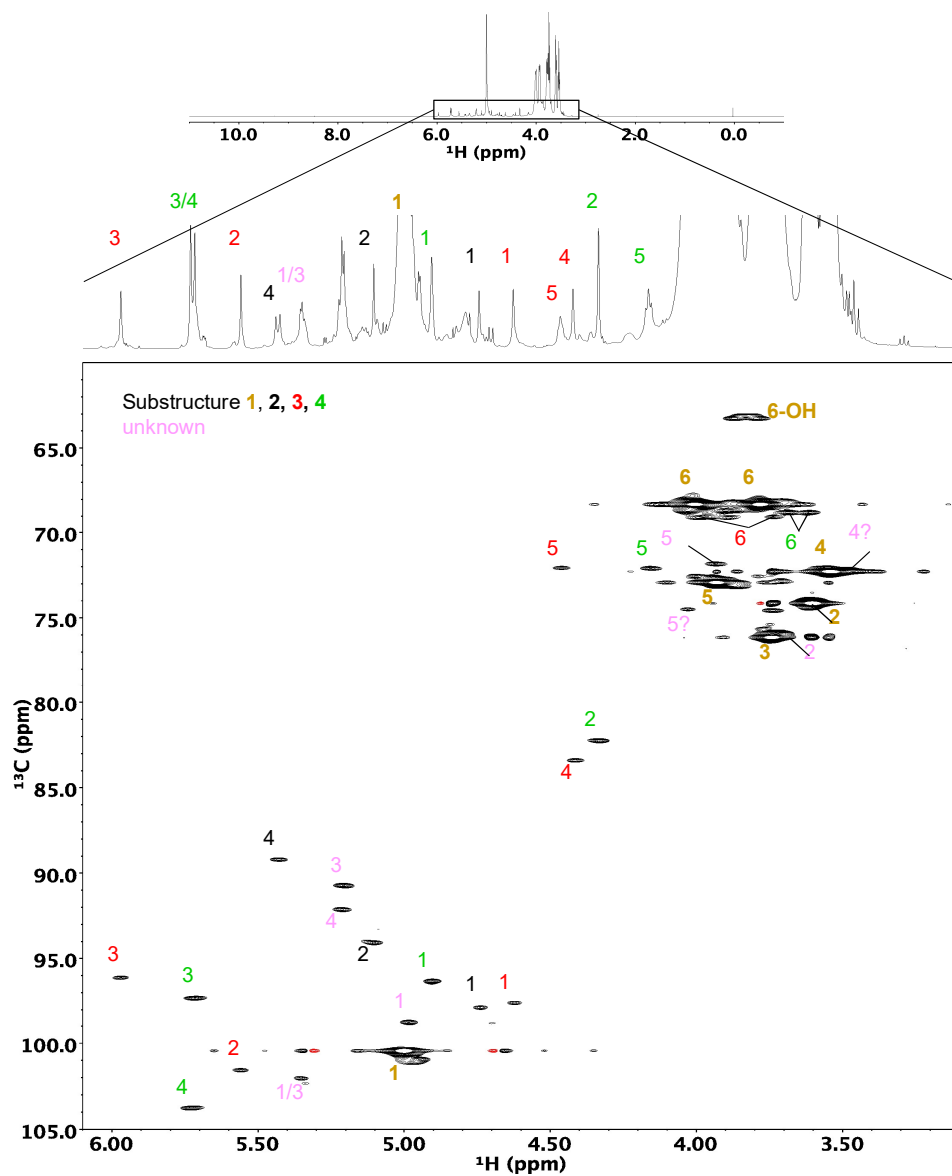


**Figure 2.11**  $^{13}\text{C}$ - $^1\text{H}$  HSQC NMR spectrum of fresh Ald-dex. Assignments of substructure 2 (black), 3 (red), and 4 (green), and non-oxidized glucose (yellow) are indicated close to NMR signals in HSQC and 1D  $^1\text{H}$  NMR. Assignment numbers represent the position of  $^1\text{H}$  and  $^{13}\text{C}$  at each substructure.

**Table 2.2** Chemical shift data for substructure of oxidized dextran.

| substructure | position | <sup>1</sup> H | <sup>13</sup> C |
|--------------|----------|----------------|-----------------|
| <b>1</b>     | 1        | 5.00           | 100.4           |
|              | 2        | 3.60           | 74.2            |
|              | 3        | 3.74           | 76.2            |
|              | 4        | 3.54           | 72.3            |
|              | 5        | 3.93           | 72.9            |
|              | 6        | 4.01/3.78      | 68.3            |
| <b>2</b>     | 1        | 4.74           | 97.9            |
|              | 2        | 5.10           | 94.1            |
|              | 4        | 5.43           | 89.2            |
|              | 5        | missing        | missing         |
|              | 6        | missing        | missing         |
| <b>3</b>     | 1        | 4.62           | 97.6            |
|              | 2        | 5.56           | 101.6           |
|              | 3        | 5.97           | 96.1            |
|              | 4        | 4.42           | 83.4            |
|              | 5        | 4.46           | 72.1            |
|              | 6        | 3.96/3.73      | 69.0            |
| <b>4</b>     | 1        | 4.90           | 96.3            |
|              | 2        | 4.33           | 82.2            |
|              | 3        | 5.71           | 97.3            |
|              | 4        | 5.73           | 103.8           |
|              | 5        | 4.16           | 72.1            |
|              | 6        | 3.69/3.61      | 68.8            |

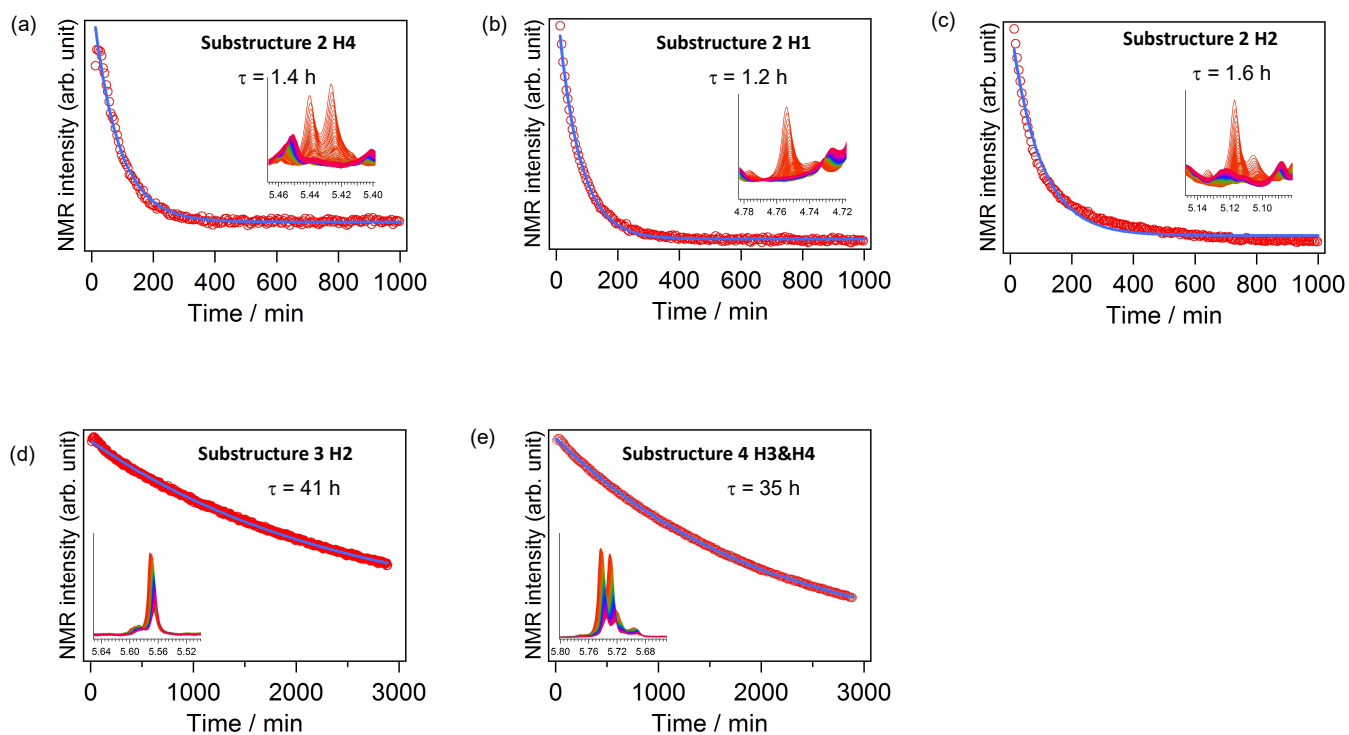


**Figure 2.12** Kinetic analysis of time course NMR spectra for substructure 2 (a, b, and c), 3 (d), and 4 (e), and methylene group (d). Blue solid lines are calculated by single exponential curve fitting and the time constants of the exponential function are shown.

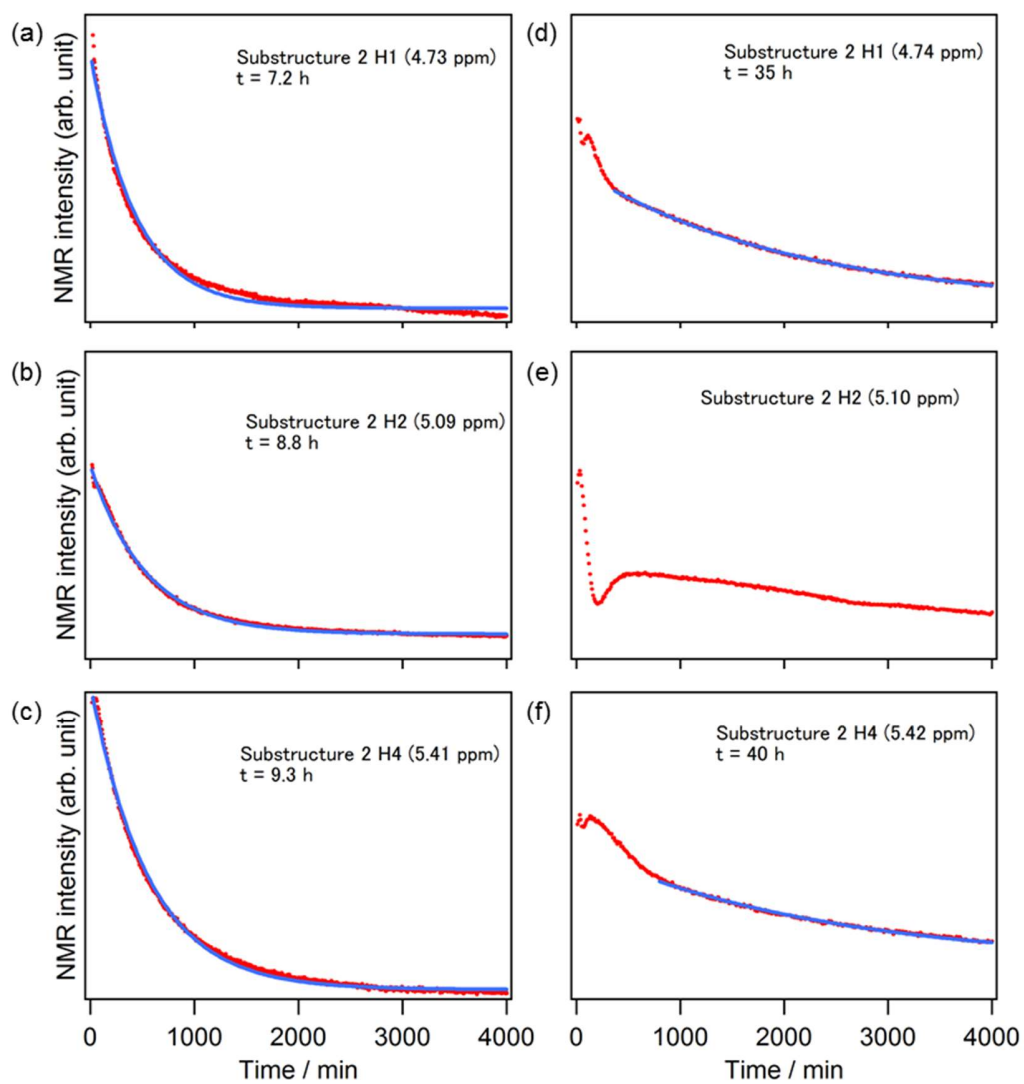


**Figure 2.14** Kinetic analysis of substructure degradation 2 in 10% oxidized dextran with 1.5% (a–c) and 0.5% (d–f) glycine solution.

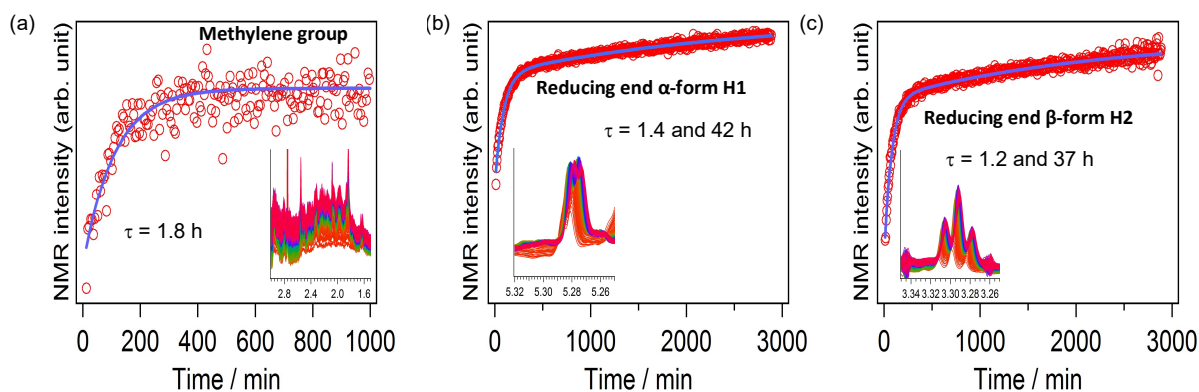


**Figure 2.15** Kinetic analysis of time course NMR spectra for methylene group (a), reducing end a-form (b) and b-form (c) H1. Blue solid lines are calculated by single exponential curve fitting for (a) and by double exponential curve fitting for (b, c), and the time constants of the exponential function are shown.

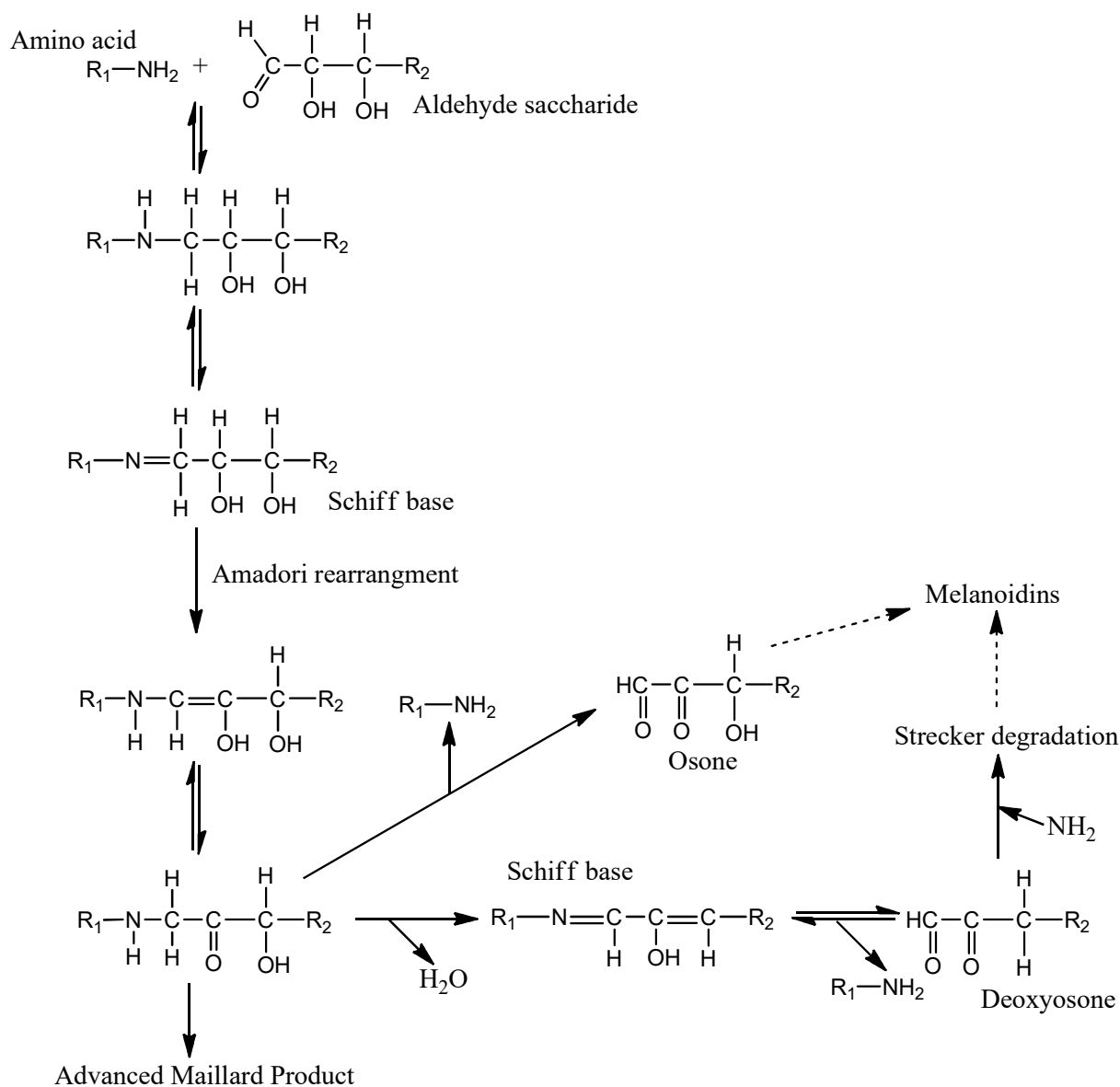


**Figure 2.16** Maillard reaction pathways by the reaction of aldehyde saccharide and amino acid.

The NMR charts of **Figure 2.15 b** and **c** show that reducing end protons were generated. To ensure curve fitting, we used double-exponential curve fitting and obtained short (1.4 and 1.2 h) and long (42 and 37 h) time constants for the  $\alpha$ -form and the  $\beta$ -form end protons, respectively (**Table 2.1**).

The degradation time constant of oxidized dextran determined by GPC was equal to that obtained by NMR kinetic analysis of substructure 2. The Schiff base formation at the substructure 2 was directly related to oxidized dextran degradation. The population of the substructure 2 was  $1.4 \pm 0.43\%$  (**Table 2.1**). The average molecular weight of 21.2%OxDex was 70000. This means that 417 glucose moieties are contained in one molecule, and that a single 21.2%OxDex chain contains 5.8 units of substructure 2. The GPC analysis indicates that the final  $M_w$  and  $M_n$  of 21.2%OxDex after reaction with 5% glycine solution was less than 20000 and 6000 respectively. (**Figure 2.9b**, **Figure 2.10a**). The degradation time constant of substructure 2 (**Table 2.1**) agreed well to the degradation profile derived by GPC. From **Figure 2.10**,  $M_w$  values obtained after 120 minutes for all the oxidized dextran samples were not much influenced by glycine concentration. However, glycine concentration greatly influenced the initial decrease rate of  $M_w$ . The degradation of oxidized dextran was probably dominated by the concentration of amino groups that reacted with the aldehyde groups on oxidized dextran. These results confirmed that substructure 2 dominantly controlled the oxidized dextran degradation. Through degradation, it is reasonable that reducing end H1 and H2 increasing with short time constants. This is the direct evidence that glycoside bonds of oxidized dextran were cleaved by the Maillard reactions triggered by Schiff base formation between aldehyde and amine groups. The Maillard reaction from substructure 2 mainly contributes to the glycine-mediate degradation of oxidized dextran. However, the mechanism behind the increasing in end protons having long time constants still remain unclear. It is likely that this complicated degradation might be related with multiple reactions, all of which cannot be detected by the NMR techniques applied here.

## **2.4 Conclusion**

Our NMR data suggests that 4 hemiacetal substructures were present during Malaprade oxidation. Substructure 2, in which C<sub>3</sub> was removed, showed a degradation time constant of  $\sim 1.5 \pm 0.43$  h, distinctly lower than those for substructures 3 and 4, which involve C<sub>2</sub>–C<sub>3</sub> and C<sub>3</sub>–C<sub>4</sub> bond cleavage, respectively. In addition, methylene was generated at time constant 1.8 h, suggesting that the degradation of oxidized dextran in glycine as the primary amino acid is related with Maillard reaction because the methylene group is the one component of 3-deoxyosone that undergoes Strecker degradation through Amadori rearrangement. This cleavage of main-chain glycoside bonds of oxidized dextran was supported by the increasing amount of end H during the reaction. Moreover, the reduction in oxidized dextran molecular weight decreased with increasing oxidation degree and glycine concentration, probably due to increased intermolecular interaction of the reactive carbonyl group with amino group of glycine, resulting in high degradation. This study revealed that main chain scission in oxidized dextran could be caused by the reaction between aldehyde and amino groups and this novel knowledge regarding the degradation of polysaccharides could help control their biodegradation and develop new biomedical applications like tissue engineering and drug delivery substrates.

## References

1. Jetten, J., et al., *Process for oxidising dialdehyde polysaccharides*. 2005.
2. Schwenke, K.D., et al., *Chemical modification of proteins. II Blocking of amino groups and basic amino acids and crosslinking of polypeptide chains in casein and field bean globulin by reaction with dialdehyde starch*. *Nahrung*, 1976. **20**(10): p. 895-904.
3. Hodge, J.E., *Dehydrated Foods, Chemistry of Browning Reactions in Model Systems*. *Journal of Agricultural and Food Chemistry*, 1953. **1**(15): p. 928-943.
4. Berg, H.E. and M.A.J.S. Van Boekel, *Degradation of lactose during heating of milk*. *Netherlands Milk and Dairy Journal*, 1994. **48**: p. 157 - 175.
5. Boekel Van, M.A.J.S. and C.M.J. Brands, *Heating of sugar-casein solutions: isomerization and Maillard reactions*. *The Maillard Reaction in Foods and Medicine*. J. O'Brien, H.E. Nursten, J. Crabbe, J.F. Ames (eds.), 1998: p. 154–158.
6. Mo, X., et al., *Soft tissue adhesive composed of modified gelatin and polysaccharides*. *Journal of Biomaterials Science, Polymer Edition*, 2000. **11**(4): p. 341-351.
7. Hyon, S.-H., et al., *Low cytotoxic tissue adhesive based on oxidized dextran and epsilon-poly-L-lysine*. *Journal of Biomedical Materials Research Part A*, 2014. **102**(8): p. 2511-2520.
8. Matsumura, K., et al., *Self-degradation of tissue adhesive based on oxidized dextran and poly-L-lysine*. *Carbohydrate Polymers*, 2014. **113**: p. 32-38.
9. Aalmo, K.M., et al., *Identification by X-ray method 6(R) -acetoxy-2(s)methoxy-1(R),5(R)-3,7,8 octane. A new compound isolated after periodate oxidation of methyl alpha -D-xylopyranoside in dimethyl sulfoxide follow by acetylation*. *Acta Chemica Scandinavica*, 1993. **47** p. 1235–1237.

10. Aalmo, K.M., et al., *Characterisation by <sup>1</sup>H- and <sup>13</sup>C-n.m.r. spectroscopy of the products from oxidation of methyl  $\alpha$ - and  $\beta$ -d-galactopyranoside with periodic acid in dimethyl sulphoxide*. Carbohydrate Research, 1981. **91**(1): p. 1-11.
11. Ishak, M.F. and T.J. Painter, *Kinetic evidence for hemiacetal formation during the oxidation of dextran in aqueous periodate*. Carbohydrate Research, 1978. **64**(0): p. 189-197.
12. Yu, R.J. and C.T. Bishop, *Novel oxidations of methyl glycopyranosides by periodic acid in dimethyl sulfoxide*. Canadian Journal of Chemistry, 1967. **45**(19): p. 2195-2203.
13. Nursten, H.E., *Recent developments in studies of the maillard reaction*. Food Chemistry, 1981. **6**(3): p. 263-277.
14. Tressl, R., et al., *Formation of Isoleucine-Specific Maillard Products from [<sup>1-13</sup>C]-D-Glucose and [<sup>1-13</sup>C]-D-Fructose*. Journal of Agricultural and Food Chemistry, 1995. **43**(5): p. 1163-1169.

*Chapter 2*  
*Dextran degradation by Malaprade reaction*

## **Chapter 3**

---

### ***Cellulose scaffold fabrication with ionic liquid and degradation control by Malaprade oxidation***

#### **3.1. Introduction**

##### **3.1.1 The oxidation of cellulose**

For several years, many researchers have been made an effort to oxidized cellulose for expanding its application. The main problem for studying the oxidized cellulose is the problem of material production which is homogenous in physical and chemical properties. Almost of oxidant manipulated are evidently not selective to the especially hydroxyl group of glucose unit in cellulose chains which are attacked. Many cellulose oxidations are topochemical. When the condition of oxidation is light, the product frequently composed of an uncharged residue of unreacted modified cellulose and oxidized portion. More harshly oxidation produces a huge oxidized cellulose portion which attaches by increased degradation. Physical degradation results to the breaking up of cellulose fiber and usually the cellulose is brittle and powders easily. The

cellulose can be the oxidized with several oxidizing agent, such as permanganate, persulfate, nitrogen dioxide, chlorine dioxide, peracetic acid and periodate.

### 3.1.1.1 Oxidation cellulose with nitrogen dioxide

The oxidation cellulose with nitrogen dioxide is a non-specific oxidation. Oxidized cellulose is obtained by nitrogen dioxide and gives a fibrous material which is not brittle. This oxidation is simple controlled to produce the oxidized cellulose of much carbonyl group content with desired degree of substitution (DS) (**Figure 3.1**). When the oxidation degree is high enough, the oxidized cellulose is completely dissolved in alkaline solution, such as 2% sodium hydroxide. The maximum of degree of substitution of this oxidation is 0.25 [1]. The oxidized cellulose products via nitrogen dioxide oxidation are yellow to brown in color, and are highly degraded [2].

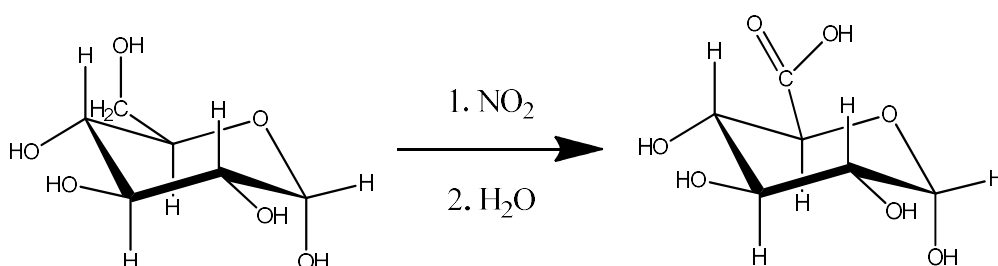


**Figure 3.1** Schematic cellulose oxidation by nitrogen dioxide.

### 3.1.1.2 Oxidation cellulose with phosphoric acid, sodium borate, sodium chlorate and sodium chlorite

With this oxidation, where the oxidizing oxyhalogen species are formed in situ, the primary alcohol groups can be completely formed resulting to carboxylic acids more than 90%. Ring is

specifically cleaved by oxidation with chlorate. The carbonyl groups are formed by oxidation of secondary hydroxyl groups and then reduced with sodium borohydride (**Figure 3.2**). The polysaccharide via this oxidation degradation differed clearly [3].

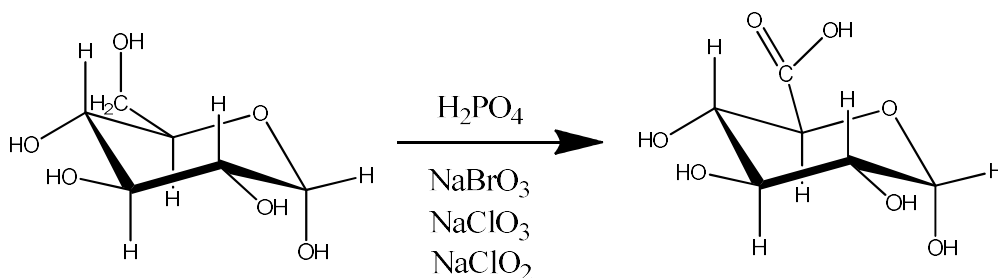


**Figure 3.2** Schematic cellulose oxidation by nitrogen dioxide halogen oxide

### 3.1.1.3 Oxidation cellulose with phosphoric acid, sodium nitrite or sodium nitrate

The oxidation cellulose with phosphoric acid, sodium nitrite or sodium nitrate is selective oxidation with sodium bromide and chloride as catalyst. Cellulose is dissolved in 85% phosphoric acid with limited hydrolysis and then treated with sodium nitrite and sodium nitrate. The oxidation between C<sub>2</sub>-C<sub>3</sub> is reduced by adding sodium borohydride. When adding with nitrate, the small excess of nitrate is needed, 4 nitrate per 3 glucose unit. When adding with nitrite, 4 nitrite per 1 glucose unit is added. Both reactions result to reduce the molecular weight of cellulose. Moreover, the reaction time is decreased by increasing the temperature. However, the oxidation is not completely selective. Therefore, the reduction step by adding sodium borohydride is important step to reduce ketone formed (10-20%) (**Figure 3.3**). The oxidation yield is high more than 95% conversion of cellulose primary alcohol to carboxylic group [3, 4].

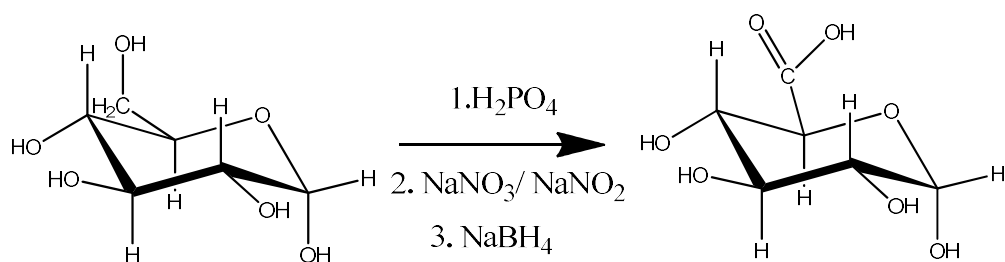


**Figure 3.3** Schematic cellulose oxidation by nitrogen dioxide

### 3.1.1.4 Oxidation cellulose by periodate

The cellulose oxidation by periodate is specific cleavage of the C<sub>2</sub>–C<sub>3</sub> bond of the glucose unit. This cleavage results in the formation of the two aldehyde groups per glucose unit resulting to 2, 3-dialdehyde cellulose (**Figure 3.4**). These aldehydes can be changed into carboxylic acid, primary alcohol or imines (Schiff bases) with primary amines through its fundamental reactivity. The oxidation cellulose with periodate is very high yield. The %conversion of cellulose to 2,3 dialdehyde cellulose is 100% which oxidized with 2.0 ratio of periodate/ cellulose , pH 5.5, reaction time 24 hour at 55 °C [5].

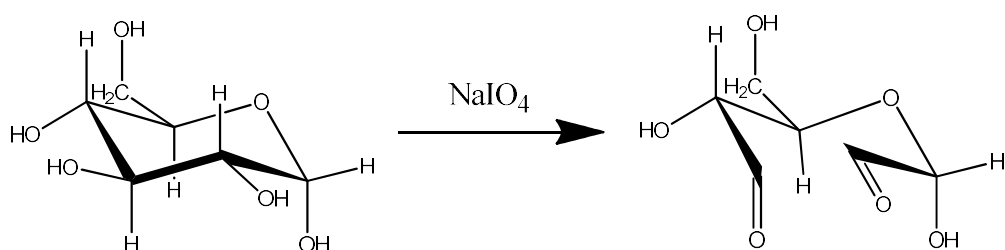


**Figure 3.4** Schematic cellulose oxidation by periodate

### 3.1.2 Scaffold biofabrication technique

In tissue engineering application, scaffold plays an important role. Tissue scaffold is the three dimensional structure which is made from biopolymer or synthetic polymer for cell growth, cell attachment, transport of nutrient and waste. Many techniques of scaffold fabrication have been developed which divided into two categories; conventional and advanced method.

#### 3.1.2.1 Particulate leaching and solvent casting

In this method, the polymer solution is equally mixed with specific salt particles. The solvent is added and evaporated after polymer mixed with salt particles planted throughout. The fluid mixture is submersed in water where the salts leach out to make the porous structure (Figure 3.5)[6]. The porosity of scaffold is high value up to 93%. The diameter of pore size can be controlled up to 500  $\mu\text{m}$  and the pore size can be varied by varying salt particles. However, this technique can be used to generate only membrane up to 3 mm thick [7].

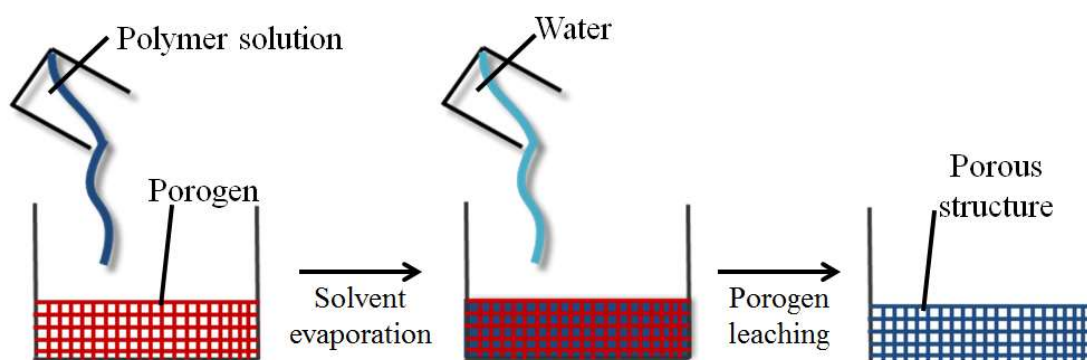


**Figure 3.5** Schematic of solvent casting and particulate leaching process

### 3.1.2.2 Gas foaming

In this method, the degradable polymer is formed in mold and pressurized with gas-foaming agents at high pressure. The example of gas foaming are nitrogen, carbon dioxide, fluoroform and water. Subsequently, the gas bubbles nucleation and growth are generated with sizes ranging between 100-500  $\mu\text{m}$  in polymer (**Figure 3.6**). The advantage of this technique is an organic solvent-free process. However, the main disadvantage is that the process may make largely unconnected pores structure and a non-porous external surface [8].

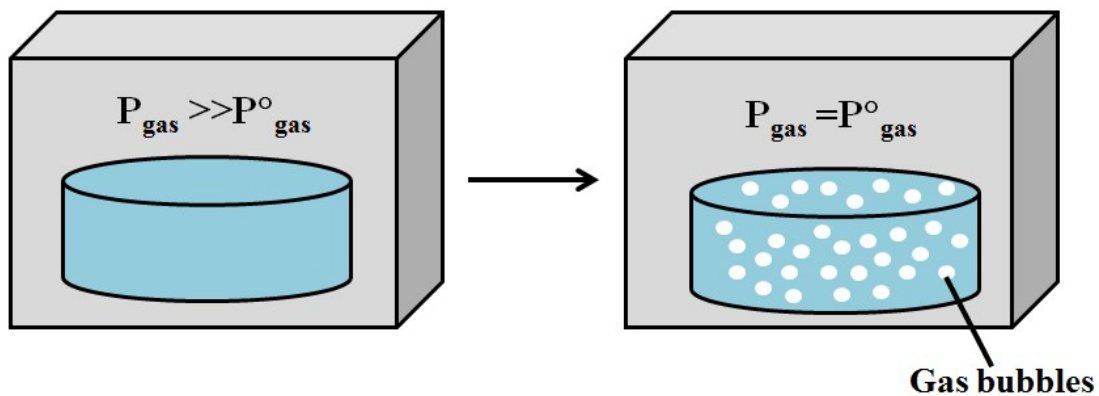


**Figure 3.6** Schematic of gas foaming process

### 3.1.2.3 Phase separation

In phase separation procedure, a polymer solution is quenched to liquid-liquid phase separation to form two phases, dividing to a polymer-poor phase and a polymer-rich phase. The polymer-rich phase becomes solid, while the polymer poor phase is discarded resulting to highly porous polymer scaffold [9] (**Figure 3.7**). The micro or macro porous in scaffold can be

controlled by varying the concentration of polymer, quenching rate and quenching temperature. The process is proceeded at low temperatures which is advantage for the corporates bioactive molecules in the scaffold.

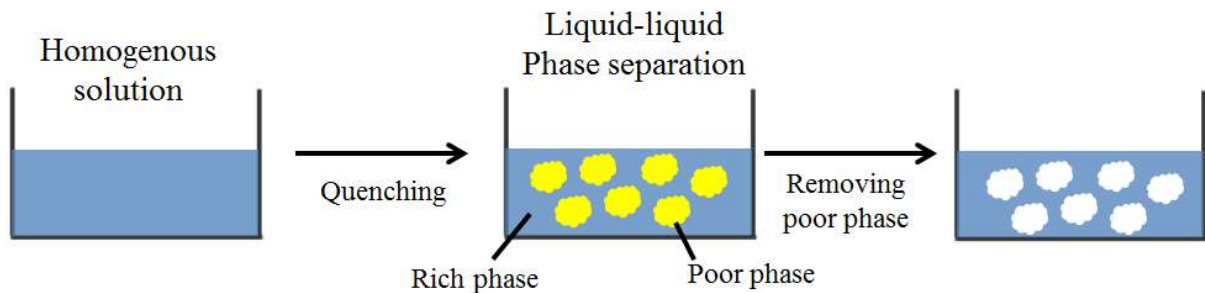


**Figure 3.7** Schematic of phase separation

#### 3.1.2.4 Melt molding

During melt molding process, the polymer powder and porogen are mixed and moved into mold then heated until the glass-transition temperature of the polymer, while pressure is applied to the mixture. The mold is removed and the porogen is leached out resulting to make pores in scaffold (Figure3.8). The advantage of this technique is non-solvent process. The shape and morphology of scaffold are independently controlled. However, the disadvantage is possibility of residual porogen and high temperatures during processing that prevent the ability to incorporate bioactive molecules[10].

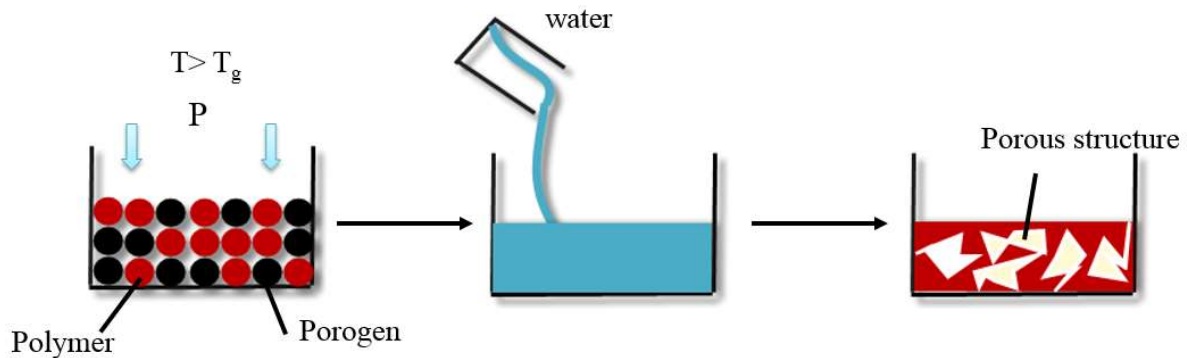


**Figure 3.8** Schematic of melt molding

### 3.1.2.5 Freeze drying

In freeze drying process, the polymer solution is cooled down to certain temperature which solvent forms ice crystals and all materials are frozen state resulting to the polymer molecules aggregation into the interstitial spaces. Subsequently, the solvent is discarded by adding pressure lower than the equilibrium vapor pressure of the frozen solvent. The solvent is completely sublimated and interconnect porous in scaffold can be obtained (Figure 3.9). The scaffold porosity is controlled by varying the polymer concentration and freezing temperature and speed.

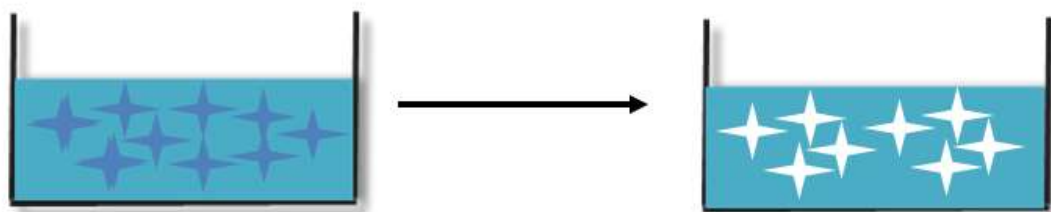


**Figure 3.9** Schematic of freeze drying

### 3.1.2.6 Electrospinning

This technique uses electrical charges to make small fibers ranging from 2 nm to several micrometers. The fibrous via electrospinning can positively affect cell spreading and binding compared to micropore from scaffold (see chapter 4). The main composition including of 3 parts, there are a syringe pump for containing the polymeric solution, a high voltage source to generate high electric field for spinning, and a collector to collect the fibers. Nanofibers with high surface area to volume ratios are most suitable for tissue engineering applications [11].

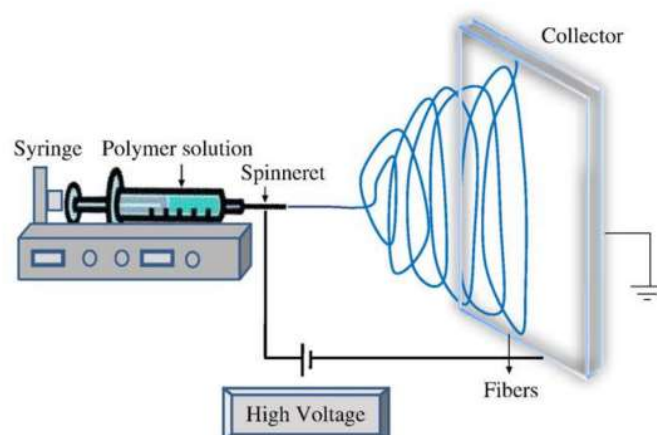
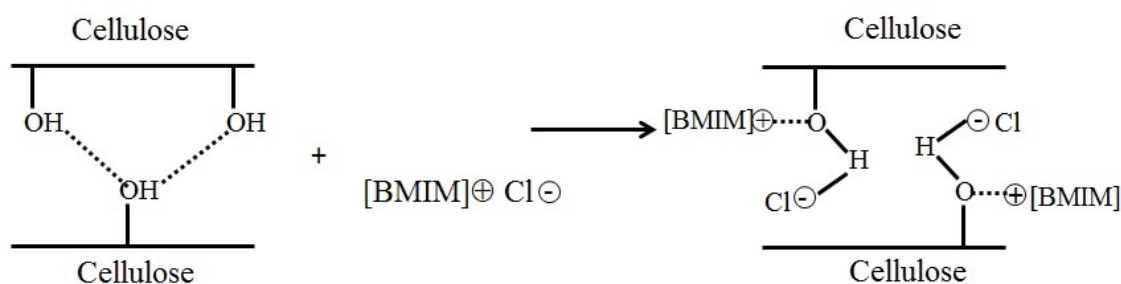


Figure 3.10 Schematic of electrospinning apparatus [12].

### 3.1.3 Ionic liquids and their interaction with cellulose

Due to highly crystalline regions in cellulose structure and the highly branched H-bonding, cellulose is insoluble in water and organic solvents. The solvents which can dissolve cellulose are such as sodium hydroxide/urea (CarbaCell), sodium hydroxide/carbon disulfide (Viscose), N-methylmorpholine-N-oxide monohydrate (NMMO). Ionic liquids (ILs) present to be highly polar

due to their ionic character, resulting in their increase in biopolymer dissolving capacity [13]. Normally, the C-H-X (X = Cl, Br) interaction is characterized as a relatively weak interaction, but it is strong in imidazolium-based halide ILs resulting to possess strong covalent character. For 1-butyl-3-methylimidazolium chloride (BMIMCl), it is suggested that both cations and anions are affected in the dissolution process. Figure 3.11 shows the proposed dissolution mechanism of cellulose in BMIMCl. The hydrogen and oxygen atoms of the cellulose form electron donor-electron acceptor complexes with the charged of the BMIMCl. It has been suggested that it exist between the C-3 and C-6 hydroxyl groups of neighbored cellulose chains [14]. This interaction results in separation of the hydroxyl groups of the different cellulose chains and leads to dissolution of the cellulose in an ionic liquid [15, 16].



**Figure 3.11** Proposed dissolution mechanism of cellulose in BMIMCl [15].

In this chapter, cellulose scaffolds were effectively prepared by NaCl leaching from ionic liquid solution BMIMCl as a green solvent. Dialdehyde cellulose scaffold was proceeded for its biodegradable and biocompatible properties. In addition, the degradation of dialdehyde was controlled by the Schiff base formation reaction.

### **3.2 Material and method**

Cellulose powder was purchased from Sigma Aldrich (St. Louis, USA). Sodium periodate, di-sodium hydrogen phosphate, sodium di-hydrogen phosphate, glycine, starch soluble, 1-butyl-3-metylimidazolium chloride and other chemical reagent were obtained from Nacalai Tesque, Inc., (Kyoto, Japan).

#### **3.2.1 Cellulose membrane degradation**

Cellulose membranes were cut into size 2×2 cm and submersed in distilled water 10 mL with different amount of NaIO<sub>4</sub> 0-2.5 g. The reaction proceeded at 50°C for 1-3 h under gentle stirring. For investigation of the effect of amino acid strength, oxidized cellulose membranes were submersed in 5, 10, 15% (w/v) glycine. After the degradation, oxidized membranes were washed with distilled water for 3 times, filtrated through Whatman paper No. 42 and dried in the oven at 45 °C. Before and after oxidation cellulose membranes were weighed.

#### **3.2.2 Cellulose scaffold fabrication**

Cellulose (0.323 g, 15% w/w for BMIMCl) was dissolved in BMIMCl (2.15 g) by heating at 100 °C for 24 h and then added sodium chloride particle size 52-450 μm as porogen. The gel paste of cellulose was cooled at room temperature and then, it was sandwiched between silicon molds (diameter 10 mm, thickness 3 mm). The material was kept at room temperature for 7 days to form the gel material. The excluded BMIMCl was removed by washing with distilled water and freeze dried. The surface of the cellulose scaffold was characterized by scanning electron

microscopy (SEM) (S4100 Hitachi, Japan). For surface characterization, a dried scaffold was coated with palladium particles in a sputter coater and was observed at 100× magnification.

### **3.2.3 Oxidized cellulose scaffold**

Cellulose scaffolds were submersed in 10 mL of distilled water with different amount of sodium periodate (0-2.5 g). The reaction was proceeded at 50°C for 1 h under gentle stirring. The oxidized cellulose scaffold was washed with distilled water 3 times and then freeze dried.

### **3.2.4 Degradation of oxidized cellulose scaffold *in vitro***

Degradation of oxidized cellulose scaffold was also examined with respect to weight loss. Weight loss of initially weighed oxidized cellulose scaffold ( $W_0$ ) was monitored as a function of incubation time both in 5% glycine and culture medium at room temperature. At specified time intervals, oxidized cellulose scaffolds were removed from the 5% glycine solution and cultured medium and then dried and weighed ( $W_t$ ). The weight loss ratio was defined as  $100 \times (W_0 - W_t)/W_0$  /%. In addition, 1% oxidized cellulose scaffold was demonstrated in cultured media at 37 °C for 1 and 2 weeks. The morphology of remained scaffold after degradation was investigated by SEM.

## **3.3 Results and discussion**

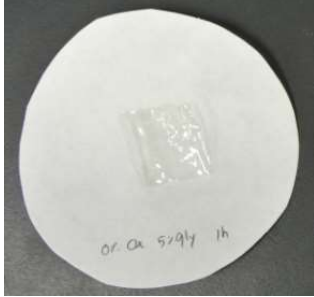
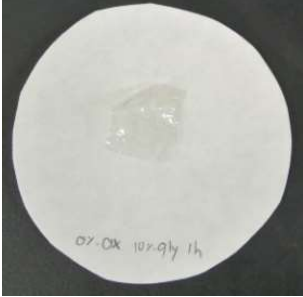
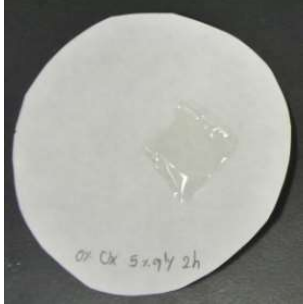
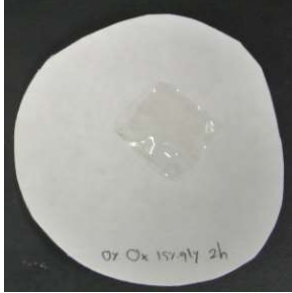
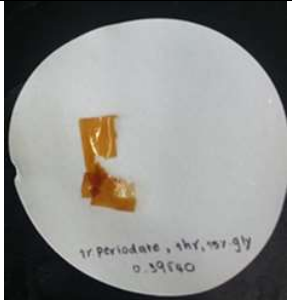
### 3.3.1 Aldehyde introduction in oxidized cellulose membrane.

For preliminary study, cellulose membrane was oxidized with 0-2.5% sodium periodate for investigation of the complete degradation time. The oxidized cellulose membranes were oxidized with various time for 1, 2, 3 hours which were submerged in 5, 10, 15% glycine solution. Cellulose membranes were weighed before and after the degradation. **Table 3.1** shows the photos of oxidized cellulose membranes with difference degree of oxidation, the reaction time and glycine concentration. Unoxidized cellulose membranes showed no degradation, even if it was submerged in glycine for 16 hr. The color of membrane did not change by submerging in glycine. In contrast, the color of oxidized cellulose membranes became brown and the intense of color according to the oxidation degree. Moreover, the mass of oxidized cellulose membrane were decreased as degree of oxidation decreased and reaction time increased. The brown color was appeared due to Millard reaction (see 1.4.3). The weight of cellulose membrane decreased as the degree of oxidation, reaction time and glycine concentration increased. In addition, 2.5% and 5% oxidized cellulose membrane in 5, 10, 15% glycine for 2 and 3 hours shows the complete degradation (**Figure 3.12**)

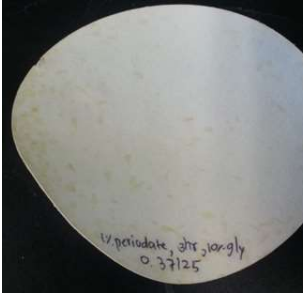
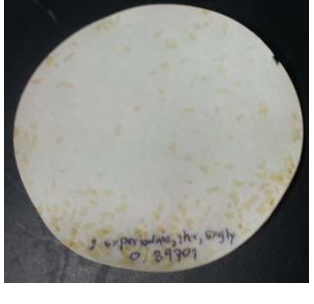
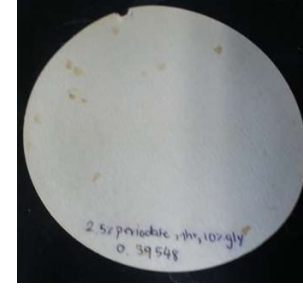
**Table 3.1** The cellulose membrane degradation with different sodium periodate concentration in 5%, 10% and 15% glycine.

| Oxidation concentration (%) | Reaction time (hour) | Glycine concentration |     |     |
|-----------------------------|----------------------|-----------------------|-----|-----|
|                             |                      | 5%                    | 10% | 15% |
|                             |                      |                       |     |     |

**Chapter 3**  
*Cellulose scaffold fabrication with ionic liquid and  
 degradation control by Malaprade oxidation*

|   |   |   |  |   |
|---|---|---|--|---|
| 0 | 1 |    |    |    |
|   | 2 |    |    |    |
|   | 3 |  |  |  |
| 1 | 1 |  |  |  |

**Chapter 3**  
*Cellulose scaffold fabrication with ionic liquid and degradation control by Malaprade oxidation*

|     |   |   |  |   |
|-----|---|---|--|---|
|     | 2 |    |    |  |
|     | 3 |    |    | *   |
| 2.5 | 1 |  |  | *   |
|     | 2 | *   | *  | *   |
|     | 3 | *   | *  | *   |

\* Completely degrade

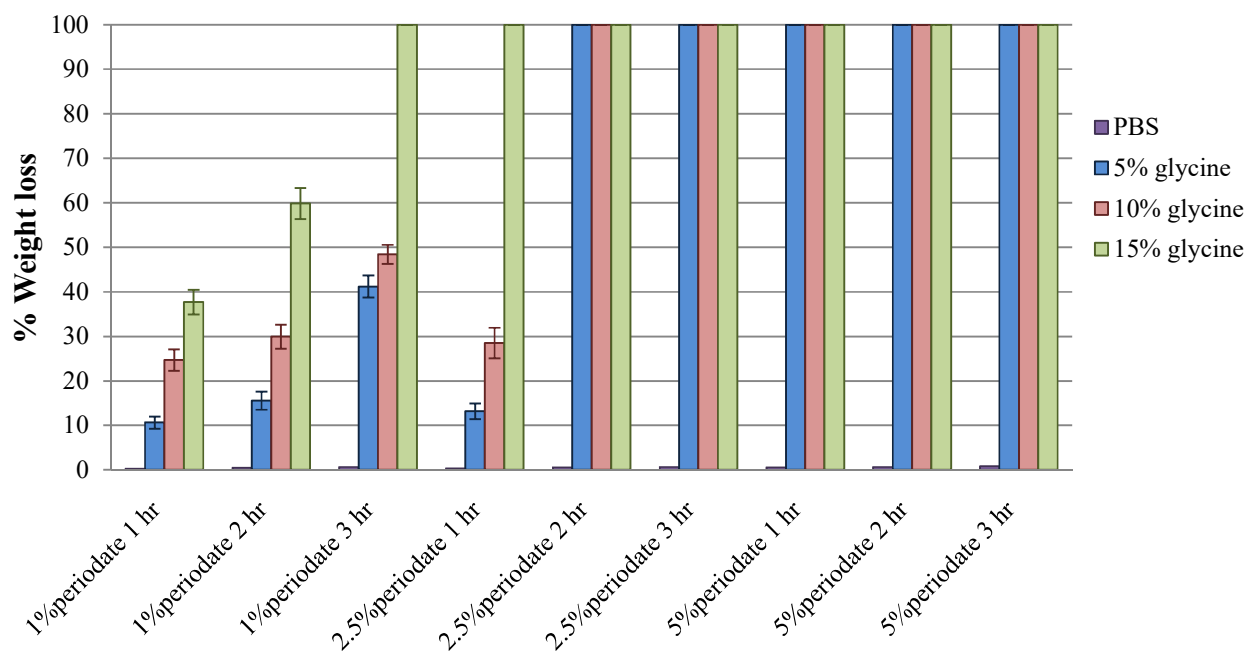


**Figure 3.12** The oxidized cellulose membrane degradation in 1%, 2.5% ,5% sodium periodate for 1, 2 ,3 hours respectively.

In the preliminary study of the effect of oxidation degree, cellulose membrane was oxidized with 0-25% sodium periodate for 1 hour. The aldehyde content was determined by simple iodometric method. **Table 3.2**, shows the aldehyde content after cellulose membrane oxidation. The aldehyde content increased as oxidation degree increased, reaching maximum value for 25% oxidation approximately 0.208 mmol /g. The result suggested that the increasing in concentration of sodium periodate dramatically increased the oxidation degree.

**Table 3.2** Aldehyde content in oxidized cellulose membrane.

| % NaIO <sub>4</sub> introduced to cellulose membrane | mmol aldehyde / weight (mmol/g) |
|--|---------------------------------|
| 1  | 0.0020                          |
| 5  | 0.0044                          |
| 10   | 0.0064                          |
| 15   | 0.0072                          |
| 20   | 0.0084                          |
| 25   | 0.0092                          |

### 3.3.2 Cellulose scaffold characterization

When the mixture of cellulose (15% w/w) and ionic liquid were heated up to 100 °C for 24 hours, the transparent homogenous material was obtained (**Figure 3.14a**). It had very high viscosity. Therefore, it could be raised from the surface as shown in **Figure 3.14b**. For the scaffold formation, the homogenous cellulose mixture was kept at room temperature for 1 week. Therefore, the excess ionic liquid was kept out from material for 7 days during the scaffold formation process. As a result, the cellulose scaffold was purified by washing with distilled water to remove the exclude excess ionic liquid (**Figure 3.13**).

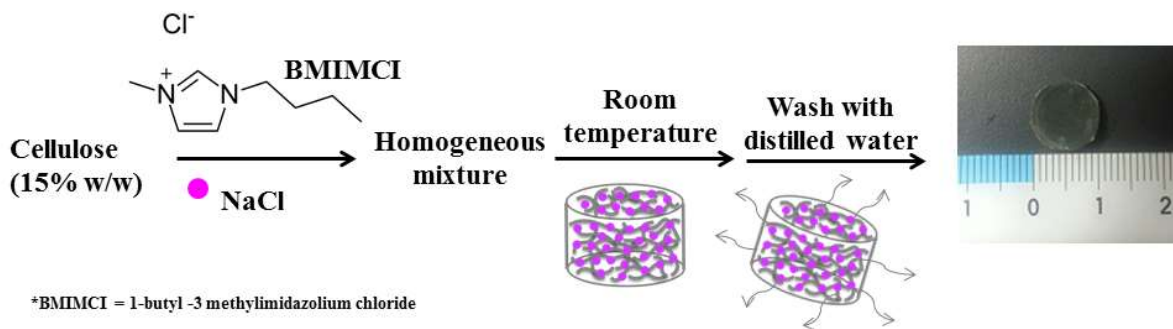


Figure 3.13 Schematic cellulose formation between cellulose powder and ionic liquid.

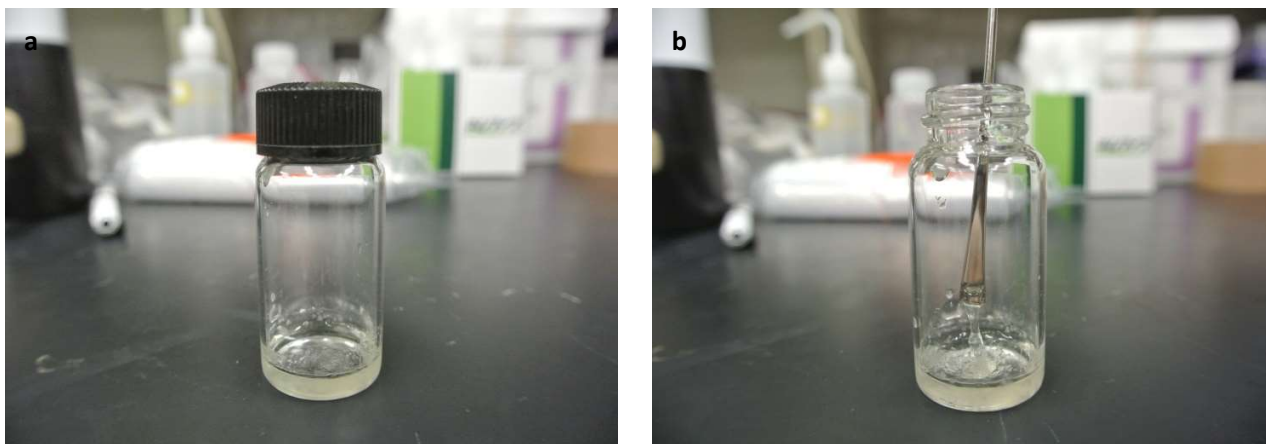
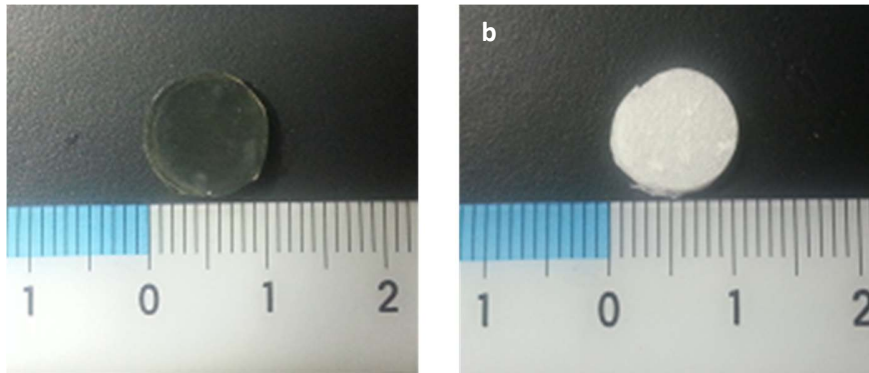


Figure 3.14 The cellulose mixed with BMIMCl as ionic liquid

As Figure 3.15, shows the cellulose scaffold before and after leaching with distilled water. Before leaching, cellulose scaffold was transparent and hard (Figure 3.15a). After leaching, it becomes turbid and firming shape (Figure 3.15b).



**Figure 3.15** Photographs of cellulose scaffolds before leaching (3.13a) and after leaching (3.13b).

**Figure 3.16** shows the interconnected pore in cellulose scaffold of SEM examination with difference in mean pore size which expanded by adding sodium chloride as the porogen. It is clearly seen that the pore size increased as the NaCl particle size increased. The pore size range was evaluated from SEM determination and found to be approximately 50-270  $\mu\text{m}$ . Moreover, NaCl content in cellulose scaffold was varied to 30-60% cooperated with NaCl mean pore size 250  $\mu\text{m}$  (**Figure 3.17**). The results showed that mean pore size of cellulose scaffold increased as NaCl content increased. Due to the increasing concentration of sodium chloride, it results to the decreasing concentration of cellulose. On decreasing concentration of cellulose, the cohesiveness decreased and tended to more porous structure. Another reason, the incomplete dispersion of cellulose due to high concentration of sodium chloride may be expanded the interconnected pore size.

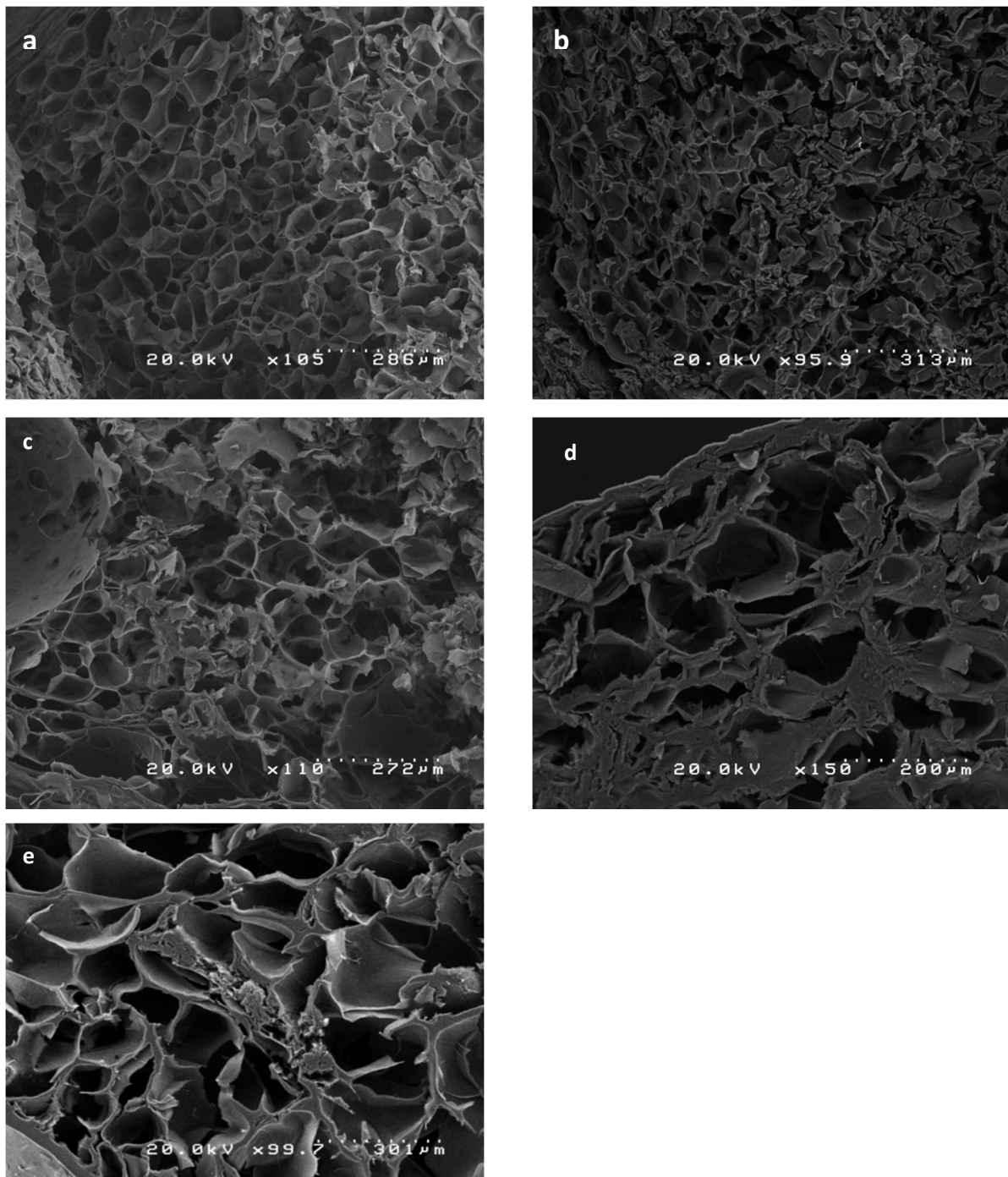


**Figure 3.16** SEM photograph of cellulose scaffold structure leaching with difference NaCl particle size 52, 75, 100, 150 and 250  $\mu\text{m}$  (3.4a, 3.4b, 3.4c, 3.4d, 3.4e).

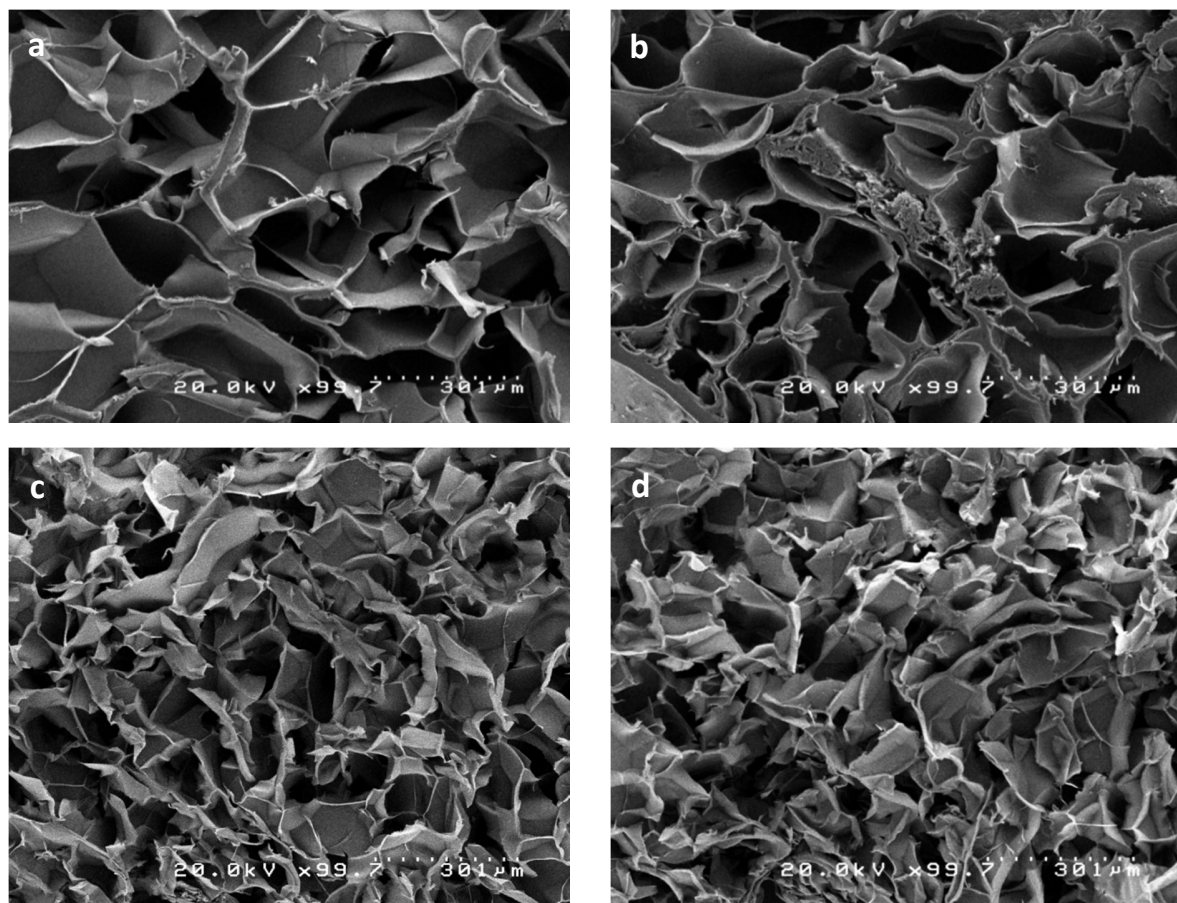


**Figure 3.17** SEM photograph of cellulose scaffold structure leaching with difference percentage of NaCl particle size 250  $\mu\text{m}$ , 60%, 50%, 40% and 30% (a, b, c, d).

### 3.3.3 Aldehyde introduction in oxidized cellulose scaffold

The aldehyde introduction in oxidized cellulose scaffold was evaluated. As a result in **Table 3.3**, the aldehyde content of oxidized cellulose scaffold was increased as the degree of oxidation increased. Moreover, the result was conformed to the cellulose membrane result. For

this experiment, the reaction was determined at 50 °C. Most studies relative with oxidation of cellulose to yield 2,3 dialdehyde cellulose was carried out at temperature 55 °C or below 55 °C. Above 55 °C, the periodate is unsteady and deteriorated to liberate iodine, which make it difficult to determine accurately the periodate consumption. While, the reaction is very slow when proceeded the reaction at room temperature or below 35 °C. Verma and Kulkarni [5] reported that oxidized cellulose with difference temperature effected on the %conversion of cellulose to 2,3 dialdehyde cellulose. At temperature 55 °C, the %conversion of cellulose to 2,3 dialdehyde cellulose was more than at 35 °C. In addition, the aldehyde content of oxidized cellulose scaffold was more than oxidized cellulose membrane at equality weight. Due the loss of crystallinity structure of cellulose powder during the fabrication of cellulose scaffold [17], it results to more susceptible structure which has more change for attacking of periodate.

**Table 3.3** Aldehyde introduction in oxidized cellulose scaffold.

| % NaIO <sub>4</sub> introduced to cellulose scaffold | mmol aldehyde / area<br>(mmol/ cm <sup>2</sup> ) |
|--|--|
| 1  | 0.64   |
| 5  | 1.34   |
| 10   | 2.06   |
| 15   | 2.33   |
| 20   | 2.67   |
| 25   | 3.03   |

### 3.3.4 Degradation of oxidized cellulose scaffold *in vitro*

The degradation of oxidized cellulose scaffolds was investigated the weight loss effect with glycine as amino acid. The degradation rate of oxidized cellulose scaffolds showed in **Figure 3.18**.

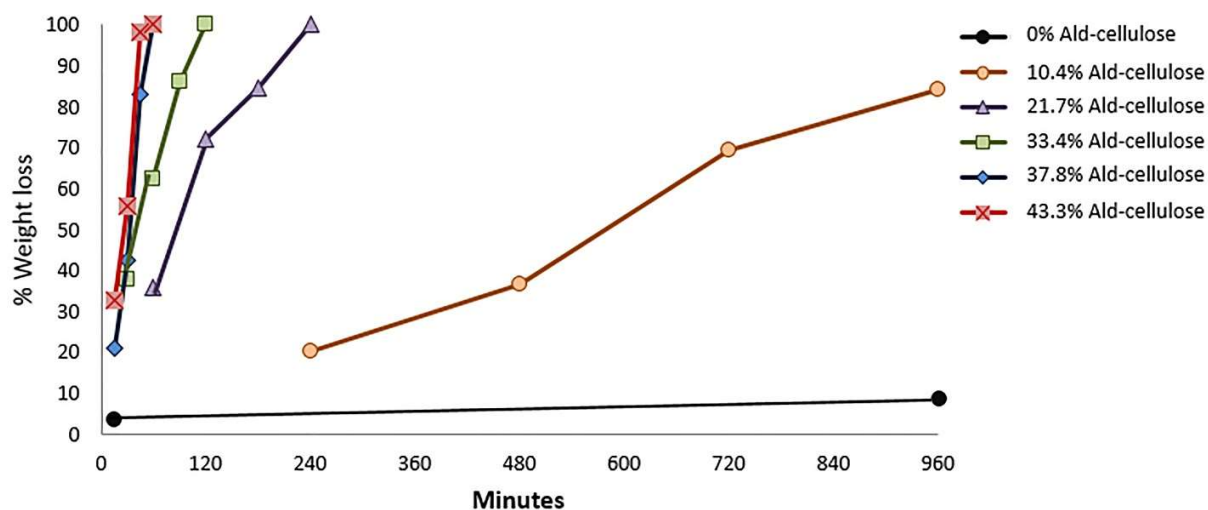


**Figure 3.18** Oxidized cellulose scaffold degradation in 5% glycine solution after 16h.

The results indicated that the degradation rate of oxidized cellulose scaffold depended on the degree of oxidation. Interestingly, 20% oxidized cellulose scaffold degradation time was fastest, completely degraded in only 45 minutes. In the meantime, unoxidized cellulose scaffold was used as a control, it was not degraded after 16 h. In other case, 15%, 10%, 5, % oxidized cellulose scaffold were completely degraded in 1, 2 and 4 hours respectively, whereas, 1% oxidized cellulose scaffold was not completely degraded after 16h. Subsequently, 0.1%, 0.25% and 0.5% oxidized cellulose scaffold were investigated the degradation time in 5% glycine solution for 8 weeks. After 8 weeks, unoxidized cellulose scaffold was partially degraded, and weight loss was 7.23%. On the other hands, 0.1%, 0.25% and 0.5% oxidized cellulose scaffold weight loss were 31.98%, 37.36% and 56.32% respectively (**Figure 3.19**).

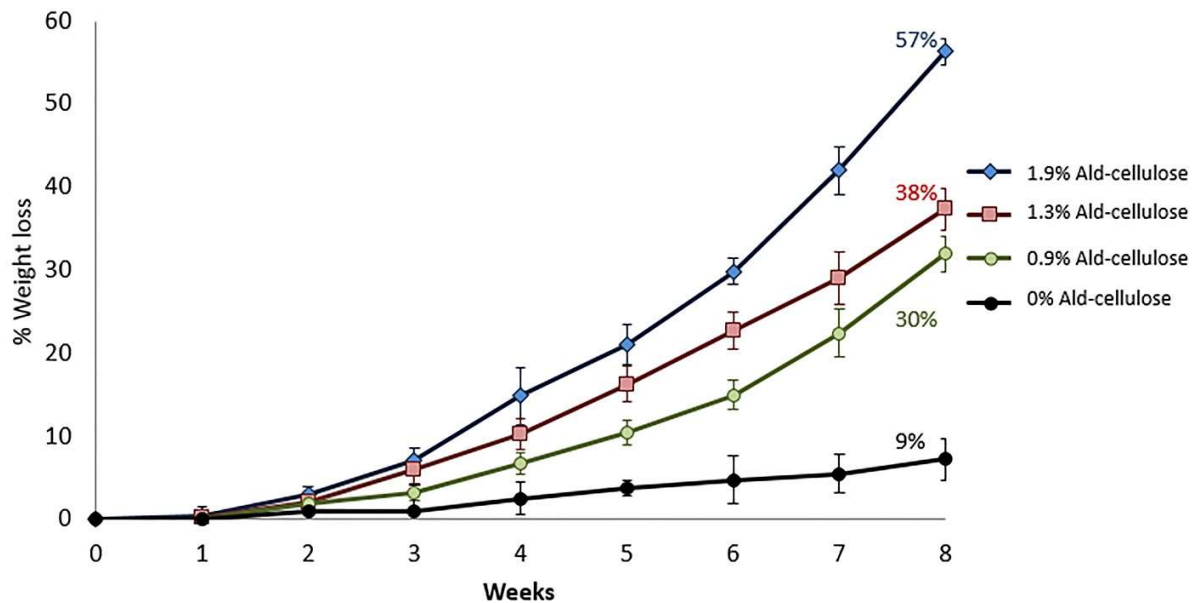


**Figure 3.19** Oxidized cellulose scaffold degradation in 5% glycine solution in 8 weeks.

Moreover, cellulose scaffold was oxidized with 0-10% sodium periodate and submerged in cultured media at 37 °C in CO<sub>2</sub> incubator without stirring and investigated the degradation time for 8 weeks. The result showed that the degradation rates of 5% and 10% oxidized cellulose scaffold were fastest, completely degraded in 15 days. Whereas, unoxidized cellulose scaffold was partially degraded, and %weight loss was 7.79% in 32 days (**Figure 3.20**).

**Chapter 3**  
*Cellulose scaffold fabrication with ionic liquid and degradation control by Malaprade oxidation*

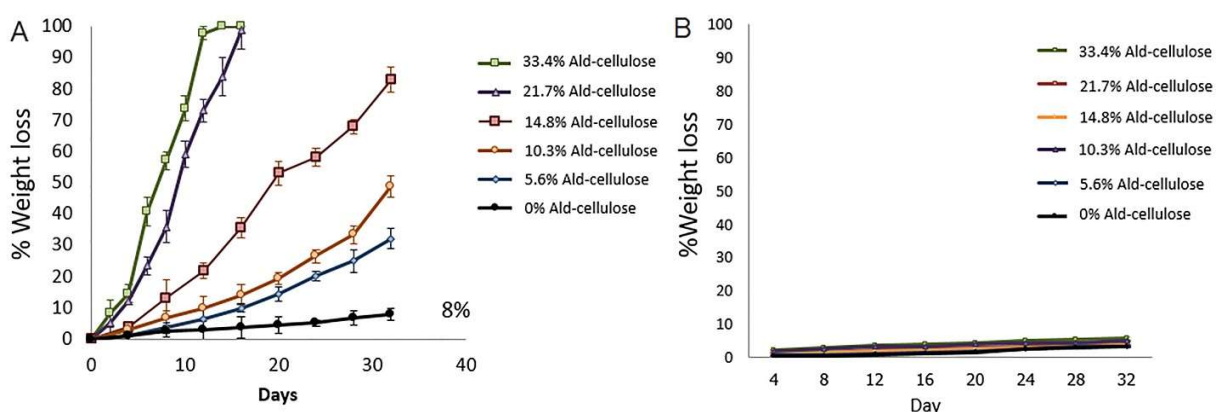


**Figure 3.20** Oxidized cellulose scaffold degradation in cultured media (a) and PBS (B) at 37 °C after 32 days.

Unoxidized cellulose scaffolds and 1% oxidized cellulose scaffolds with mean pore size of 250  $\mu\text{m}$  were submersed in cultured media to investigate scaffold degradation for 1 and 2 weeks and the oxidized cellulose scaffold morphology was determined by SEM (**Figure 3.21**). The results showed that the morphology of unoxidized cellulose scaffold before and after submerging for 1 and 2 weeks in culture media was very similar with initial structure, whole scaffolds was almost remained (**Figure 3.21a, 3.21b**). Interestingly, morphology of 1% oxidized cellulose scaffold after 1 week showed partial degradation. Subsequently, the morphology after 2 weeks was moderately deteriorated (**Figure 3.21c, 3.21d**). The result suggested that oxidized cellulose scaffold was more degraded than unoxidized one.

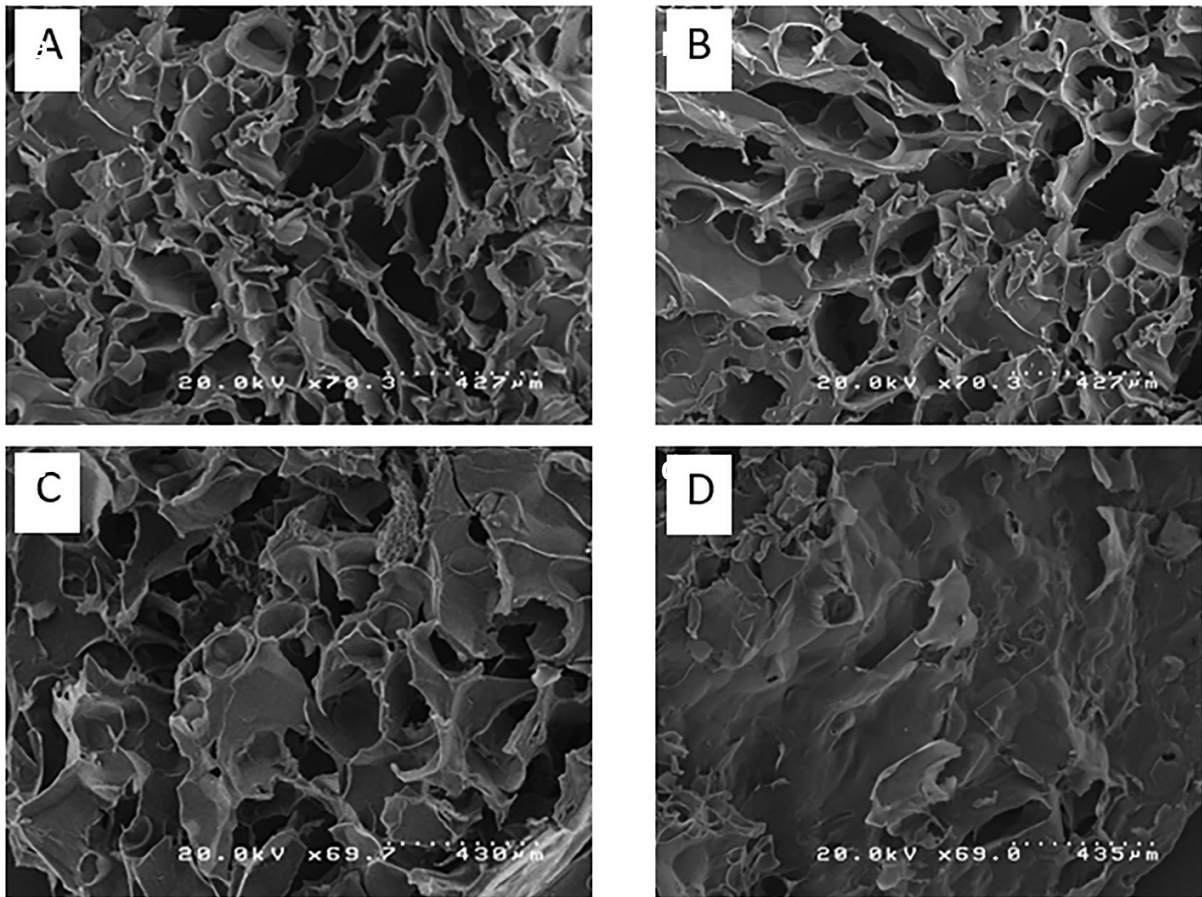


**Figure 3.21** SEM photograph of cellulose scaffold degradation in culture media; unoxidized cellulose scaffold for 1 and 2 week (a, b), 1% oxidized cellulose scaffold for 1 and 2 week (c, d).

Ideally, scaffold completely degraded and displaced by regenerated extra cellular matrix (ECM), eliminating the need for surgical scaffold dismissal but the scaffold should be degraded under controlling rate. Sung et al. [18] studied the effect of the degradation rate on cell viability and cell migration. The result showed that the rapid degradation negatively affects cell viability and cell migration *in vitro* and *in vivo*.

**Chapter 3**  
*Cellulose scaffold fabrication with ionic liquid and degradation control by Malaprade oxidation*

Precisely, enzymatic degradation could activate polymer breakdown. In my study, I proceeded to determine the degradation *in vitro* and *in vivo* (chapter 4). I did not proceed testing using the mimicking the enzyme fluid system.

There are many applications like long term culture for tissue engineering and therapeutically production, which needs the scaffold to be continued culture for 2 or 3 months. Consequently, *in vitro* degradation was considerable.

## **Conclusion**

In this chapter, I fabricated cellulose scaffold with open porous structure using 1-butyl 3-methylimidazolium chloride (BMIMCl) as ionic liquid and NaCl leaching method. BMIMCl is green solvent that dissolved native cellulose. The use of ionic liquid is uncomplicated method for preparation scaffold with unmodified cellulose fiber. The interconnected pore size was controlled by varying the diameter of NaCl particle size ranging from 50-250  $\mu\text{m}$ . The cellulose scaffold was oxidized with periodate via Malaprade oxidation. In this study, I use the knowledge of the controlling polysaccharide degradation for controlling the degradation scaffold for tissue engineering application. The degradation of scaffold is depended on the degree of oxidation. Subsequently, the degradation of oxidized cellulose scaffold was initially started when adding with the amino acid. This result is correlated with chapter 2 which indicated that the polysaccharide degradation is associated with Schiff base and Maillard reaction. The degradation time was fastest when cellulose was oxidized with 10% periodate, the cellulose was completely degraded after 16 days. Whereas, unoxidized cellulose scaffold showed very low degradation approximately 8% in

CO<sub>2</sub> incubator at 37 °C after 1 month. Moreover, the morphology of degraded cellulose scaffold after 2 weeks showed more deteriorated than 1 week.

## References

1. Yackel, E.C. and W.O. Kenyon, *The Oxidation of Cellulose by Nitrogen Dioxide\**. Journal of the American Chemical Society, 1942. **64**(1): p. 121-127.
2. Painter, T.J., *Preparation and periodate oxidation of C-6-oxycellulose: conformational interpretation of hemiacetal stability*. Carbohydrate Research, 1977. **55**(1): p. 95-103.
3. Pagliaro, M., *Autocatalytic oxidations of primary hydroxyl groups of cellulose in phosphoric acid with halogen oxides*. Carbohydrate Research, 1998. **308**(7): p. 311-317.
4. Arendt, J.H., et al., *Oxidation of cellulose by acid-sodium nitrite systems*. Journal of Polymer Science: Polymer Symposia, 1973. **42**(3): p. 1521-1529.
5. Varma, A.J. and M.P. Kulkarni, *Oxidation of cellulose under controlled conditions*. Polymer Degradation and Stability, 2002. **77**(1): p. 25-27.
6. Mikos, A.G., et al., *Preparation and characterization of poly(l-lactic acid) foams*. Polymer, 1994. **35**(5): p. 1068-1077.
7. Mikos, A.G., et al., *Biocompatible polymer membranes and methods of preparation of three dimensional membrane structures*. 1996: United States.
8. Quirk, R.A., et al., *Supercritical fluid technologies and tissue engineering scaffolds*. Current Opinion in Solid State and Materials Science, 2004. **8**(3-4): p. 313-321.
9. Lee, K.-W.D., P.K. Chan, and X. Feng, *Morphology development and characterization of the phase-separated structure resulting from the thermal-induced phase separation*

- phenomenon in polymer solutions under a temperature gradient*. Chemical Engineering Science, 2004. **59**(7): p. 1491-1504.
10. Thomson, R.C., et al., *Biodegradable polymer scaffolds to regenerate organs*, in *Biopolymers II*, N. Peppas and R. Langer, Editors. 1995, Springer Berlin Heidelberg. p. 245-274.
  11. Jain, K.K., *Role of nanotechnology in developing new therapies for diseases of the nervous system*. Nanomedicine (Lond), 2006. **1**(1): p. 9-12.
  12. Bhardwaj, N. and S.C. Kundu, *Electrospinning: A fascinating fiber fabrication technique*. Biotechnology Advances, 2010. **28**(3): p. 325-347.
  13. Pinkert, A., et al., *Ionic Liquids and Their Interaction with Cellulose*. Chemical Reviews, 2009. **109**(12): p. 6712-6728.
  14. Kosan, B., C. Michels, and F. Meister, *Dissolution and forming of cellulose with ionic liquids*. Cellulose, 2008. **15**(1): p. 59-66.
  15. Feng, L. and Z.-l. Chen, *Research progress on dissolution and functional modification of cellulose in ionic liquids*. Journal of Molecular Liquids, 2008. **142**(1-3): p. 1-5.
  16. Zhang, H., et al., *1-Allyl-3-methylimidazolium Chloride Room Temperature Ionic Liquid: A New and Powerful Nonderivatizing Solvent for Cellulose*. Macromolecules, 2005. **38**(20): p. 8272-8277.
  17. Shin, E., et al., *Fabrication of cellulose-based scaffold with microarchitecture using a leaching technique for biomedical applications*. Cellulose, 2014. **21**(5): p. 3515-3525.
  18. Sung, H.-J., et al., *The effect of scaffold degradation rate on three-dimensional cell growth and angiogenesis*. Biomaterials, 2004. **25**(26): p. 5735-5742.

**Chapter 3**  
*Cellulose scaffold fabrication with ionic liquid and  
degradation control by Malaprade oxidation*

# Chapter 4

---

## *In vitro and in vivo study of oxidized cellulose scaffold*

### 4.1 Introduction

#### 4.1.1 Protein adsorption

##### 4.1.1.2 Relevance

Protein interaction with solid surface is an important issue in the field of biocompatible material. Nowadays, products and medical devices become an important role in biomedical area, such as implants and surgical tools. When the foreign comes into the body, the immune system is operated. Subsequently, plasma proteins and extracellular matrix are aggregated in attempt to neutralize certain and eliminate the injurious agent. Fibroblasts and osteoblasts can encourage the cell attachment for repairing cell. Moreover, the material can cover with specific bioactive material to adsorb specific protein, wound healing or fibrous capsule formation. After endothelium formation, the body is disclosed to the foreign material and immune system will stop.

For tissue engineering application, the protein adsorption properties to non-specific surface considerably affected whether cells adhered to surface of scaffold. For example, artificial joint is

necessitated for protein integration with patient tissue and protein adsorption supports this integration. On the other hand, protein adsorption onto artificial blood vessel can be exceedingly disadvantageous event. For example, clotting factor adhesion can induce thrombosis leading to blockage and stroke. For this reason, the surgical tools or biomaterials surface is usually sterilized to prevent protein adsorption and contamination.

#### **4.1.2.2 Protein and surface interaction**

##### **a. Protein properties**

The interaction between protein and surface is evaluated by their properties of both protein and surface. The protein properties have the effect on their interaction with biomaterials surface, such as charge, size, structure alteration and amphipathicity. For the effect of size, the large molecule has more chance to interact or attach to the surface more than the small molecule (**Figure4.1**). For example, fibrinogen ( $M_w$  340 kDa) can contact with silica substrate approximately 703 contacts per molecule, whereas albumin ( $M_w$  67 kDa) can contact with silica substrate only 77 contacts per molecule[1]. However, size of protein is not only one determinant because hemoglobin (65 kDa) as small molecule showed high efficiency to attach the surface more than fibrinogen.

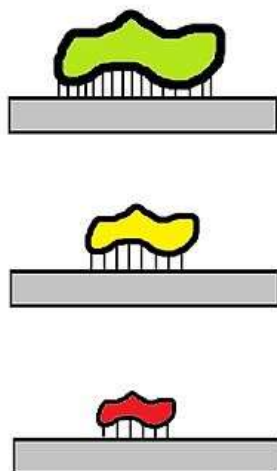


**Figure 4.1** Schematic of the size effect of protein to adsorb with material surface

Normally, charged amino acids are frequently placed on the outside of proteins molecule resulting to readily interact with material surface. Therefore, the charge distribution on protein surface is an important effect for protein adsorption. In the same case, charge is not only one determinant. Protein shows high efficiency for absorption near their isoelectric point (pI) because at pI the charge of protein is zero. Subsequently, protein molecule cannot interact with protein in isolation form. At pI point, electrostatic repulsion of uncharged protein is reduced for interaction with the surface. For another reason, the protein structure alteration is changed as the charge change. As a result, other amino acids can show up on protein surface resulting in changing the way for protein binding.

Moreover, the unfolding of protein is the one effect for protein adsorption. Unfolded protein shows more possibility or more sites on interaction with surface (**Figure4.2**). Consequently, the rate of unfolding protein has the effect on that rate of protein adsorption. For

example, glutamic acid in hemoglobin is substituted by hydrophobic valine resulting in unstable of hemoglobin. The destabilized hemoglobin results to accelerate fibrous and twist red blood cell[2].

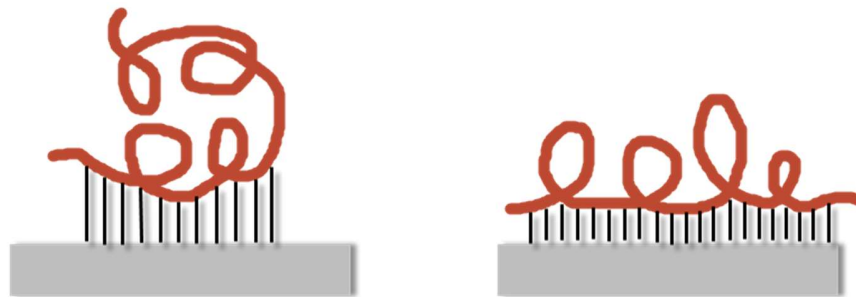


**Figure4.2** Illustration of the effect of protein unfolding on interaction with a surface.

In addition, protein has amphipathic, negative and positive charge, polar, non-polar spread on the molecule surface (**Figure4.3**). Even though, hydrophobic part usually located on the inside, whereas hydrophilic and charge normally locate outside. Hydrophobic amino acid may be located on protein surface for interaction with material surface.

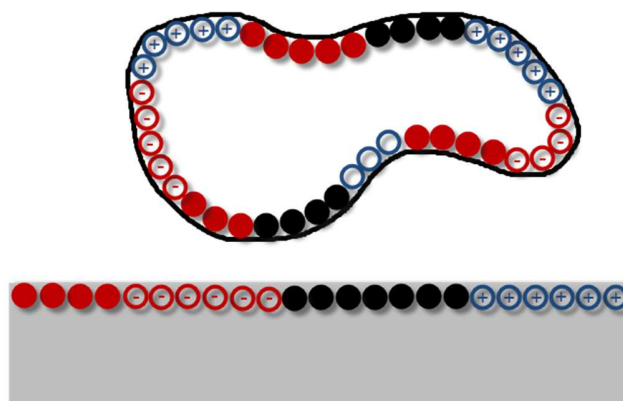


**Figure4.3** Illustration of both protein molecule and surface properties in determining protein-surface interactions.

## **b. Surface properties**

The important properties of surface for protein adsorption can be divided into 2 categories; chemical, geometric and electrical. The surface with high topographical will express more surface area to interact with protein. For example, material surfaces with more pores or grooves have more surface area when compare with flat surface. Many methods have been developed for modified biomaterial surface to enhance the possibility of protein adsorption.

Acid chloride and acid anhydrides were used for modification of chitosan film. The chitosan film showed more hydrophobic than the non-modified one because the film was grafted with stearyl group and showed more efficiency of protein adsorption [3]. To generate a calcium phosphate-rich surface layer, porous hydroxyapatite (HA) was treated with tris-buffered electrolyte solution. The treated porous showed high protein adsorption more than untreated porous HA. Consequently, cell adhered on modified porous HA greater than untreated porous HA[4]. In contrast, polyethylene glycol (PEG) usually used to resist protein adsorption for avoidance the immune system. Zhang et al. modified superparamagnetic magnetite nanoparticles surface by PEG and folic acid. After uptake in to macrophage cell, PEG modified nanoparticle showed low uptake than unmodified nanoparticle. Consequently, folic acid and PEG modified magnetite nanoparticles can be useful to prevent the protein adsorption resulting in avoidance the macrophage cells recognition[5]. Moreover, poly (ether urethane) was grafted with PEG and Pluronic PE9400 as amphiphilic polymer additive. The result showed that both PE9400 and PEG reduced fibrinogen adsorption[6].

#### 4.1.2 Cell and polymer interaction

For studying the cell interaction with polymer, cells are cultured on surface of polymer and evaluated the cell spreading and cell adhesion on polymer surface were evaluated. The important factors during cell cultivation on polymer surface are cell function, cell viability and cell motility. Although, *in vitro* experiment cannot procreate total cellular response which can observe in *in vivo*, and the controlling environment for culturing is easily more than *in vivo*.

For cell adhesion and cell spreading, cell adhesion is crucial factor because it oversteps other factor, such as, cell spreading, cell migration, cell function and cell differentiation. The simple procedure for evaluation the adhesion of cells on polymer surface include of 3 steps; (1) cell suspension over the polymer surface, (2) cultivation cells with polymer surface in cultured medium, (3) disconnection between adhered cell and polymer surface. The amount of adhered cells are determined with various methods, such as fluorescent labeled cells, radiolabeled cells, measurement of the concentration of the binding of dye to specific component such as DNA. For studying of cell migration, it is essential phenomenon for tissue engineering application because the cell potential for moving, it neither state the association of cell with polymer surface nor the other cell. Moreover, the cell aggregation is important for studying the interaction between cell and cell during the cell differentiation, cell migration, cell viability and cell formation. The cell aggregation morphology allows reconstruction of cell-cell interaction usually present in tissue. Consequently, cell function and survival are normally increased in aggregated culture [7, 8]. Hence, the cell aggregation may be benefit for tissue engineering, such as re-constitution tissue transplant [9] and increasing the cell function on artificial organ [10]. For tissue engineering application, cell function is frequently enhanced to promote and support cell-specific function. For

example, the production of extra cellular matrix (ECM) protein is essential for cell physiology, such as osteoblast [11], chondrocyte [12] and fibroblast [13].

### **4.1.3 Effect of polymer chemistry on cell behavior**

#### **4.1.3.1 Synthetic polymer**

For cell attachment on polymer surface, cell function and cell adhesion are depend on properties of polymer surface. For example, hydrophobic and hydrophilic plays an important role for cell attachment. Klebe et al. [14] stated that hydrophobic polymer surfaces are repeated for cell attachment and growth. This reason is based on the investigation of involving polymers with ester groups. Therefore, The enhancing of the nonhydrophilic polymer poly(vinyl acetate) blends with polyHEMA showed the increasing of cell attachment, whereas, hydrophilic poly-2-hydroxyethyl methacrylate (polyHEMA) showed non adhered for CHO cells[14]. In addition, the modification of cultured plate polystyrene with poly (2- hydroxyethyl methacrylate) (pHEMA) showed that cell attachment increased as pHEMA concentration increased [15, 16]. Consequently, it can be concluded that the hydrophobic/ hydrophilic character of polymer surface is important for cell attachment and cell function (Figure 4.4).

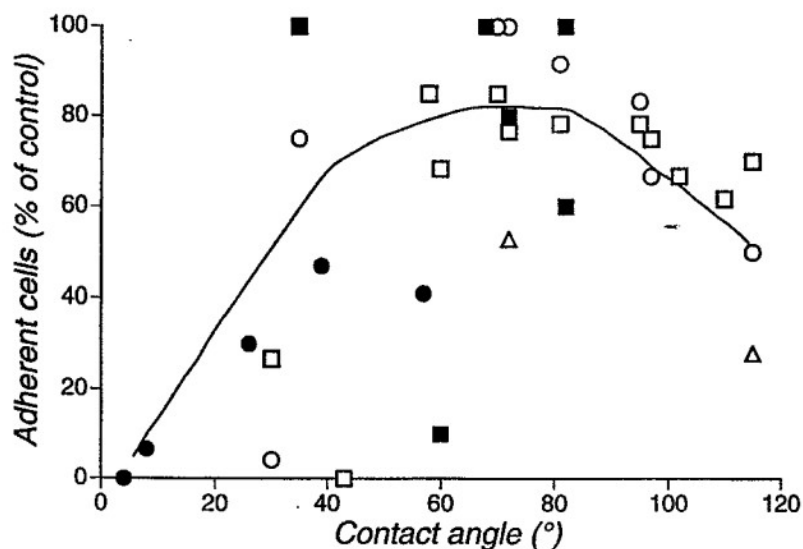


**Figure 4.4** The relationship between water in air contact angle and cell adhesion for variety surface; (□) fibroblast [13], (○) L cell [17], (△) endothelial cell [18], (●) endothelial cell [19], (■) fibroblast [20].

On most polymer surface, serum protein was required for cell adhesion, therefore, it is further supported that cell adhesion is related with protein adsorption (see 4.1.1), such as fibronectin [21]. In non-attendance of serum, cell adhesion is increased on positively charged polymer surface [19]. Many factor of polymer surface modification present to increase the protein adsorption, such as vitronectin and fibronectin, to the surface. Some researchers reported that specific chemical group has the effect cell adhesion onto polymer surface such as C-O surface [22] and -OH surface [23]. Furthermore, the interaction between cell adhesion and implanted polymer in *in vivo* are affected by chemical properties of implant surface. For example, the macrophages can form multinucleated giant cell on implanted polymer surface when the surface is present with difference chemical group. The macrophage increase in the order  $-\text{COOH}(\text{COONa}) > -\text{SO}_3\text{H} > -\text{OH} = -\text{CO}-\text{NH} > (\text{CH}_3)_2\text{N}$  [24, 25]. Lee et al. showed the similar hierarchy CHO cell adhesion on

polymer [26]. CHO cell growth and adhesion were in the order;  $-\text{COOH} > -\text{CONH}_2 > -\text{CH}_2\text{OH} > -\text{CH}_2\text{NH}_2$ .

#### 4.1.3.2 Biodegradable polymer

Ideally, degradable polymer should be wholly degraded and replaced by revived extra cellular matrix. Degradable polymer may allow a supplementary level for controlling over the interaction of cell; during the degradation of polymer, the polymer surface should be continually renewed, giving a dynamic of surface for cell growth and cell attachment. The biodegradable films of poly(glycolic acid) (PGA), poly(lactic acid) (PLA) and poly(lactide-co-glycolide) (PLGA) were treated with chloric acid (CA) to increase wettability and improve cell proliferation and cell adhesion of human chondrocytes and NIH/3T3 fibroblasts [26]. Moreover, PLGA was cooperated with poly(D,L-lactide-co-glycolide) as porogen for extending pores in scaffold. The degradation of polymer showed biphasic pattern, the initial rapid degradation for 20–30 days come after by a slower degradation rate [27]. For long term implant in tissue engineering application, polycaprolactone is usually used because the degradation rate is very slow for pure polycaprolactone, approximately 2-3 years. To increase the degradation speed of polycaprolactone, it is frequently combine with poly(L-lactic acid) (PLLA)[28, 29], poly(lactide-co-glycolide) (PLGA)[30, 31], poly (D,L lactic acid)(PDLLA)[32, 33]. Moreover, Poly(propylene fumarate) (PPF) is favorable for tissue engineering application because PPF is injectable liquid becomes solid during crosslinking. Consequently, it is usually used for filling bone depot [34, 35] and defect, extending of ocular drugs delivery [36, 37].

## **4.2 Materials and method**

### **4.2.1 Protein adsorption**

Protein adsorption was performed by incubating the scaffolds in culture medium containing 10% fetal bovine serum (FBS). The 0%, 0.5%, 2.5%, 5% oxidized cellulose scaffold with 1.0 cm in diameter and 0.3 cm in thickness without cell were incubated for 1 day and then, the culture in medium was removed. Two hundred microliter of PBS (0.1M, pH 7.4) was replaced. The scaffolds were washed twice or more with PBS and then, incubated with 0.1 mL sodium dodecyl sulfate solution for 1h at 37 °C. The concentration of the protein adsorption was quantified with a commercial protein assay kit, BCA (Thermo Scientific, Rockford, US), using bovine serum albumin (BSA) standards.

### **4.2.2 Cell growth investigation**

The experiments were divided into two groups; first group is using 5% oxidized cellulose scaffold for investigation cell growth on different scaffold pore size ; second group is using 0%, 0.5%, 2.5% and 5% oxidized cellulose scaffold for investigation of the effect of the oxidation degree for cell growth on scaffold with mean pore size 250  $\mu\text{m}$ . Before culturing cell with scaffold, the scaffolds were sterilized by soaking in 70% ethanol, and then ethanol solution was removed by distilled water for 3 times and then dried. The scaffolds were put into a 12-well plate and seeded with 2 mL of culture medium containing mesenchymal stem cell (MSC)  $2.5 \times 10^5$  cells/ml. Cells were cultured with oxidized cellulose scaffold for 3, 5, 7 days in the CO<sub>2</sub> incubator without stirring at 37 °C. Cell numbers were counted with CCK-8 kit (Dojindo Molecular Technologies, Inc., Rockville, US).

### **4.2.3 Cell fixation on oxidized cellulose scaffold**

MSCs were plated on oxidized cellulose scaffold at  $2.5 \times 10^5$  /scaffold oxidized cellulose scaffold and prepared for SEM (Hitachi, Tokyo, Japan) after 1 and 2 week of culture. SEM was utilized to observe the morphology of cells on the oxidized cellulose scaffold. The pore of oxidized cellulose scaffolds with cells were blotted to dry with absorbent papers and washed with phosphate buffered saline (PBS), pH 7.4. Cells were fixed with glutaraldehyde (4% v/v in PBS) for 24 hours at room temperature. Then, glutaraldehyde was discarded and oxidized cellulose scaffold with cells were washed with PBS. The oxidized cellulose scaffolds with cells were subjected to sequential dehydration in graded ethanol (60%, 70%, 80%, 90%, and 100%). The scaffolds were taken out, dried and stored at 4 °C till observation. The cell morphology was evaluated by SEM.

### **4.2.4 Animal implantation**

Implantation of 0%, 0.5%, 2.5%, 5% oxidized cellulose scaffolds under the skin of the flank of rat (SD rat, 9 weeks, male) were performed under sterilized conditions in a clean room. All experiments were performed according to the guidelines of the Animal Welfare Committee of the university. The oxidized cellulose scaffolds were sterilized by submerged into 70% (v/v) ethanol for 15 min and washing with PBS (pH 7.4) 3 times for 10 min. Before implantation, the hair of skin was shaved. Then all rat were anesthetized by 2% isoflurane. All oxidized cellulose scaffolds were subcutaneously implanted under the skin. The rats were sacrificed after 1 week, 1 month and 3 months. At harvest, the implantation sites were cut in a full thickness manner.

#### 4.2.5 Histological study

The specimen was fixed with 4% *p*-formaldehyde solution for overnight and submerged in 30% sucrose in PBS for 2-4 days. Subsequently, it was dehydrated by sequential dehydration in graded ethanol (70%, 80%, 90%) for 1 hour. After the immersion in 100% ethanol for 20 min, it was submerged for embedding in the xylene-ethanol mixture (xylene : ethanol = 3 : 1) for 30 min, 100% xylene for 3 min in twice, 1:1 xylene: paraffin at 65- 75 °C for 30 min, and 3 times 100% paraffin for 30 min, respectively. Then, the specimen was immersed into paraffin solution at 65 °C, and this solution was cooled on the ice bath to firm the paraffin containing the tissue sample.

Paraffine sections (thickness: 10 µm) were prepared by microtome (RM2235, Leica Biosystems, Tokyo, Japan) and affixed to slide glass. These slide glasses were immersed two times for 3 min into xylene to remove the paraffine. And then, slide glasses were immersed to ethanol for 2 min in twice, 90% ethanol for 2 min, 80% ethanol for 2 min, and 70% ethanol for 2 min. Finally, these samples were replaced to water by the immersion in water for 30 min and dried overnight at room temperature.

Tissue sections on slide glass were treated with blocking reagent (20% Blocking One (Nacalai Tesque, Kyoto, Japan) in PBS) for 2 hours. Then, the blocking solution containing anti-monocytes/macrophages antibody (1:100, mouse monoclonal (ED1) IgG<sub>1</sub>, Millipore, Temecula, CA, USA) was mounted to the tissue section and reacted for 2 h. After washing with PBS-T, tissue section was stained with anti-mouse IgG<sub>1</sub>-Alexa 594 antibody (ThermoFisher, Waltham, MA, USA) and Hoechst33258 (Dojindo, Kumamoto, Japan) for 30 min. these samples were washed with PBS. The localization of secondary antibody was analyzed with an fluorescent microscope (IX70, Olympus Optical Co. Ltd., Tokyo, Japan).

## 4.3 Results and discussion

### 4.3.1 Protein adsorption

The interaction between cell and protein directly related with cell differentiation, growth, adhesion, migration and apoptosis [38]. The adsorption of protein to scaffold was evaluated for understanding cell behavior on scaffold. The 0%, 0.5%, 2.5%, 5% oxidized cellulose scaffolds with different mean pore size were submerged in 10% FBS containing medium and determined protein adsorption by BCA assay kit. As BCA assay, peptide containing three or more amino acid residues is form a purple colored chelate complex with cupric ions ( $\text{Cu}^{2+}$ ) in an alkaline environment containing sodium potassium tartrate.

**Figure 4.5** showed the protein adsorption of 0%, 0.5%, 2.5% and 5% oxidized cellulose scaffold with different mean pore size 52, 75, 100, 150 and 250  $\mu\text{m}$ . For 5% oxidized cellulose scaffold with mean pore size 250  $\mu\text{m}$ , showed the highest protein adsorption approximately 1155.56  $\mu\text{g}$ . When compared with the different mean pore size with the same degree of oxidation, it showed that the protein adsorption increased as the mean pore size increased,  $250 > 150 > 100 > 75 > 52$   $\mu\text{m}$  respectively. Moreover, protein adsorption of various oxidation degree with the same mean pore size was compared. This result is supported by Woo et al. [38] they made nanofibrous scaffolds with phase separation technique and porogen leaching. The results suggested that the pores of nanofibrous scaffolds (pore size ranging 50–500 nm) increased protein adsorption more than solid scaffold (pore size ranging 250–420  $\mu\text{m}$ ) of the same material [38].

Moreover, the result indicated that the protein adsorption increased with increase in oxidation degree. Due to the Malaprade reaction, results in many amount of carbonyl groups,

amine can react with carbonyl group via Schiff base reaction, whereas, hydroxyl group in glucopyranose ring can not react with amine group. Therefore, it might induce protein interaction.

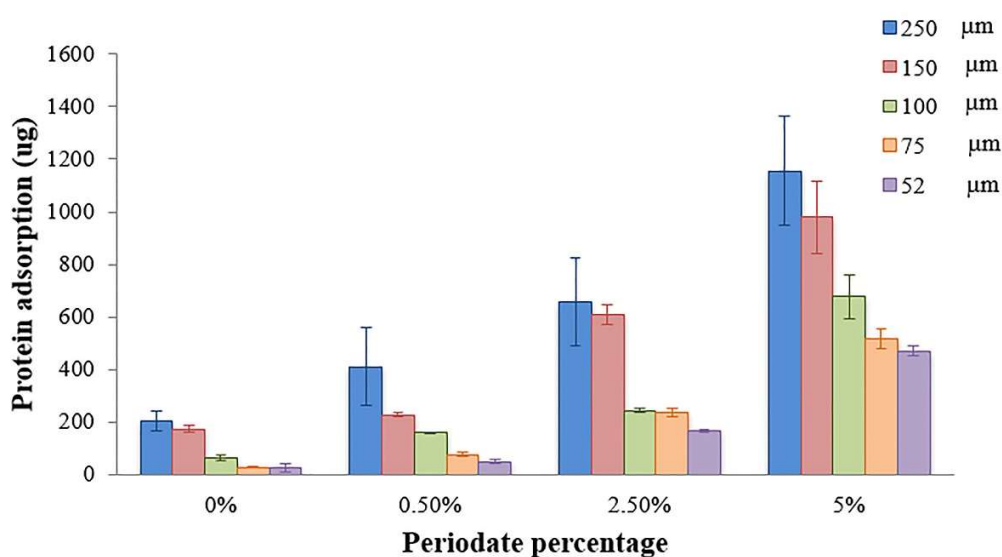


**Figure 4.5** Protein adsorption on 0%, 0.5%, 2.5%, 5% oxidized cellulose scaffold difference mean pore size.

#### 4.3.2 Pore size effect to cell growth

For pore size effect on cell growth, MSCs were cultured on 1% oxidized cellulose scaffold for 3, 5 and 7 days (**Figure 4.6**). The result showed that cell number on 5% oxidized cellulose scaffold with mean pore size of 250 μm was highest at approximately  $5.77 \times 10^5$  cells after 7 days. In the meantime, cell numbers on 1% oxidized cellulose scaffold with mean pore size of 52, 75, 100, 120 μm were  $3.07 \times 10^5$ ,  $3.24 \times 10^5$ ,  $3.74 \times 10^5$  and  $4.16 \times 10^5$  cell respectively. The results

indicated that cell growth increased with increase in mean pore sized of scaffolds. This result is conflicted with previous report [38] which stated that scaffold with small pore size is high specific volume and promote protein adsorption and cell attachment.

However, our result is supported by the report of Murphy et al [39] . They fabricated collagen–glycosaminoglycan scaffolds with pore size ranging 85-325  $\mu\text{m}$  for bone tissue engineering and investigated the effect of pore size on cell growth. The result suggested that cell number on collagen–glycosaminoglycan scaffolds with the biggest pore size 325  $\mu\text{m}$  was highest. Consequently, larger pore size allowed for improve of cellular infiltration. The larger pore reduced cell aggregation along the edges of the scaffold, promoting cell proliferation and migration into the center of the scaffold [40]

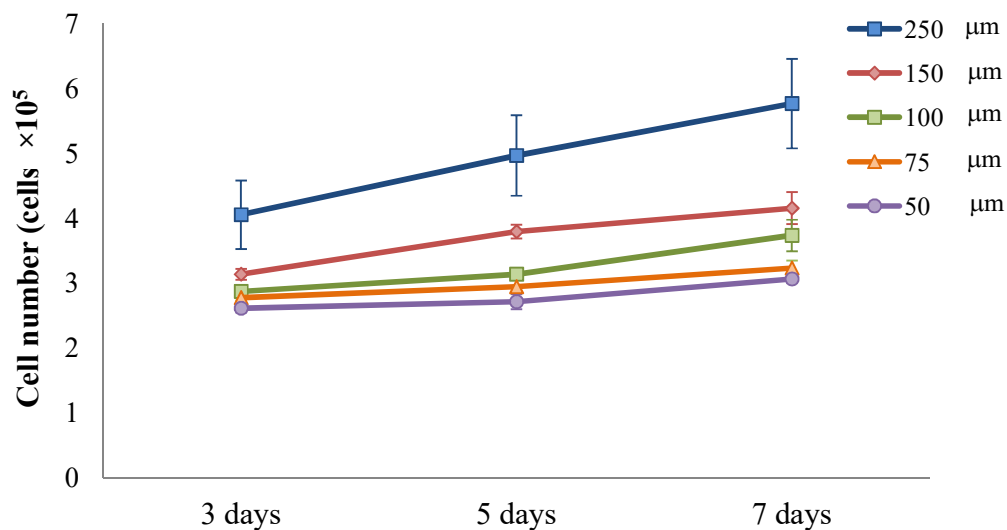


**Figure 4.6** Effect of mean pore size of scaffold on cell number. Cells were cultured with 5% oxidized cellulose scaffold with difference mean pore size 52, 75, 100, 150, 250  $\mu\text{m}$  respectively.

### 4.3.3 The degree of oxidation effect to cell growth

For the degree of oxidation effect on cell growth, MSCs was cultured with 0%, 0.5%, 2.5%, 5% oxidized cellulose scaffold for 3, 5 and 7 days (**Figure 4.7**). The result showed that cell number with 5% oxidized cellulose scaffold was highest of approximately  $6.71 \times 10^5$  cells/ scaffold. Meanwhile, cell number on 0%, 0.5%, 2.5% were  $4.63 \times 10^5$ ,  $4.91 \times 10^5$ ,  $5.70 \times 10^5$  cells/ scaffold respectively. The results indicated that cell numbers increased with increase in the degree of oxidation in scaffold. The reaction of cells with aldehydes scaffold may be anticipated with two effects. One is the production of an anionic surface by elimination of free amino groups. Another one is more lipophilic by attachment of the aliphatic group. Either of these effects could increase the affinity of the cell for proteins through salt-like or non-ionic forces [41]. In fact, before cells adhesion, adsorption of cell adhesive proteins onto the polymer surface occurs first. Subsequently, cells attached onto protein leading to adhesion of all on polymer surface. Hence, the cell growth result is correlated with protein adsorption result.

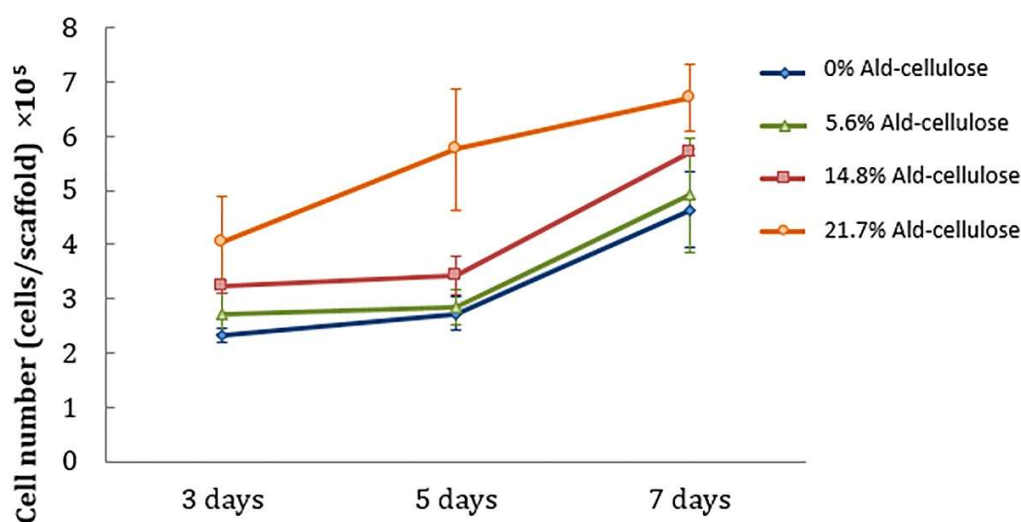
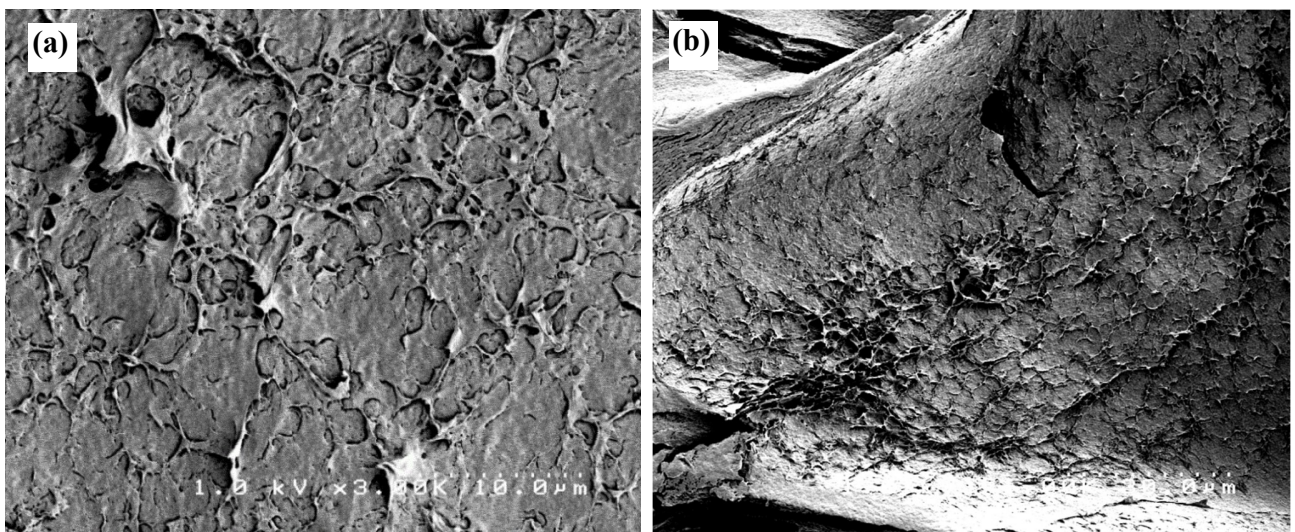


Figure4.7

Effect of oxidation degree of cellulose scaffold mean pore size 250 for 3, 5, 7 days to cell growth.

In addition, 5% oxidized cellulose scaffold was selected to observe the biocompatibility. SEM photographs of cultivated fibroblast (**Figure4.8a**) and MSCs (**Figure4.8b**) after 1 week showed that cell adhered well on oxidized cellulose scaffold surface. It is indicated that oxidized cellulose scaffold is promoted fibroblast and MSC growth.



**Figure4.8** SEM photograph showing fibroblast (a) and MSC (b) on 5% oxidized cellulose scaffold after 1 week.

#### 4.3.4 Animal test

For preliminary study, 0%, 0.5%, 5% oxidized cellulose scaffolds were subcutaneously implanted on mice back and then, the mice were sacrificed after 1 week. As **Figure 4.9a**, unoxidized cellulose scaffold showed no degradation because the whole construct of scaffold was remained. While, 0.5% oxidized cellulose scaffold was partially degraded (**Figure 4.9b**). In mean time, 5% oxidized cellulose scaffold was moderately degraded after 1 week (**Figure 4.9c**).

However, all scaffolds showed highly inflammation because the host tissue could not heal itself after surgical only 1 week.



**Figure 4.9** Implantation of 0% (a), 0.5% (b), 5% (c) oxidized cellulose scaffold under mouse backs after 1 week.

The oxidized cellulose scaffolds were subcutaneously implanted on mice back. The mice were sacrificed after 1 week, 1 month and 3 months. As **Figure 4.10a, 4.10b, 4.10c** showed the interaction between 0% oxidized cellulose scaffold and host tissue. After 1 week, it does not clearly showed the morphology of scaffold because it appeared of high inflammation due to the surgical and bleeding. For 0% oxidized cellulose scaffold after 1 month and 3 months (**Figure 4.10b, 4.10c**), the scaffold can kept the whole construct of scaffold. Cell infiltration into the scaffold (**Figure 4.10b**) was not seen. While, partially cells were infiltrated into the scaffold after 3 months. The cells were accumulated around the outside near the edge of scaffold. It is not clearly seen the inflammation of host tissue because it has been encapsulated by fibrous tissue after 3 months (**Figure 4.10c**).

In the case of 0.5% oxidized cellulose scaffold after 1 month and 3 months (**Figure 4.10e, 4.10f**), showed that the cells moderately infiltrated into the scaffold and a few cells spread around

the scaffold. However, degradation of scaffold does not occur, whereas, the inflammation initially started (**Figure 4.10e**). Interestingly, 0.5% oxidized cellulose scaffold after 3 months showed a large number of cells infiltration into cellulose scaffold. At the same time, the inflammation continued for 1 month (**Figure 4.10f**).

Interestingly, 2.5% oxidized cellulose scaffold showed high degradation with low inflammation after 1 month and 3 months (**Figure 4.10h, 4.10i**). After 1 month, almost cell can infiltrate in the scaffold with high degradation, while, the scaffold showed the less inflammation of host tissue (**Figure 4.10h**). Subsequently, 2.5% oxidized cellulose scaffold after 3 months was almost degraded; the construct of scaffold was still remained (black arrow). Moreover, the host tissue at the center of scaffold and adjacent area became plenary when compare with without implantation host tissue (**Figure 4.10i**).

In the case of 5% oxidized cellulose scaffold after 1 month, the degradation of scaffold was more than 0.5% and 2.5% oxidized cellulose scaffold resulting to a few construct of scaffold. After 1 month, the scaffold became lean and small (black arrow). A large number of cells spreads around in the scaffold (**Figure 4.10k**). However, the host tissue showed high inflammation and it continued until 3 months. After 3 months, 5% oxidized cellulose scaffold became tattered. It showed 3 specimen (black arrow) which suggested that the scaffold was battered, though, the host tissue showed highly inflammation due to high degree of oxidation of the scaffold (**Figure 4.10l**).

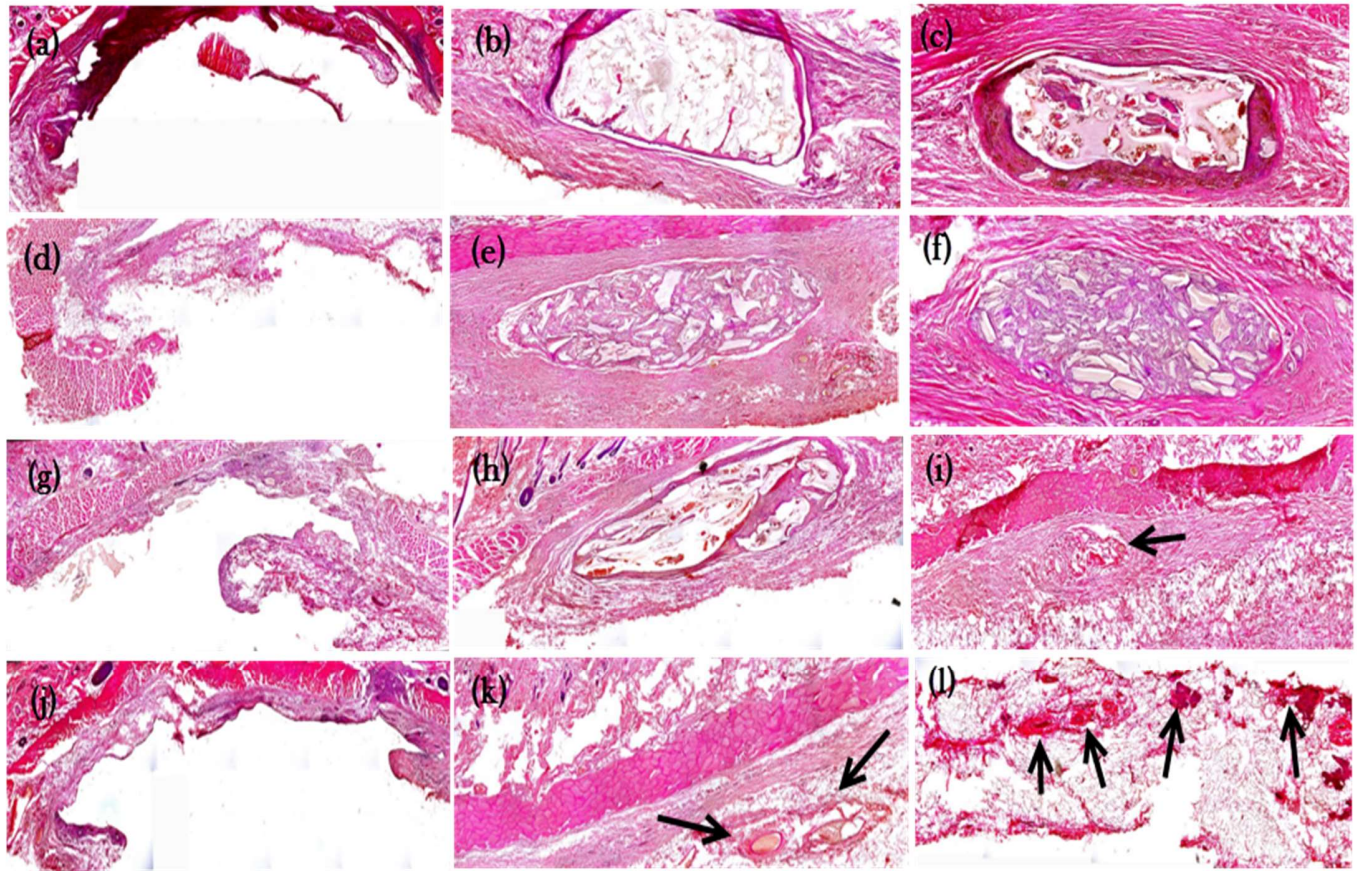


**Figure 4.10** H&E staining was performed to investigate real time interaction between oxidized cellulose scaffold and host, unoxidized cellulose scaffold after 1 week (a), 1 month (b), 3 months (c), 0.5% cellulose scaffold after 1 week (d), 1 month (e), 3 months (f), 2.5% cellulose scaffold after 1 week (g), 1 month (h), 3 months (i), 5.0% cellulose scaffold after 1 week (j), 1 month (k), 3 months (l).

Moreover, the inflammation during implantation the oxidized cellulose scaffold was observed by immuno staining of macrophage. After 1 week of implantation, 2.5% and 5% oxidized cellulose scaffold showed high inflammation (red spot) surrounding outside of scaffold (white dash line) (**Figure 4.11g, 4.11j**) because only 1 week has passed from operation. After 1 month of implantation, 0.5% oxidized cellulose scaffold showed very high inflammation of host tissue

where infiltrated into the scaffold (**Figure 4.11e**). After 3 months, inflammation was remaining with all oxidized cellulose scaffold (**Figure 4.11c, 4.11f, 4.11i, 4.11l**). Interestingly, 2.5% oxidized cellulose scaffold showed lowest inflammation after 3 months (**Figure 4.11i**). This result is further supported and correlated with H&E staining.

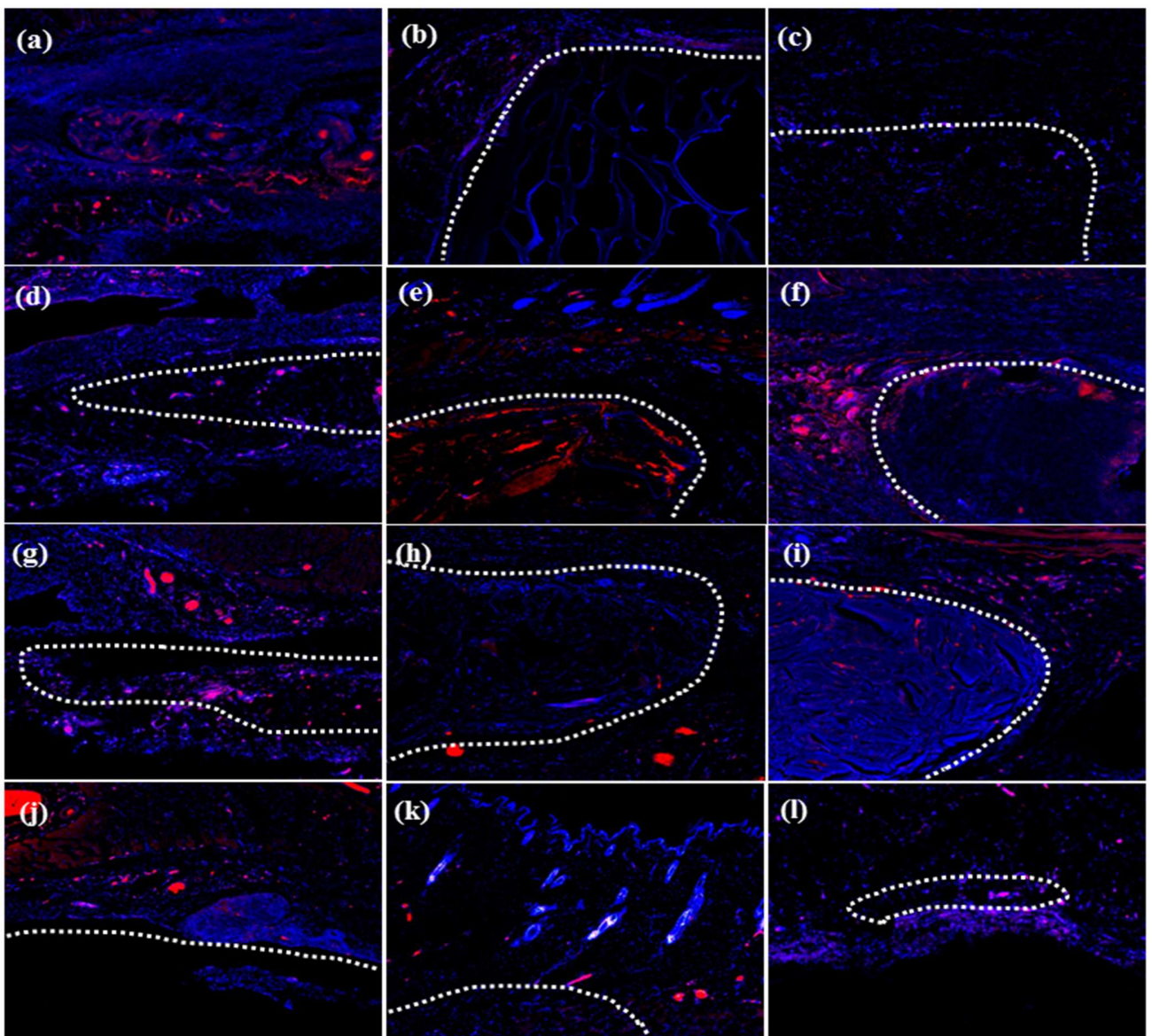


**Figure 4.11** Hoechst33258 staining was performed to investigate the inflammation during implantation, unoxidized cellulose scaffold after 1 week (a), 1 month (b), 3 months (c), 0.5% cellulose scaffold after 1 week (d), 1 month (e), 3 months (f), 2.5% cellulose scaffold after 1 week (g), 1 month (h), 3 months (i), 5.0% cellulose scaffold after 1 week (j), 1 month (k), 3 months (l).

#### **4.4 Conclusion**

In this chapter, the protein adsorption and cell attachment were observed. Protein adsorption is an important factor for judgement of the biocompatibility of material. In the meantime, cell growth on scaffold is a very important role for identity of biocompatibility. Interestingly, the protein adsorption on oxidized cellulose scaffold increased with increase in pore size of scaffold and degree of oxidation. In the case of pore size, large pore size promoted cell infiltration and penetration into the center of scaffold and reduced cell accumulation on the edge of scaffold. In the case of degree of oxidation, high aldehyde content such as high reactive carbonyl group can interact with amine in polypeptide chain resulting in high protein adsorption. Subsequently, cell number which attached on oxidized cellulose scaffold was increased with increase in oxidation degree. From histological study, 2.5% oxidized cellulose scaffold showed high degradation with low inflammation after 1 and 3 months. Although, 5% oxidized cellulose scaffold was completely degraded after 3 months the inflammation was very high due to high degree of oxidation resulting in toxicity to host tissue.

#### **References**

1. Roach, P., D. Farrar, and C.C. Perry, *Surface Tailoring for Controlled Protein Adsorption: Effect of Topography at the Nanometer Scale and Chemistry*. Journal of the American Chemical Society, 2006. **128**(12): p. 3939-3945.
2. Arends, T., et al., *Haemoglobin North Shore-Caracas  $\beta$ 134 (H12) valine  $\rightarrow$  glutamic acid*. FEBS Letters, 1977. **80**(2): p. 261-265.
3. Tangpasuthadol, V., N. Pongchaisirikul, and V.P. Hoven, *Surface modification of chitosan films.: Effects of hydrophobicity on protein adsorption*. Carbohydrate Research, 2003. **338**(9): p. 937-942.
4. El-Ghannam, A., P. Ducheyne, and I.M. Shapiro, *Effect of serum proteins on osteoblast adhesion to surface-modified bioactive glass and hydroxyapatite*. Journal of Orthopaedic Research, 1999. **17**(3): p. 340-345.
5. Zhang, Y., N. Kohler, and M. Zhang, *Surface modification of superparamagnetic magnetite nanoparticles and their intracellular uptake*. Biomaterials, 2002. **23**(7): p. 1553-1561.
6. Wesslen, B., et al., *Protein adsorption of poly(ether urethane) surfaces modified by amphiphilic and hydrophilic polymers*. Biomaterials, 1994. **15**(4): p. 278-84.
7. Koide, N., et al., *Continued high albumin production by multicellular spheroids of adult rat hepatocytes formed in the presence of liver-derived proteoglycans*. Biochemical and Biophysical Research Communications, 1989. **161**(1): p. 385-391.
8. Landry, J., et al., *Spheroidal aggregate culture of rat liver cells: histotypic reorganization, biomatrix deposition, and maintenance of functional activities*. The Journal of Cell Biology, 1985. **101**(3): p. 914-923.
9. Langer, R. and J.P. Vacanti, *Tissue engineering*. Science, 1993. **260**(5110): p. 920-6.

10. Nyberg, S.L., et al., *Evaluation of a Hepatocyte-Entrapment Hollow Fiber Bioreactor: A Potential Bioartificial Liver* Biotechnology and Bioengineering, 1992. **41**(2): p. 194-203.
11. Ishaug, S.L., et al., *Osteoblast function on synthetic biodegradable polymers*. Journal of Biomedical Materials Research, 1994. **28**(12): p. 1445-1453.
12. Benya, P.D. and J.D. Shaffer, *Dedifferentiated chondrocytes reexpress the differentiated collagen phenotype when cultured in agarose gels*. Cell, 1982. **30**(1): p. 215-24.
13. Tamada, Y. and Y. Ikada, *Fibroblast growth on polymer surfaces and biosynthesis of collagen*. J Biomed Mater Res, 1994. **28**(7): p. 783-9.
14. Klebe, R.J., K.L. Bentley, and R.C. Schoen, *Adhesive substrates for fibronectin*. Journal of Cellular Physiology, 1981. **109**(3): p. 481-488.
15. Grinnell, F. and M.K. Feld, *Adsorption characteristics of plasma fibronectin in relationship to biological activity*. J Biomed Mater Res, 1981. **15**(3): p. 363-81.
16. Grinnell, F. and M.K. Feld, *Fibronectin Adsorption on Hydrophilic and Hydrophobic Surfaces Detected by Antibody Binding and Analyzed during Cell Adhesion in Serum-containing Medium*. THE JOURNAL OF BIOLOGICAL CHEMISTRY, 1982. **257**(10): p. 4888-4893.
17. Ikada, Y., *Proceedings of the 4th International Conference Biointeractions '93 Molecular Aspects of Biomaterials Surface modification of polymers for medical applications*. Biomaterials, 1994. **15**(10): p. 725-736.
18. Hasson, J.E., D.H. Wiebe, and M.W. Abbott, *Adult Human Vascular Endothelial Cell Attachment and Migration on Novel Bioabsorbable Polymers*. Archives of Surgery, 1987. **122**(4): p. 428-430.

19. van Wachem, P.B., et al., *Adhesion of cultured human endothelial cells onto methacrylate polymers with varying surface wettability and charge*. *Biomaterials*, 1987. **8**(5): p. 323-328.
20. Saltzman, W.M., et al., *Fibroblast and hepatocyte behavior on synthetic polymer surfaces*. *Journal of Biomedical Materials Research*, 1991. **25**(6): p. 741-759.
21. Horbett, T.A. and M.B. Schway, *Correlations between mouse 3T3 cell spreading and serum fibronectin adsorption on glass and hydroxyethylmethacrylate–ethylmethacrylate copolymers*. *Journal of Biomedical Materials Research*, 1988. **22**(9): p. 763-793.
22. Chinn, J.A., et al., *Enhancement of serum fibronectin adsorption and the clonal plating efficiencies of Swiss mouse 3T3 fibroblast and MMI4 mouse myoblast cells on polymer substrates modified by radiofrequency plasma deposition*. *Journal of Colloid and Interface Science*, 1989. **127**(1): p. 67-87.
23. Curtis, A. and J. Forrester, *Adhesion of cells to polystyrene surfaces*. *The Journal of Cell Biology*, 1983. **97**(5): p. 1500-1506.
24. Smetana, K., *Cell biology of hydrogels*. *Biomaterials*, 1993. **14**(14): p. 1046-1050.
25. Smetana, K., et al., *The influence of hydrogel functional groups on cell behavior*. *Journal of Biomedical Materials Research*, 1990. **24**(4): p. 463-470.
26. Lee, S.J., et al., *Interaction of human chondrocytes and NIH/3T3 fibroblasts on chloric acid-treated biodegradable polymer surfaces*. *J Biomater Sci Polym Ed*, 2002. **13**(2): p. 197-212.
27. Panyam, J., et al., *Polymer degradation and in vitro release of a model protein from poly(d,l-lactide-co-glycolide) nano- and microparticles*. *Journal of Controlled Release*, 2003. **92**(1–2): p. 173-187.

28. Ito, Y., et al., *Three-layered microcapsules as a long-term sustained release injection preparation*. International Journal of Pharmaceutics, 2010. **384**(1–2): p. 53-59.
29. Lu, X.L., et al., *Study on the shape memory effects of poly(l-lactide-co-ε-caprolactone) biodegradable polymers*. Journal of Materials Science: Materials in Medicine, 2008. **19**(1): p. 395-399.
30. Singh, A., et al., *Efficient Modulation of T-cell Response by Dual-mode, Single-carrier Delivery of Cytokine-targeted siRNA and DNA Vaccine to Antigen-presenting Cells*. Mol Ther, 2008. **16**(12): p. 2011-2021.
31. Singh, J., et al., *Diphtheria toxoid loaded poly-(ε-caprolactone) nanoparticles as mucosal vaccine delivery systems*. Methods, 2006. **38**(2): p. 96-105.
32. Richter, A., et al., *Solubilization of Sagopilone, a poorly water-soluble anticancer drug, using polymeric micelles for parenteral delivery*. International Journal of Pharmaceutics, 2010. **389**(1–2): p. 244-253.
33. Rieger, J., et al., *Polyester Nanoparticles Presenting Mannose Residues: Toward the Development of New Vaccine Delivery Systems Combining Biodegradability and Targeting Properties*. Biomacromolecules, 2009. **10**(3): p. 651-657.
34. Christenson, E.M., et al., *Biodegradable Fumarate-Based PolyHIPEs as Tissue Engineering Scaffolds*. Biomacromolecules, 2007. **8**(12): p. 3806-3814.
35. Kim, C.W., et al., *Characterization of porous injectable poly-(propylene fumarate)-based bone graft substitute*. Journal of Biomedical Materials Research Part A, 2008. **85A**(4): p. 1114-1119.
36. Haesslein, A., et al., *Long-term release of fluocinolone acetonide using biodegradable fumarate-based polymers*. Journal of Controlled Release, 2006. **114**(2): p. 251-260.

37. Ueda, H., et al., *Injectable, in situ forming poly(propylene fumarate)-based ocular drug delivery systems*. Journal of Biomedical Materials Research Part A, 2007. **83A**(3): p. 656-666.
38. Woo, K.M., V.J. Chen, and P.X. Ma, *Nano-fibrous scaffolding architecture selectively enhances protein adsorption contributing to cell attachment*. Journal of biomedical materials Research Part A, 2003. **67A**(2): p. 531-537.
39. Murphy, C.M., M.G. Haugh, and F.J. O'Brien, *The effect of mean pore size on cell attachment, proliferation and migration in collagen-glycosaminoglycan scaffolds for bone tissue engineering*. Biomaterials, 2010. **31**(3): p. 461-6.
40. Murphy, C.M., M.G. Haugh, and F.J. O'Brien, *The effect of mean pore size on cell attachment, proliferation and migration in collagen-glycosaminoglycan scaffolds for bone tissue engineering*. Biomaterials, 2010. **31**(3): p. 461-466.
41. Ling, N.R., *The Attachment of Proteins to Aldehyde-Tanned Cells*. British Journal of Haematology, 1961. **7**(3): p. 299-302.

## Chapter 5

---

### *Conclusion*

By the objective of this research, we want to explore the controlling of degradation mechanism of polysaccharide for tissue engineering application. Our 2-dimensional NMR data suggests that 4 substructures of hemiacetal were presence via Malaprade oxidation. Substructure 2 which C<sub>3</sub> was removed showed time constant of degradation approximately  $1.5 \pm 0.43$  h. It was excellently faster than substructure 3 and substructure 4 which cleavage between C<sub>2</sub>-C<sub>3</sub> and C<sub>3</sub>-C<sub>4</sub> respectively. In addition, methylene was generated at time constant 1.8 h. It suggested that the degradation of oxidized dextran in glycine as primary amino acid is related with Maillard reaction because methylene is the one component of 3-deoxyosone which undergo to Strecker degradation and formic acid. Moreover, the decreasing of oxidized dextran molecular weight was decreased as oxidation degree and glycine concentration increased. It might be increased the intermolecular interaction of carbonyl reactive group with amine group of glycine resulting in high degradation. It stated that the mechanism of polysaccharide degradation by Malaprade reaction was explored. The oxidized polysaccharide is controlled by varying the concentration of periodate and primary amino acid.

Moreover, we fabricated cellulose scaffold with open porous structure using 1-butyl 3-methylimidazolium chloride (BMIMCl) as ionic liquid and NaCl leaching method. BMIMCl is green solvent that dissolved native cellulose. The use of ionic liquid is uncomplicated method for preparation scaffold with unmodified cellulose fiber. The interconnected pore size was controlled by varying the diameter of NaCl particle size ranging from 50-250  $\mu\text{m}$ . The cellulose scaffold was oxidized with periodate for converting hydroxyl group in glucopyranose ring to reactive aldehyde and underwent to degradation with same mechanism of oxidized dextran via Malaprade oxidation and Maillard reaction. The degradation of oxidized cellulose scaffold was increased with increase in oxidation degree increased. It can conclude that the degradation of oxidized polysaccharide scaffold was controlled by varying the concentration of periodate. Moreover, the degradation was initially started by adding primary amino acid which correlated with the oxidized dextran degradation mechanism.

Interestingly, the protein adsorption on oxidized cellulose scaffold was increased with increase in pore sized of scaffold and degree of oxidation. In the case of pore size, large pore size promotes cell infiltration and penetration into the center of scaffold and reduces cell accumulation on the edge of scaffold. In the case of degree of oxidation, high aldehyde content such high reactive carbonyl group can interact with amine in polypeptide chain resulting in high protein adsorption. Subsequently, cell number which attached on oxidized cellulose scaffold was increased as oxidation degree increased. For histological study, 2.5% oxidized cellulose scaffold showed high degradation with low inflammation after 1 and 3 months. Even though, 5% oxidized cellulose scaffold was completely degraded after 3 months but the inflammation was very high due to high degree oxidation resulting in toxicity to host tissue.

In this research, we can explore the mechanism of oxidized polysaccharide by Malaprade oxidation via oxidized dextran which directly related with Maillard reaction. In addition, we use this mechanism for controlling the oxidized polysaccharide scaffold via cellulose scaffold for tissue engineering. For future work, we will study the controlled release of important substance for cell growth via oxidized polysaccharide scaffold by Malaprade oxidation for tissue engineering application.

# Achievement

---

## Conference

Wichchulada KONKUMNERD, Suong-Hyu HYON, Kazuaki MATSUMURA

62<sup>th</sup> Symposium on Macromolecule, 2013/9/11-13, Kanazawa

Degradation control of polysaccharides by Malaprade oxidation

Wichchulada Konkumnerd, Suong Hyu Hyon, Kazuaki Matsumura

MRS Fall meeting 2013, 2013/12/1-6, Boston, USA

Degradation control of cellulose by Malaprade oxidation for tissue engineering application

Wichchulada Konkumnerd, Kazuaki Matsumura

第二回日本バイオマテリアル学会北陸若手研究発表会 12/16 富山

Degradation control of cellulose scaffold by Malaprade reaction for tissue engineering.

Wichchulada KONKUMNERD、 Suong-Hyu HYON, Kazuaki MATSUMURA

64<sup>th</sup> Symposium on Macromolecule, 2015/9/14-17, Sendai

Degradation control of polysaccharide by Malaprade oxidation for tissue engineering

Wichchulada Konkumnerd , Tadashi Nakaji-Hirabayashi, Suong-Hyu Hyon4, Kazuaki Matsumura

PACCON 2016, 2016/ 2/9-11, Bangkok, Thailand

Polysaccharide degradation control by Malaprade oxidation for tissue engineering (Best poster presentation award)

## **Publication**

Chimpibul, W., Nagashima, T., Hayashi, F., Nakajima, N., Hyon, S. and Matsumura, K. 2016.

Dextran Oxidized by a Malaprade Reaction Shows Main Chain Scission Through a Maillard Reaction Triggered by Schiff Base Formation Between Aldehydes and Amines. *Journal of Polymer Science, Part A: Polymer Chemistry*. (Article in press)

# Acknowledgements

---

Firstly and foremost I would like to express the appreciation to my supervisor, Assoc. Prof. Kazuaki Matsumura for supporting, educating, supervision, and give me motivation throughout the completion of my doctoral study. I am grateful for his advice and teaching. It is a great honor for me to be a member in Matsumura's laboratory. I appreciate all his contributions of time, opinion, and funding to make my Ph.D. experience productive and stimulating. Without his supports, I would not have achieved this far and this thesis would not have been completed.

I am profoundly grateful to Assoc. Prof. Tadashi Nakaji-Hirabayashi from University of Toyama for animal study, Dr. Toshio Nagashima, unit leader and Dr. Fumiaki Hayashi from Division of Structural and Synthetic Biology, RIKEN Center for Life Science for NMR analysis. I also deeply appreciate the members of my committee: Prof. Masayuki Yamaguchi, Prof. Kohki Ebitani and Assoc. Prof. Tatsuo Kaneko. Further I would like to thank dual degree program (CU-JAIST) Scholarships for financial support during my doctoral study. Without these facilities and sponsorship, I would not have been able to achieve and complete my study.

I would like to express my appreciation to Assoc. Prof. Supason Wanichwecharungreung for valuable advice during my completion minor research. Without her, I would not have been able to achieve and complete my study.